Overview of CACTI datasets, ongoing research, and future opportunities

Adam Varble[1], Zhe Feng[1], James Marquis[1], Zhixiao Zhang[2], Paloma Borque[1], Joseph Hardin[1], and Peter Veals[2]

[1]Pacific Northwest National Laboratory
[2]University of Utah

2022 ARM/ASR Joint User Facility and PI Meeting

October 25, 2022

PNNL is operated by Battelle for the U.S. Department of Energy

Early stages of the 25 January 2019 storm that reached nearly 21 km ASL. Photo courtesy of Ramón Alberto Acuña (SMN).

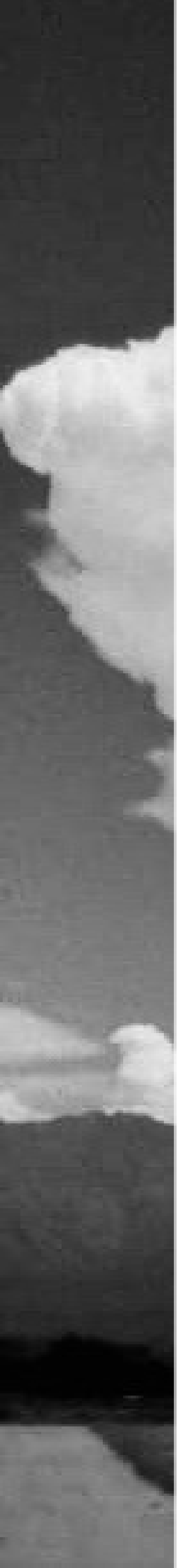

Cloud, Aerosol, and Complex Terrain Interactions (CACTI) Logistics

First deployment of the CSAPR2 with over 50 ARM Mobile Facility (AMF) instruments between Oct 2018 and Apr 2019 in the Sierras de Córdoba range of central Argentina.

IOP coincident with the RELAMPAGO field campaign between 1 Nov and 15 Dec with 22 flights performed by the G-1 (8 Deep CI, 8 Cu, 3 microphysics, 3 clear air).

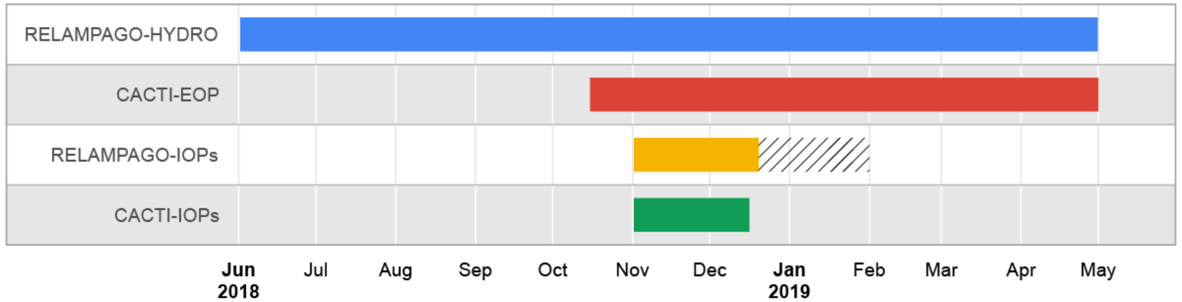

Amongst the most ARM data streams produced of any AMF campaign including comprehensive, calibrated scanning Ka-, X-, and C-band radar datasets.

https://www.arm.gov/research/campaigns/amf2018cacti

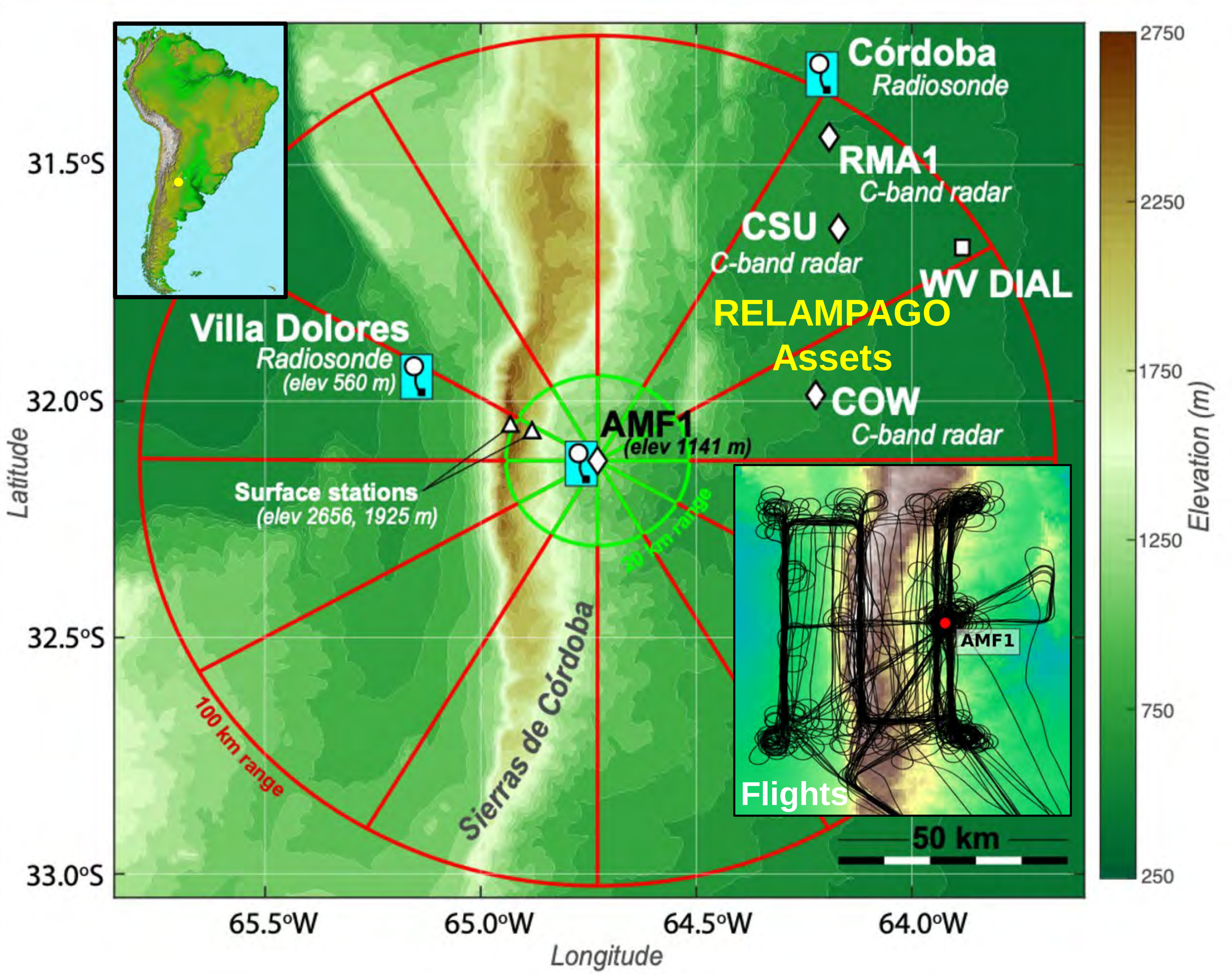

Varble, A. C., et al., 2021: Utilizing a Storm-Generating Hotspot to Study Convective Cloud Transitions: The CACTI Experiment. *BAMS*, 102, E1597-E1620, doi:10.1175/BAMS-D-20-0030.1.

CACTI Objectives

Varble, A. C., et al., 2021: Utilizing a Storm-Generating Hotspot to Study Convective Cloud Transitions: The CACTI Experiment. *BAMS,* 102, E1597-E1620, doi:10.1175/BAMS-D-20-0030.1.

Nesbitt S. W., et al., 2021: A Storm Safari in Subtropical South America: Proyecto RELAMPAGO. *BAMS,* 102, E1621-E1644, doi:10.1175/BAMS-D-20-0029.1.

AMS special collection: https://journals.ametsoc.org/collection/RELAMPAGO-CACTI

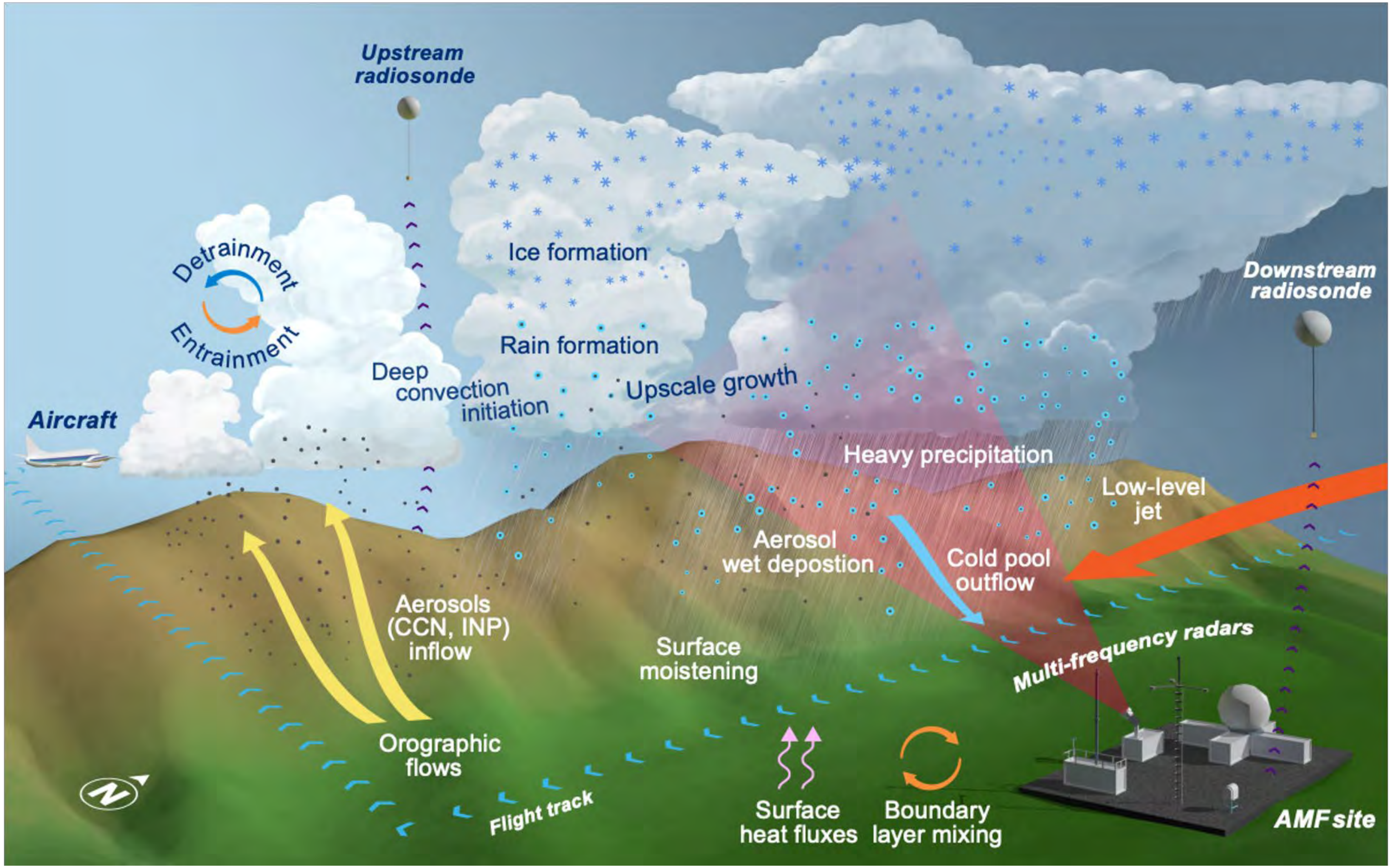

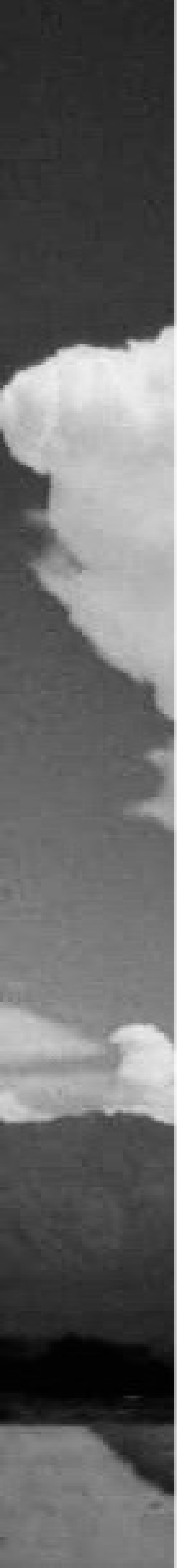

Pacific Northwest
NATIONAL LABORATORY

Cloud and Precipitation Conditions

Shallow clouds were observed directly overhead on 191 of 212 days, 165 of which had liquid clouds lasting 30 minutes or longer, many of which produced drizzle.

About 160 deep convective systems passed directly over the site on 83 separate days with a wide range of depth and organization.

Varble, A. C., et al., 2021, *BAMS*, doi:10.1175/BAMS-D-20-0030.1.

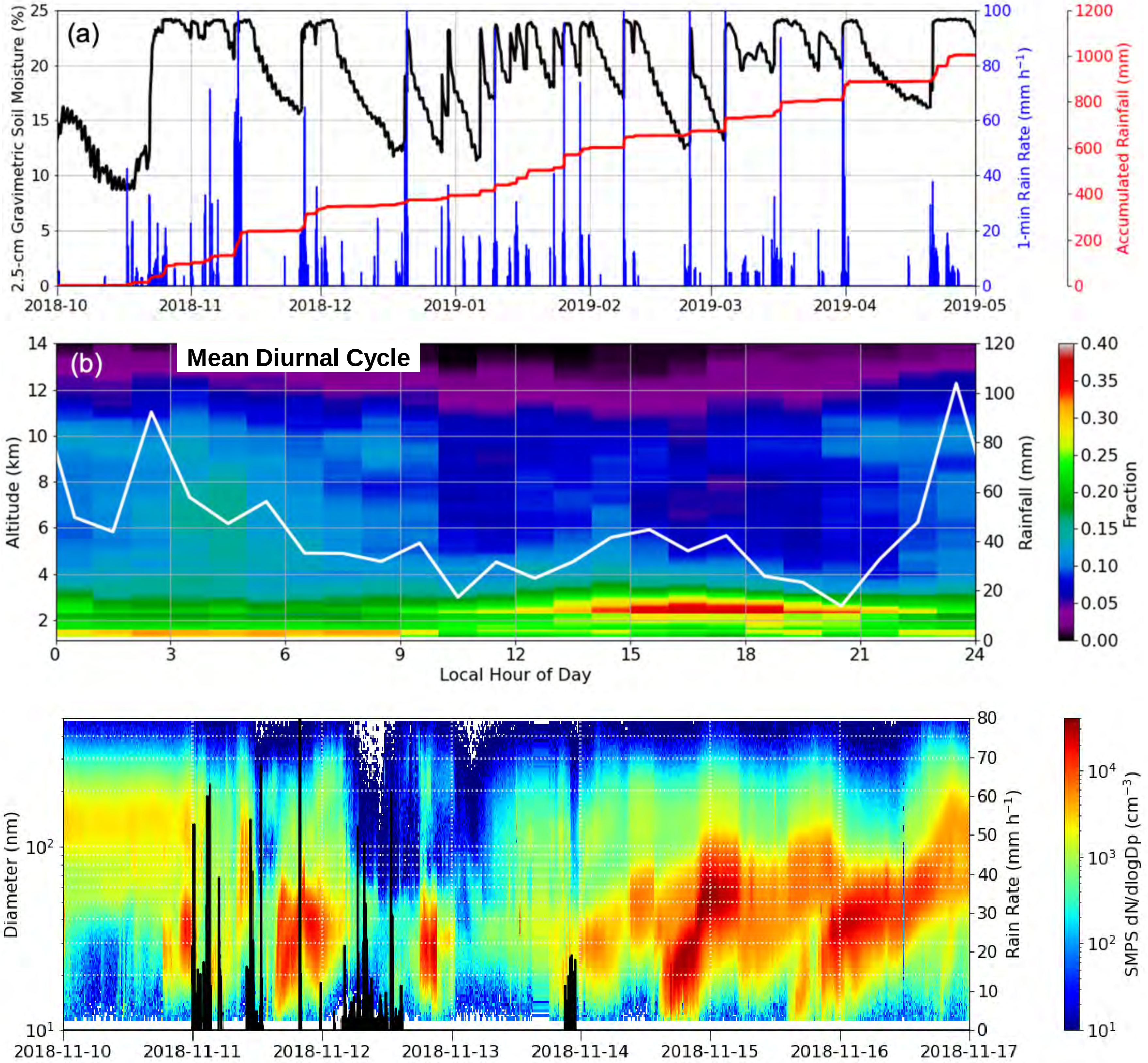

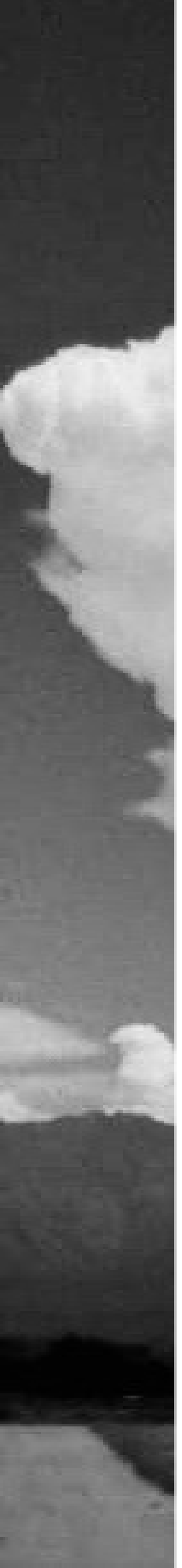

Aerosol and Aerosol-Cloud Interaction Observations

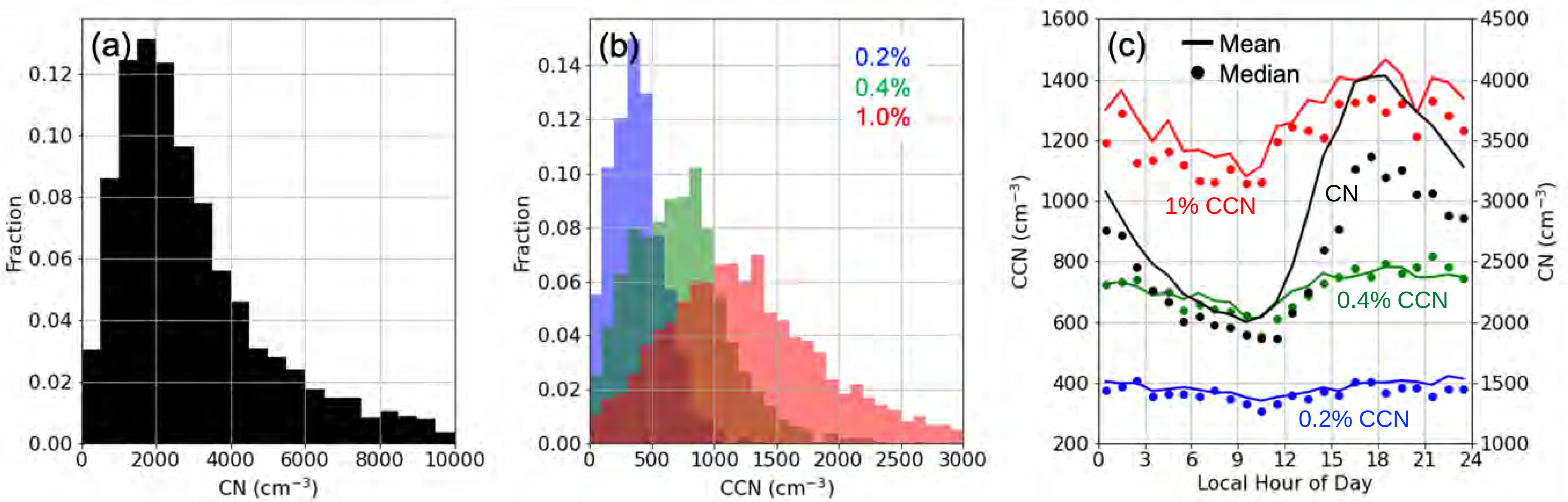

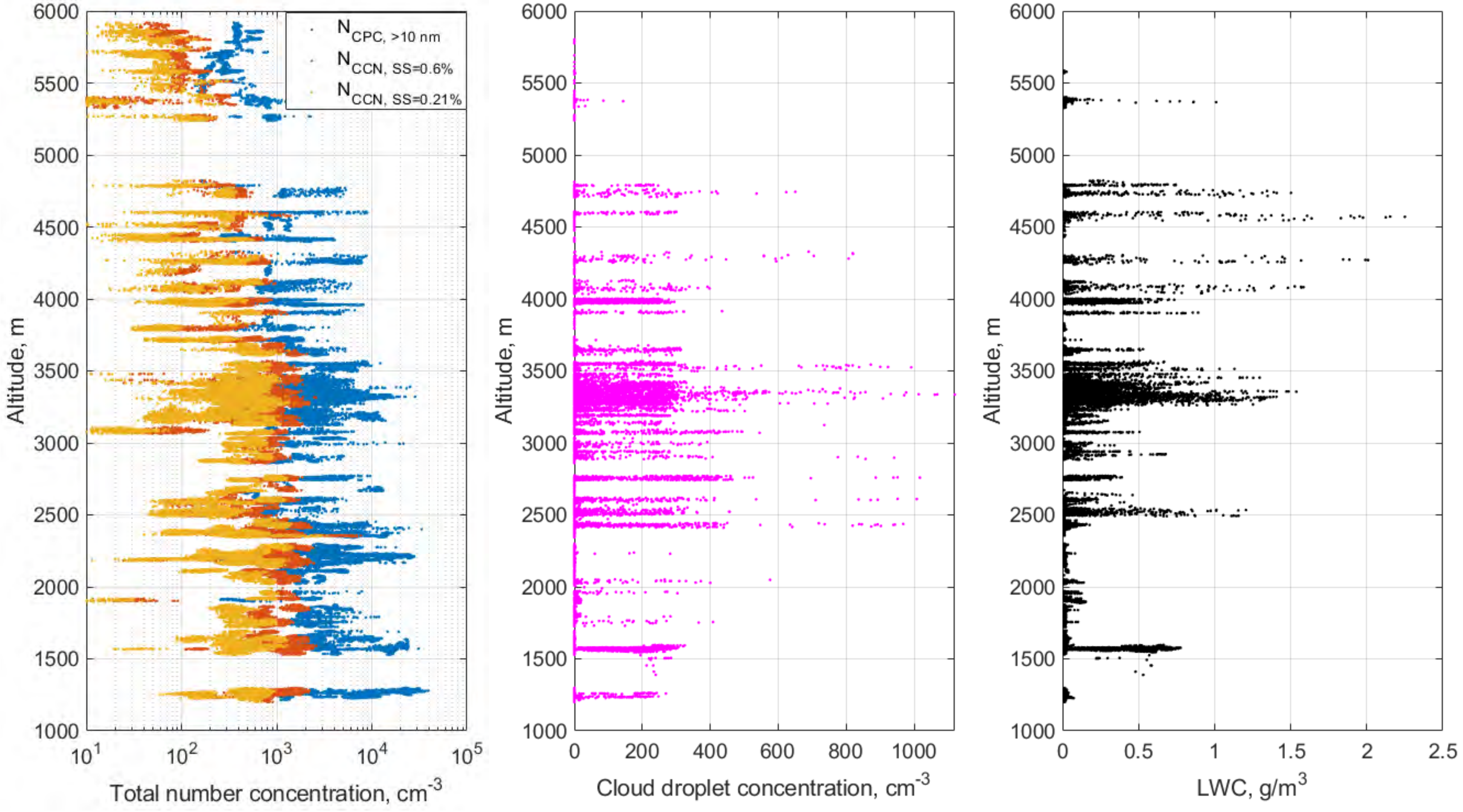

Varble, A. C., et al., 2021, *BAMS*, doi:10.1175/BAMS-D-20-0030.1.

INP-Precipitation Interactions (Testa, Hill, Demott, and coauthors)

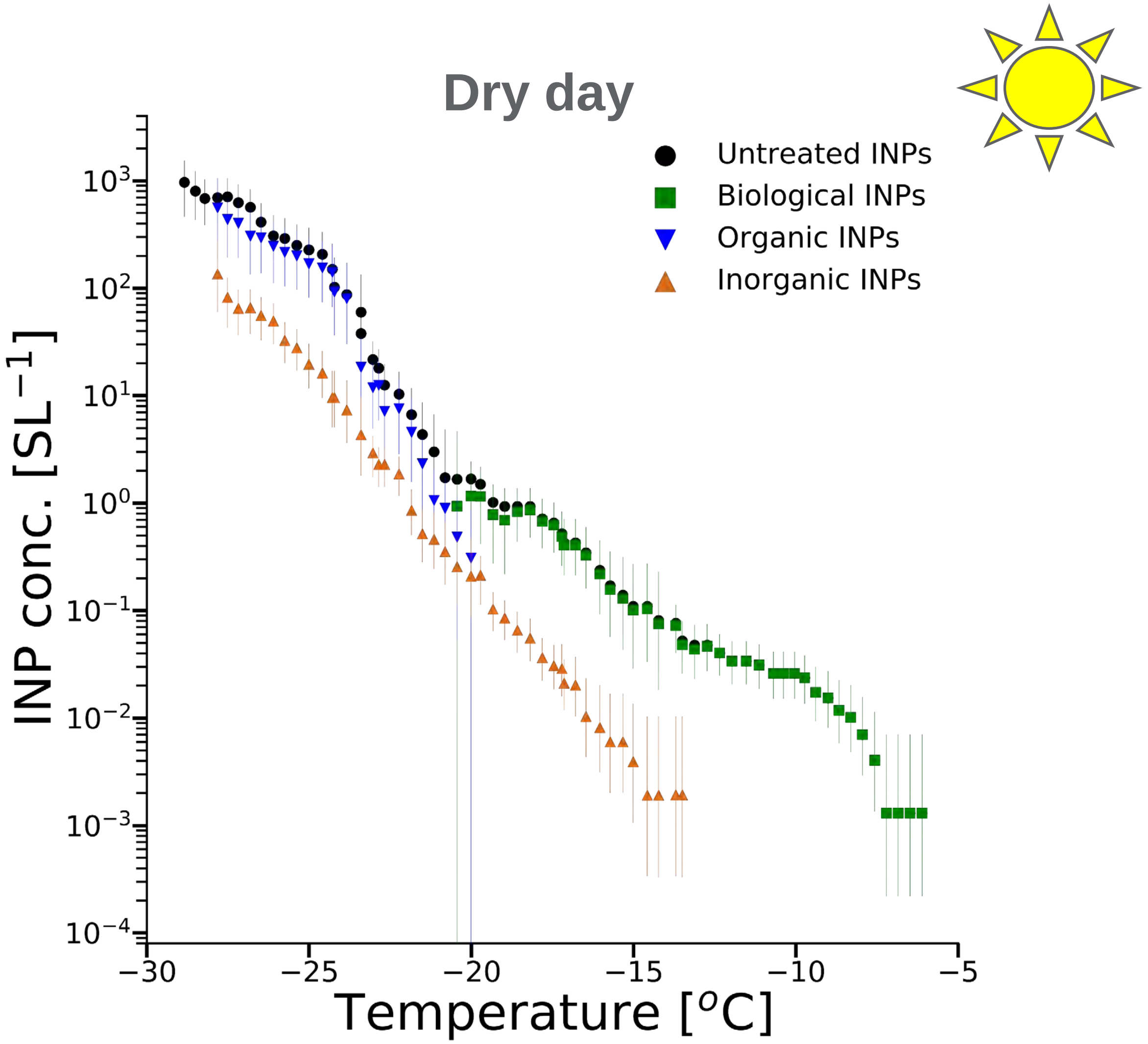

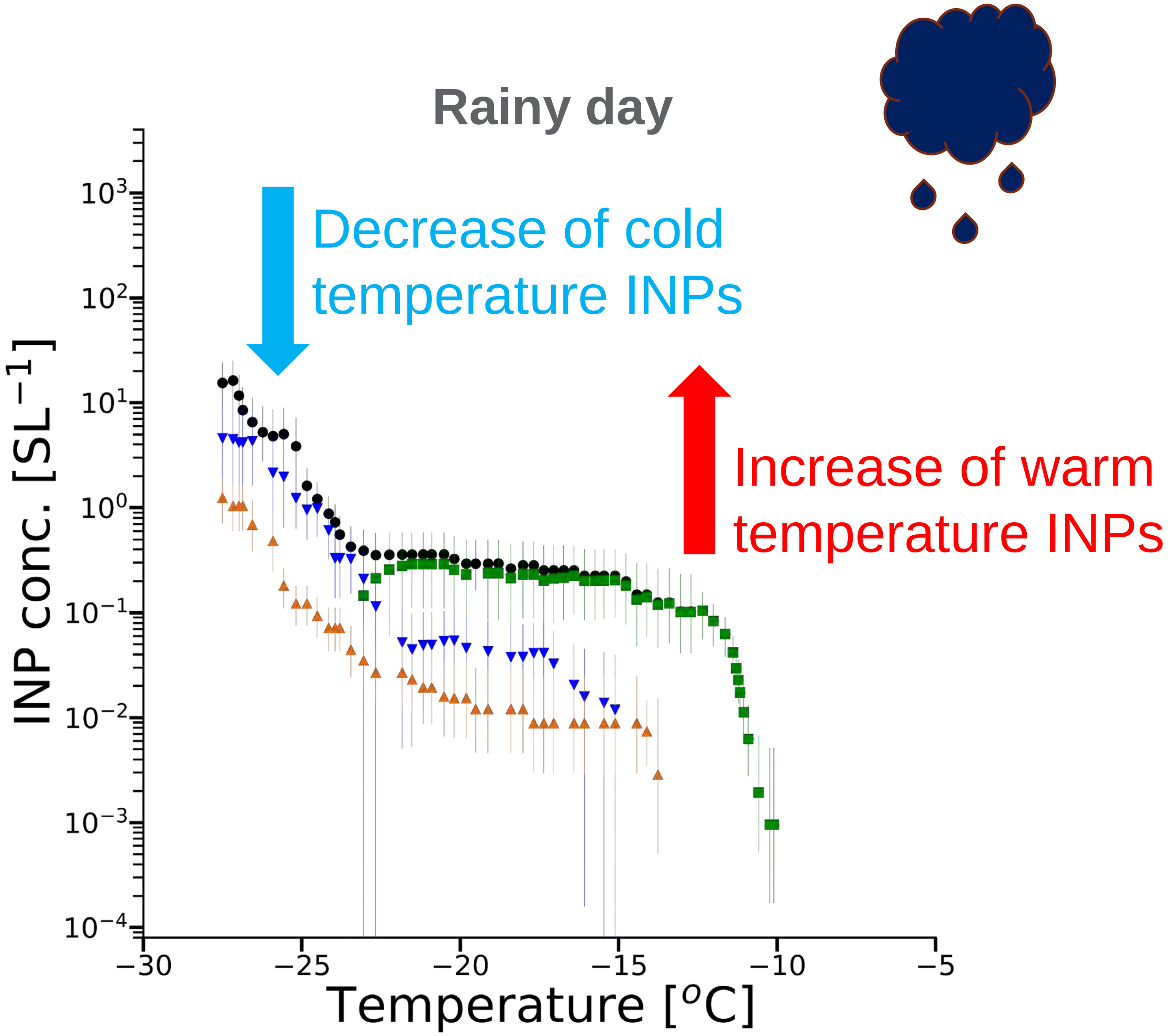

Testa, B., et al., 2021: Ice nucleating particle connections to regional Argentinian land surface emissions and weather during the Cloud, Aerosol, and Complex Terrain Interactions experiment, *J. Geophys. Res. Atmos*., 126, doi:10.1029/2021JD035186.

Warm Cloud Processes

Borque, P., et al., 2022: Peak rain rate sensitivity to observed cloud condensation nuclei and turbulence in continental warm shallow clouds during CACTI. *J. Geophys. Res. Atmos.*, 127, doi:10.1029/2022JD036864.

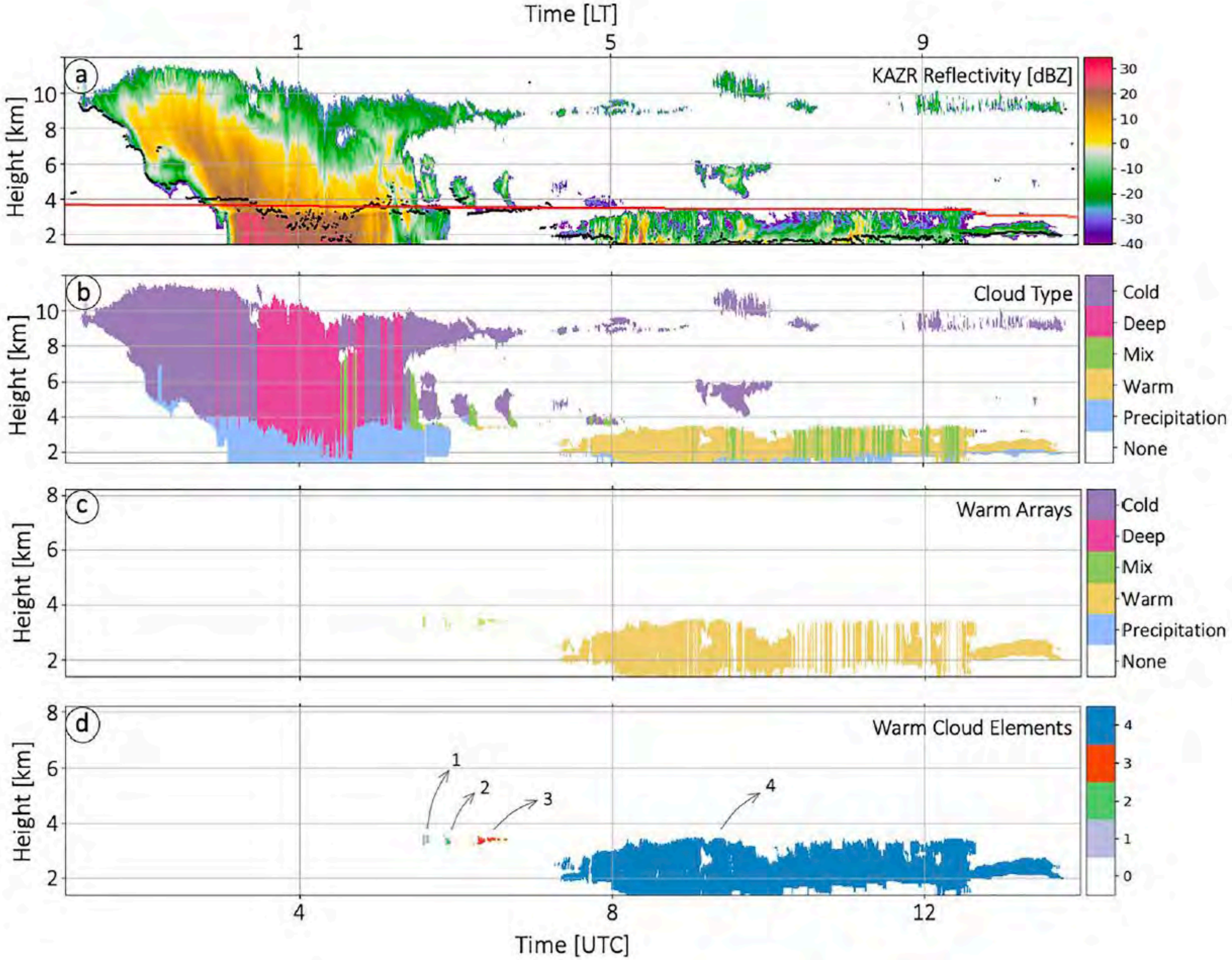

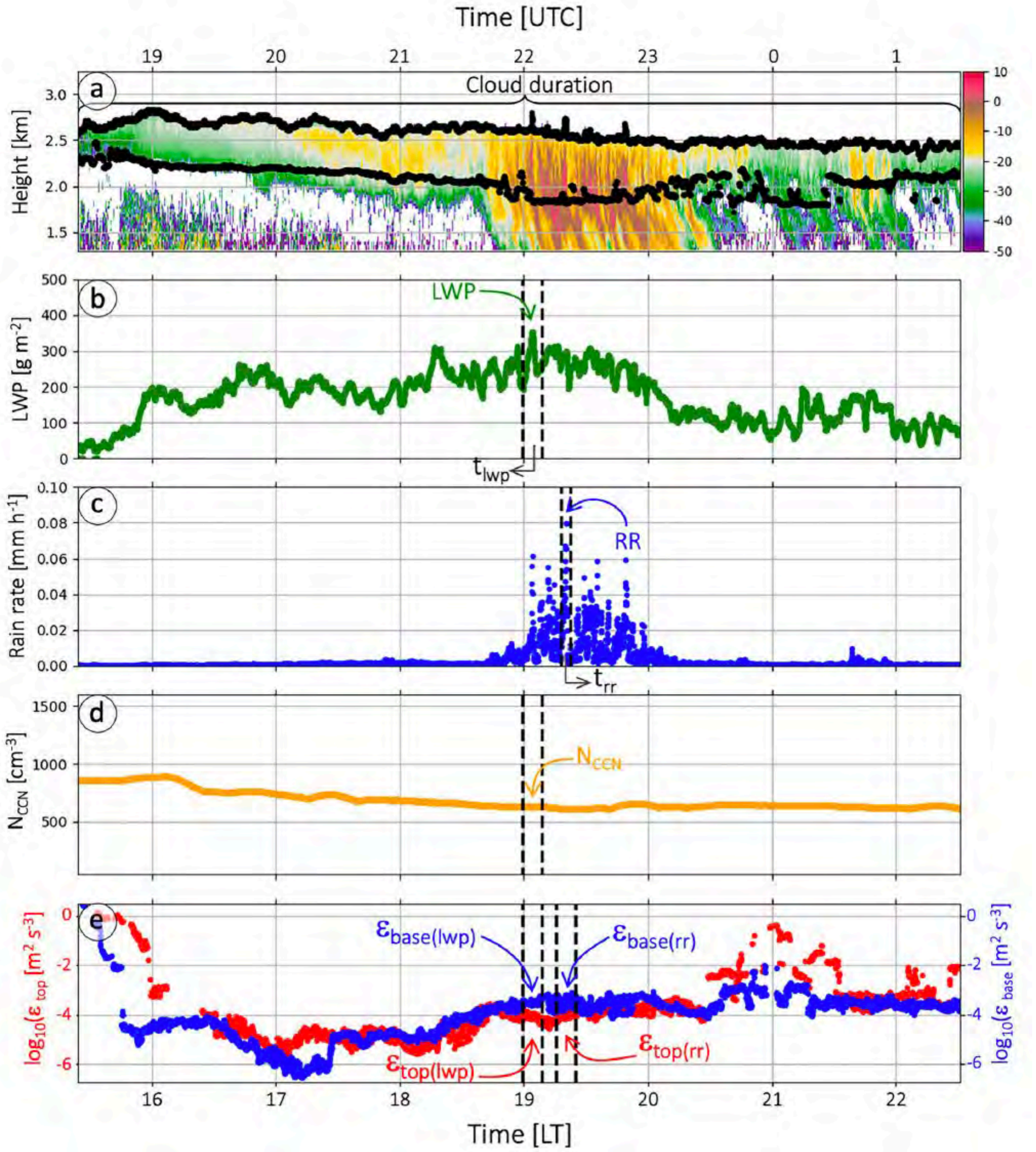

3342 warm cloud objects, 2173 mixed cloud objects, 152 deep cloud objects merged with cold clouds

CCN impact on warm cloud drizzle rate

Borque, P., et al., 2022: Peak rain rate sensitivity to observed cloud condensation nuclei and turbulence in continental warm shallow clouds during CACTI. *J. Geophys. Res. Atmos.*, 127, doi:10.1029/2022JD036864.

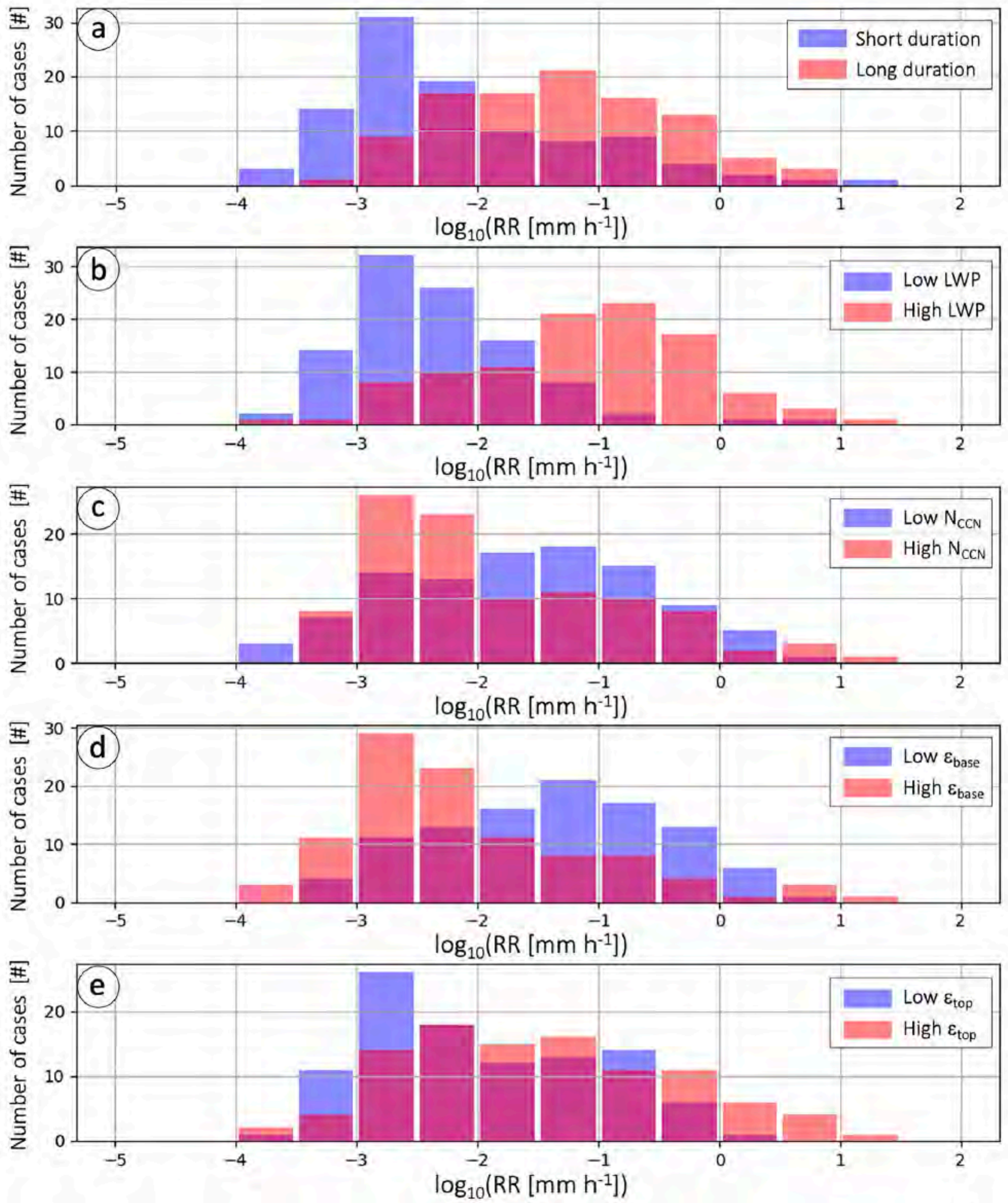

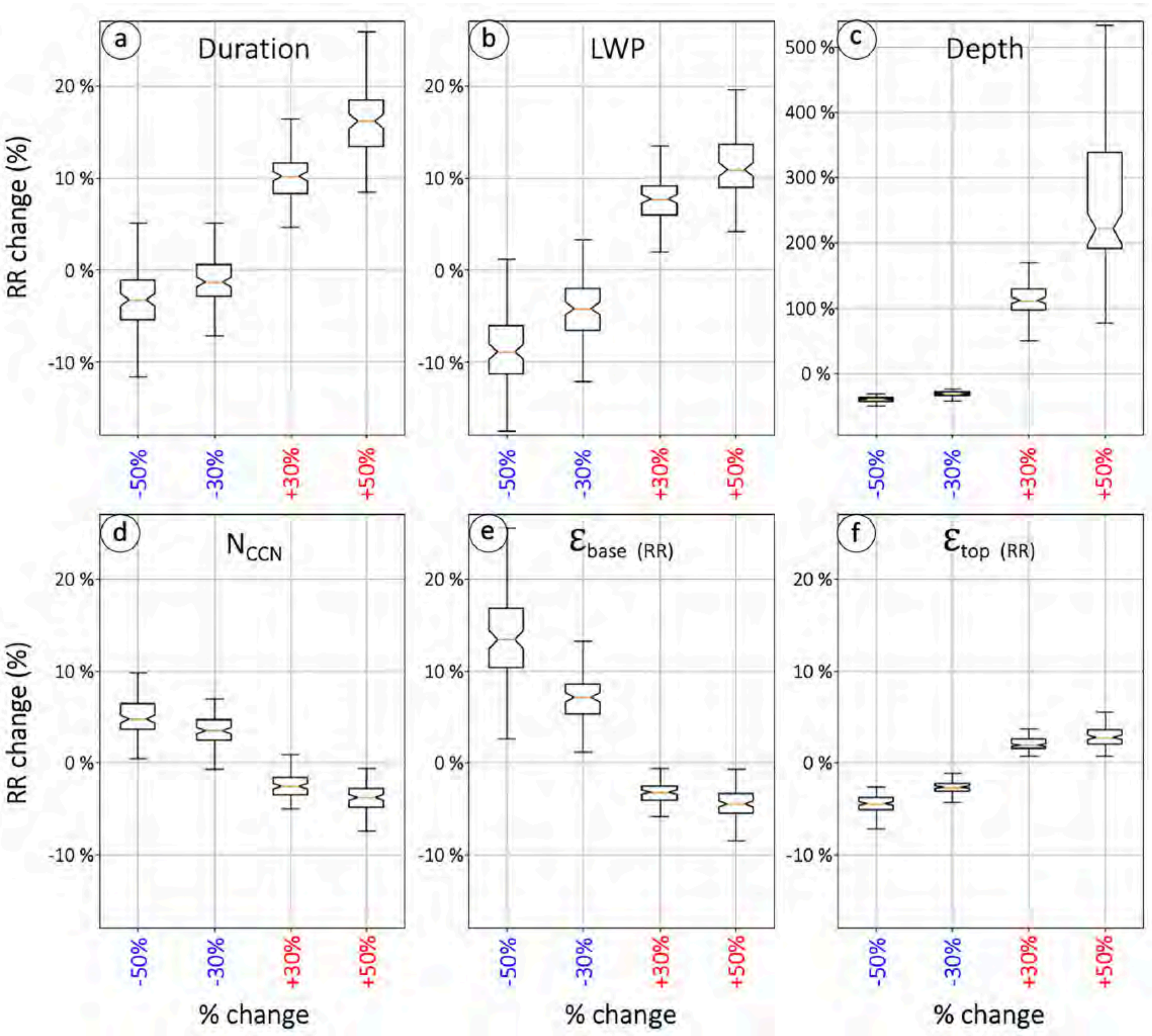

Shallow Cloud Research Opportunities

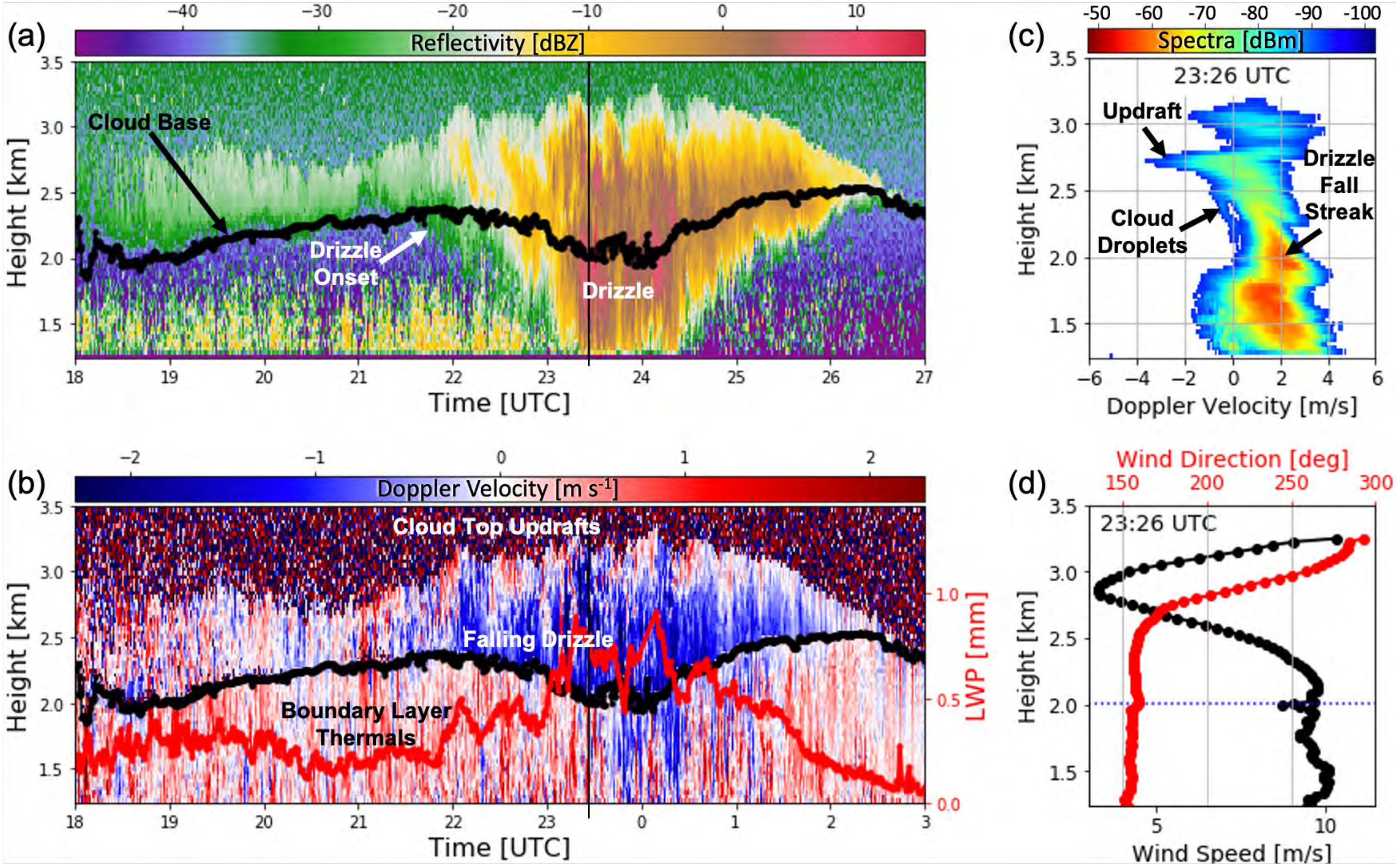

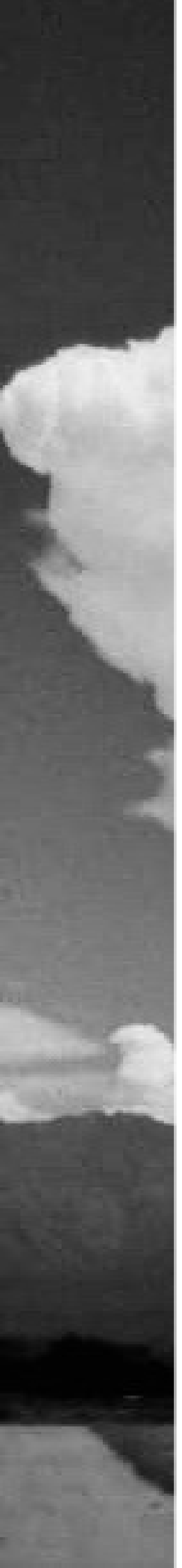

Pacific Northwest NATIONAL LABORATORY

Congestus Deepening Processes (Andrew Geiss, Rusen Öktem, David Romps)

+

=

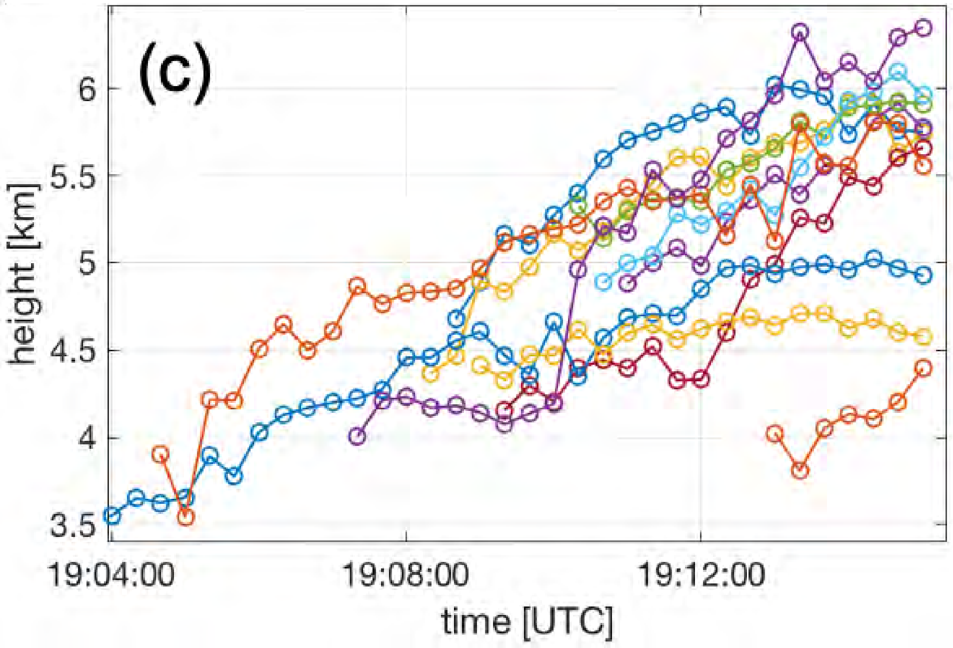

- Location
- Width
- Depth
- Lifetime
- Ascent Rate

Deep Convection Initiation (CI)

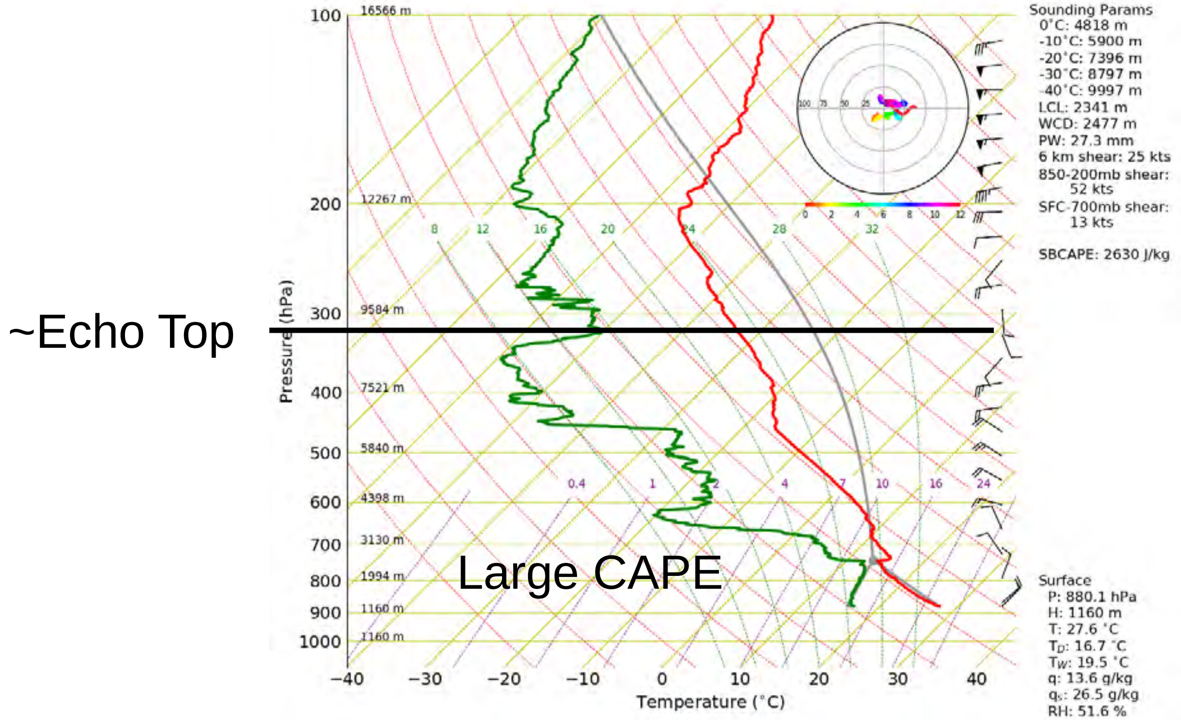

Ka-band Reflectivity Evolution

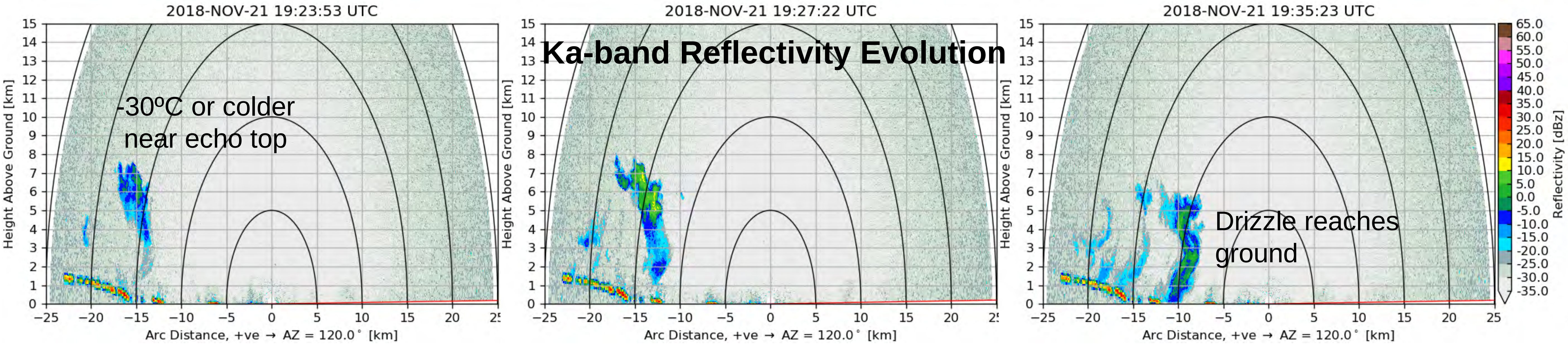

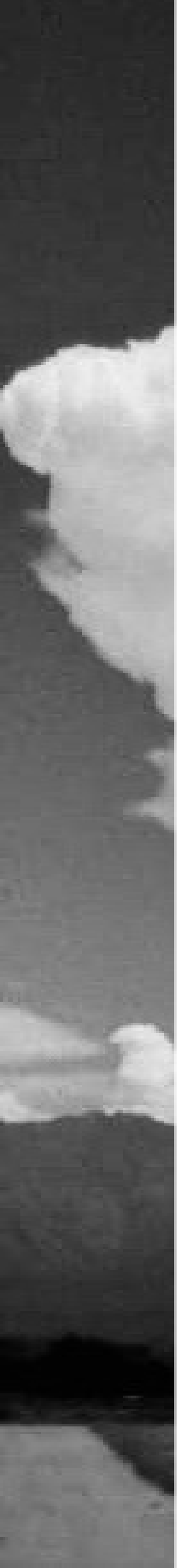

Pacific Northwest NATIONAL LABORATORY

Deep Convection Initiation Processes

With frequent orographic clouds and favorable deep convective thermodynamic conditions, many deep convection initiation (CI) success and failure cases were observed.

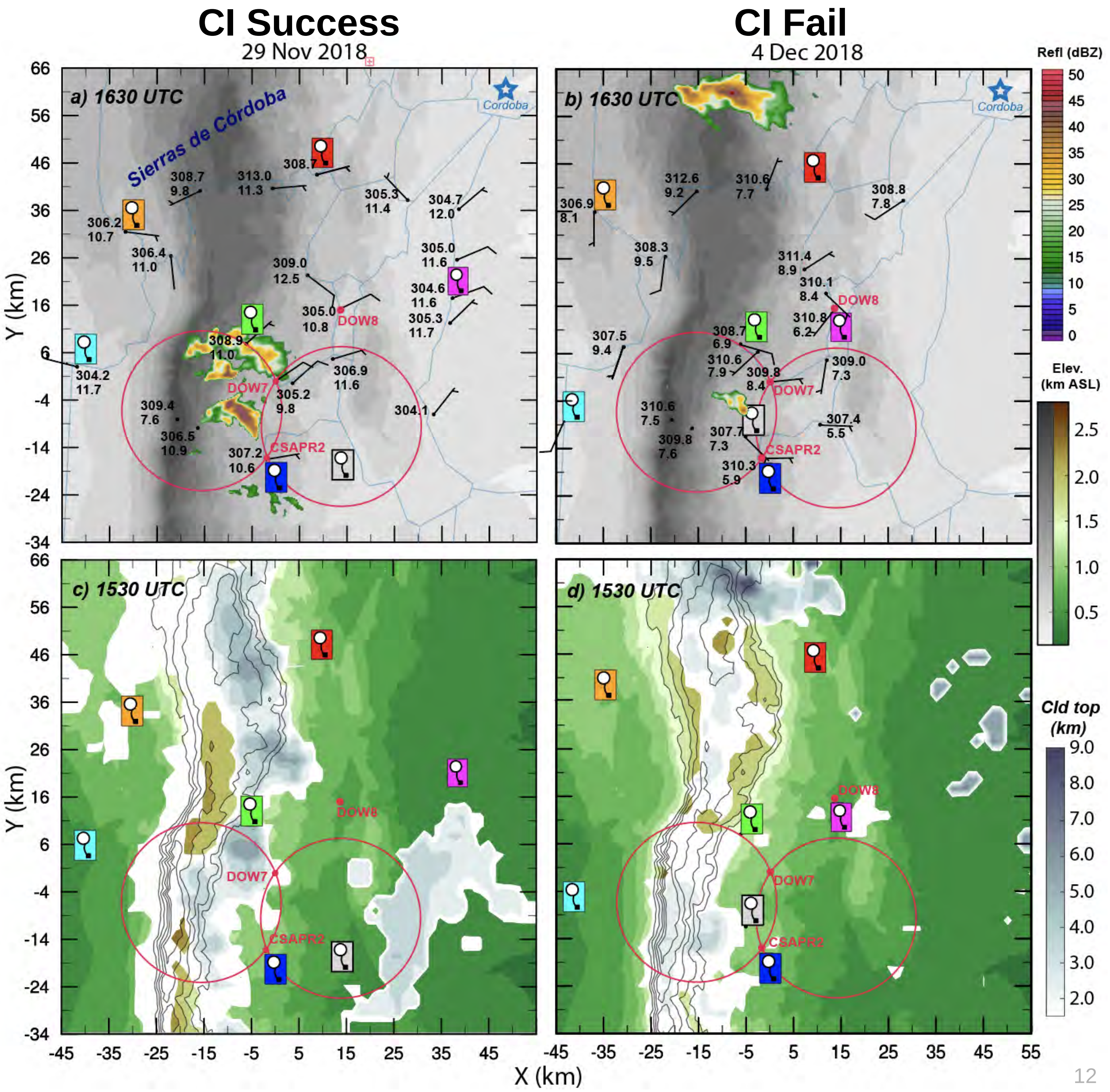

Marquis J. N., et al., 2021: Low-level Mesoscale and Cloud-scale Interactions Promoting Deep Convective Initiation. *Mon. Wea. Rev*., 149, 2473-2495, doi:10.1175/MWR-D-20-0391.1.

Nelson T. C., et al., 2021: Radiosonde Observations of Environments Supporting Deep Moist Convection Initiation during RELAMPAGO-CACTI. *Mon. Wea. Rev.*, 149, 289–309. doi:10.1175/MWR-D-20-0148.1.

Tracking Convective Cells for the Whole Campaign

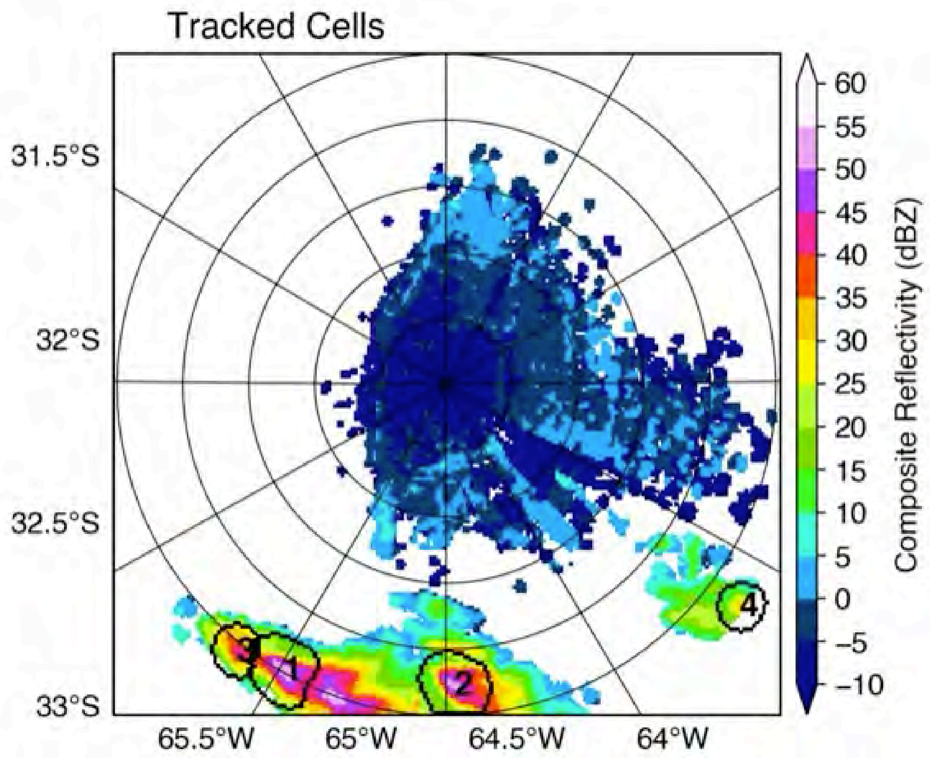

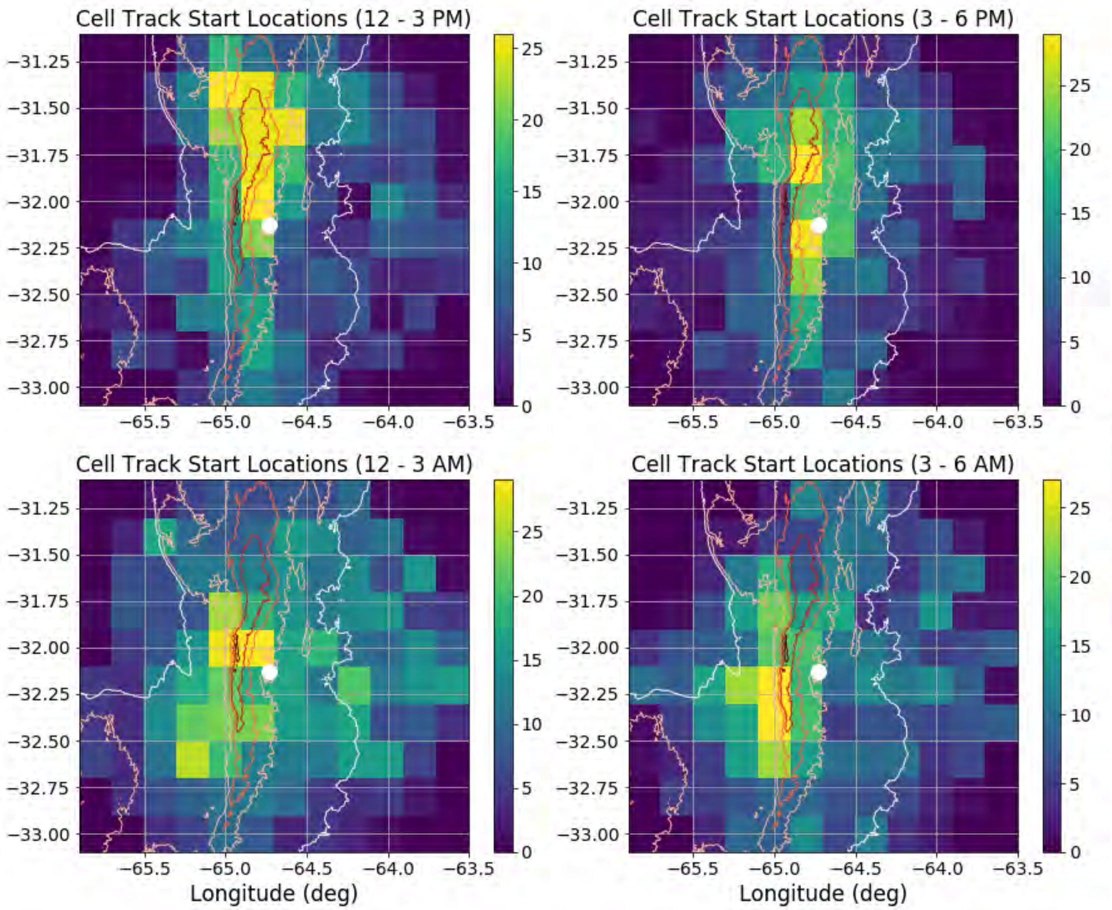

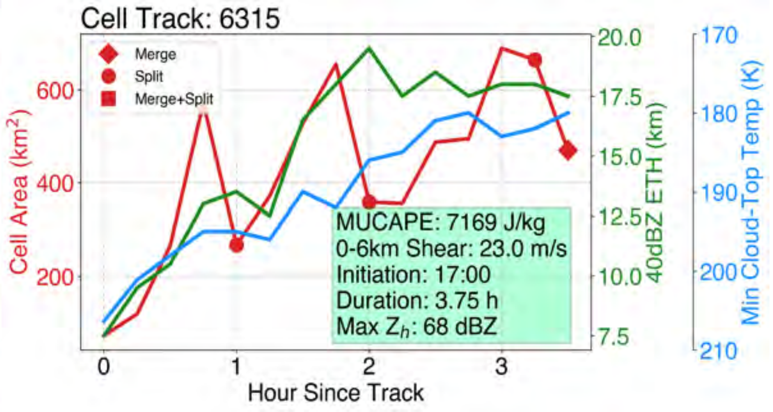

FLEXTRKR was used to separate, track, and save properties of ~6,900 observed convective cells on 74 days, matching them to sounding-derived atmospheric conditions.

Feng, Z, et al., 2022: Deep Convection Initiation, Growth, and Environments in the Complex Terrain of Central Argentina during CACTI, *Mon. Wea. Rev.*, 150, 1135-1155, doi:10.1175/MWR-D-21-0237.1.

Feng, Z., et al., 2023: PyFLEXTRKR: A Flexible Python Feature Tracking Software for Convective Cloud Analysis. *GMD*, submitted.

Cell Lifetime-Max Width-Depth-Reflectivity Relationships

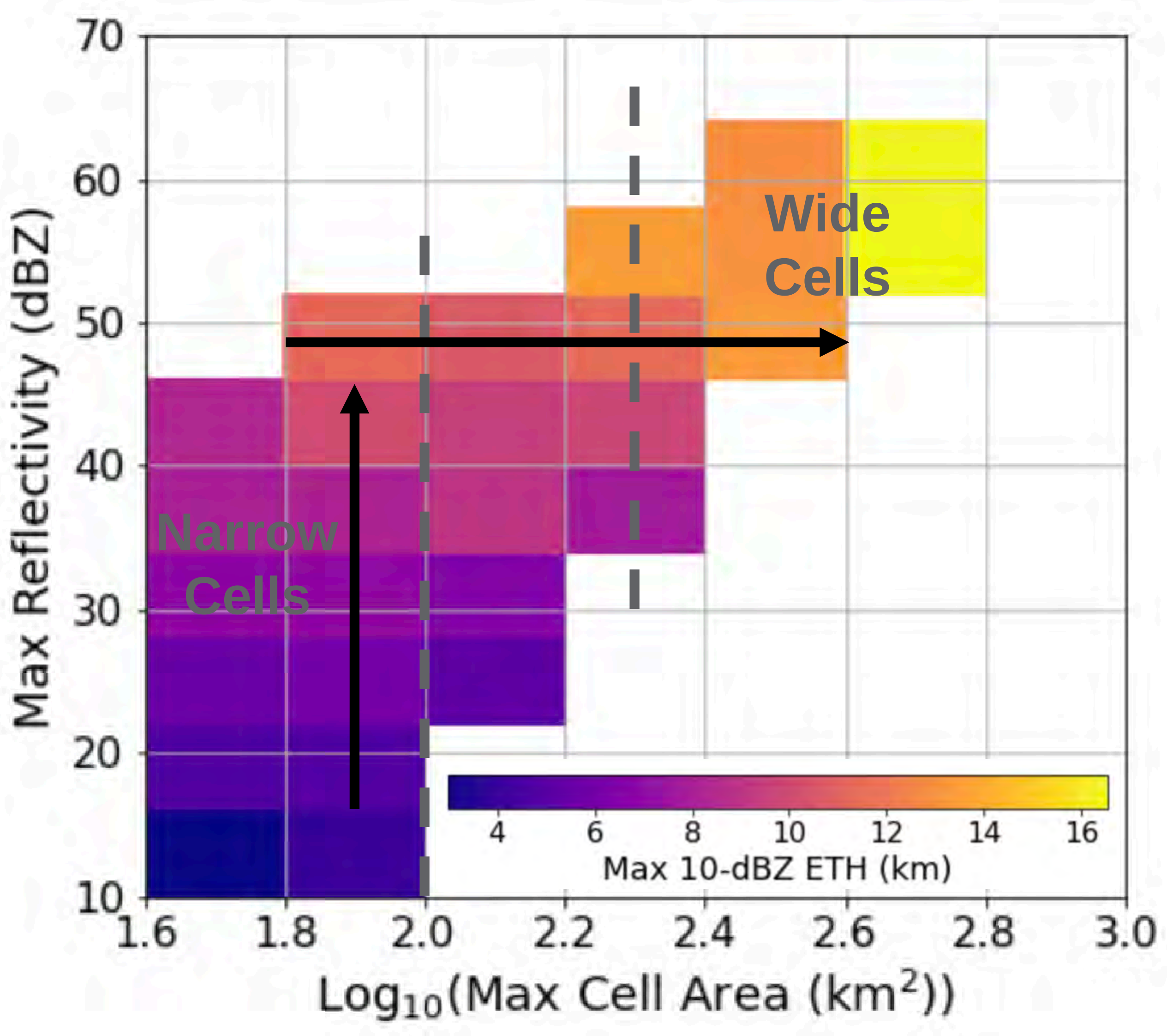

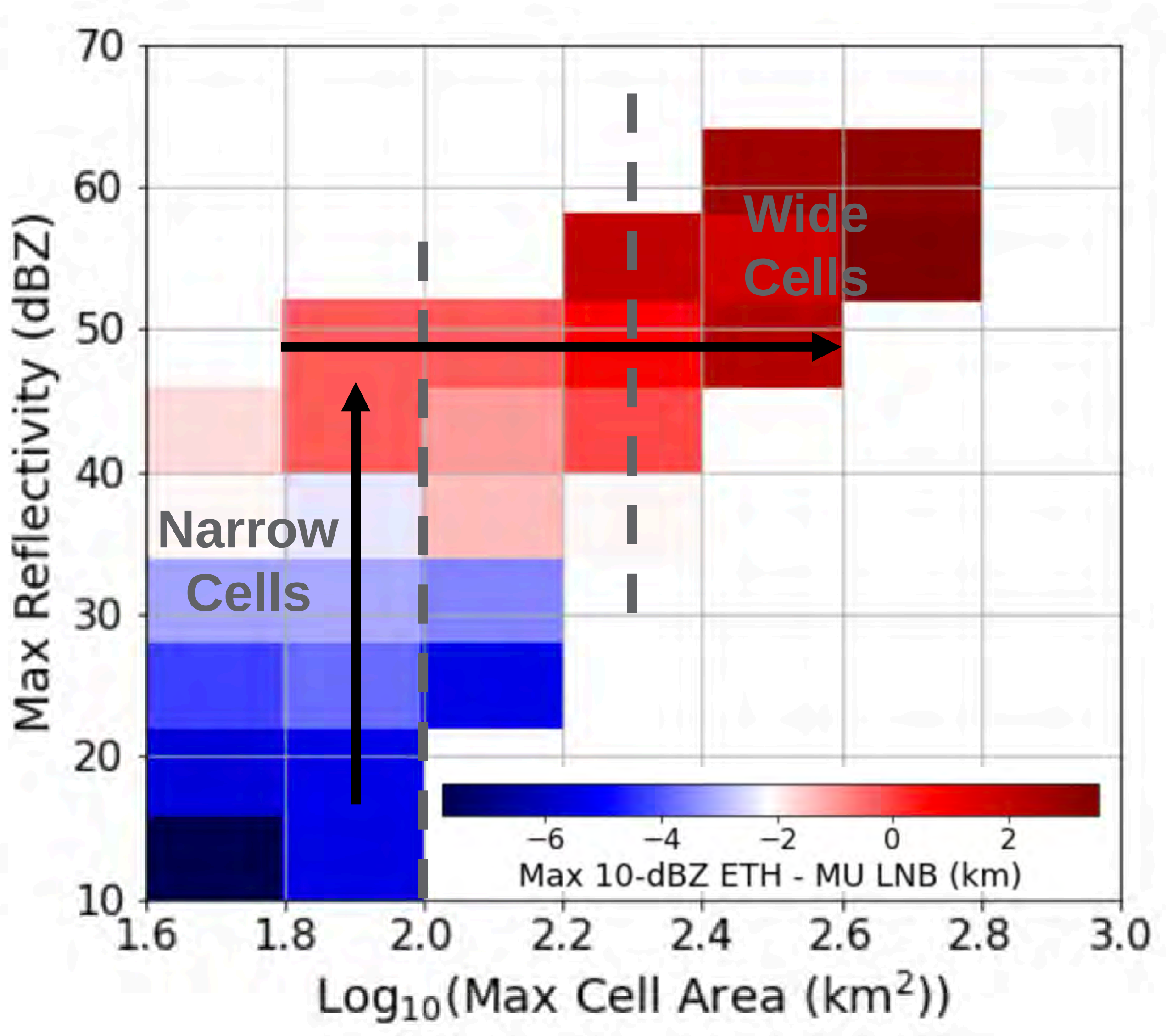

What conditions correlate with narrow cell deepening and precipitation intensification?

- **MUCAPE** ✗
- **MU EL** ✗
- **Vertical Wind Shear** ✗
- **# of Cell Mergers** ✗
- MUCIN ✓
- ACBL RH ✓
- Cell Inflow ✓
- Cell Depth ✓
- Lifetime —

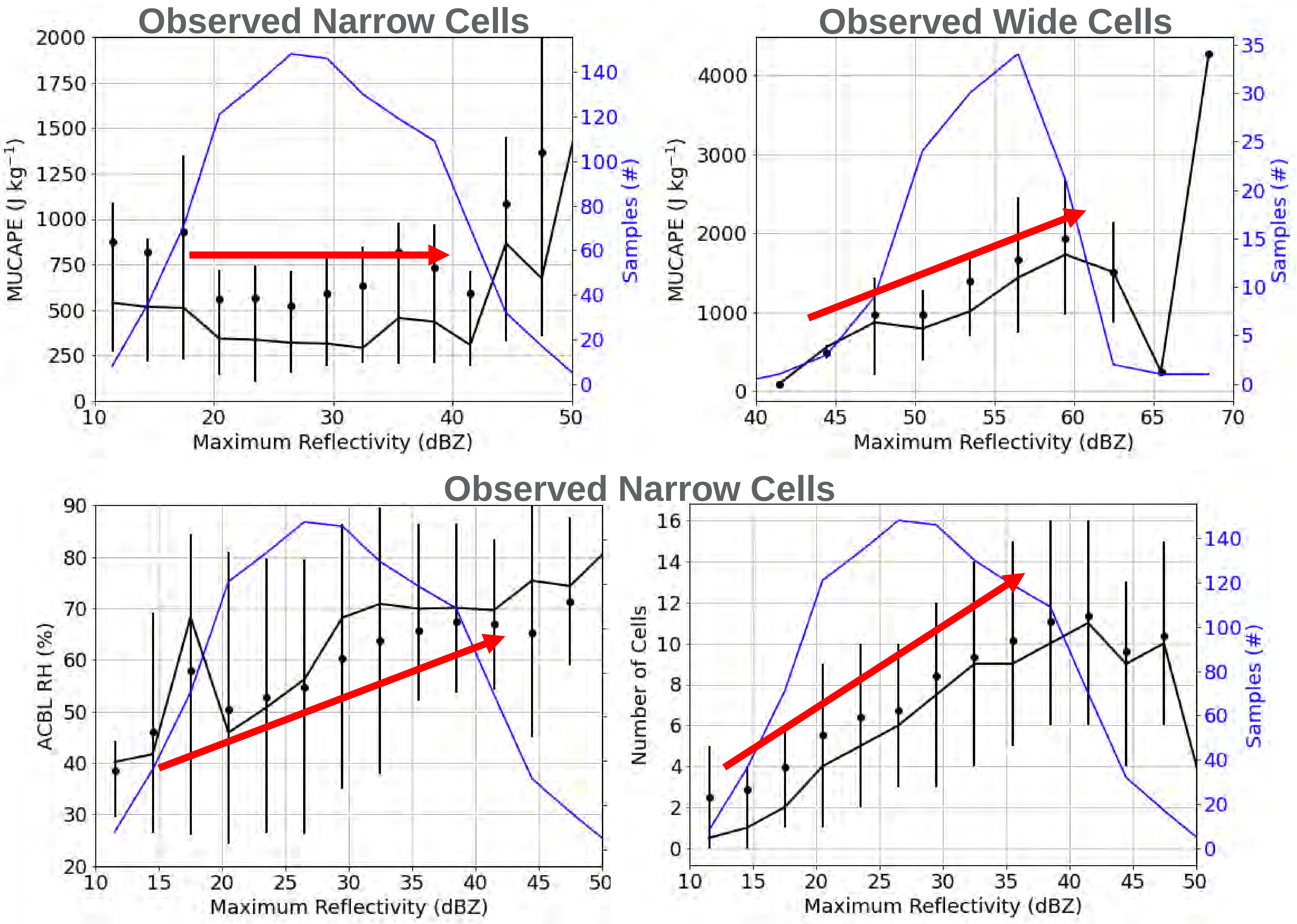

Simulated MCS Evaluation

Zhang, Z., et al., 2021: Growth of Mesoscale Convective Systems in Observation and a Seasonal Convection-Permitting Simulation over Argentina. *Mon. Wea. Rev.*, 149, 3469-3490, doi:10.1175/MWR-D-20-0411.1.

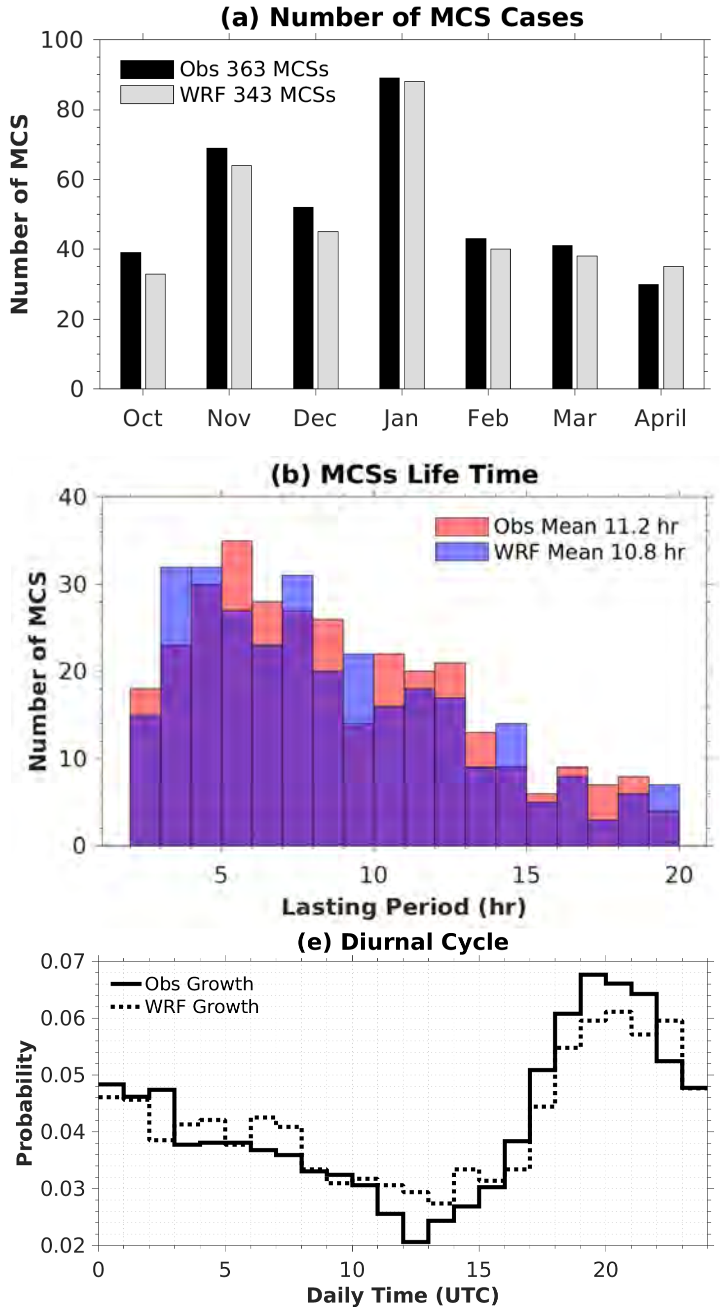

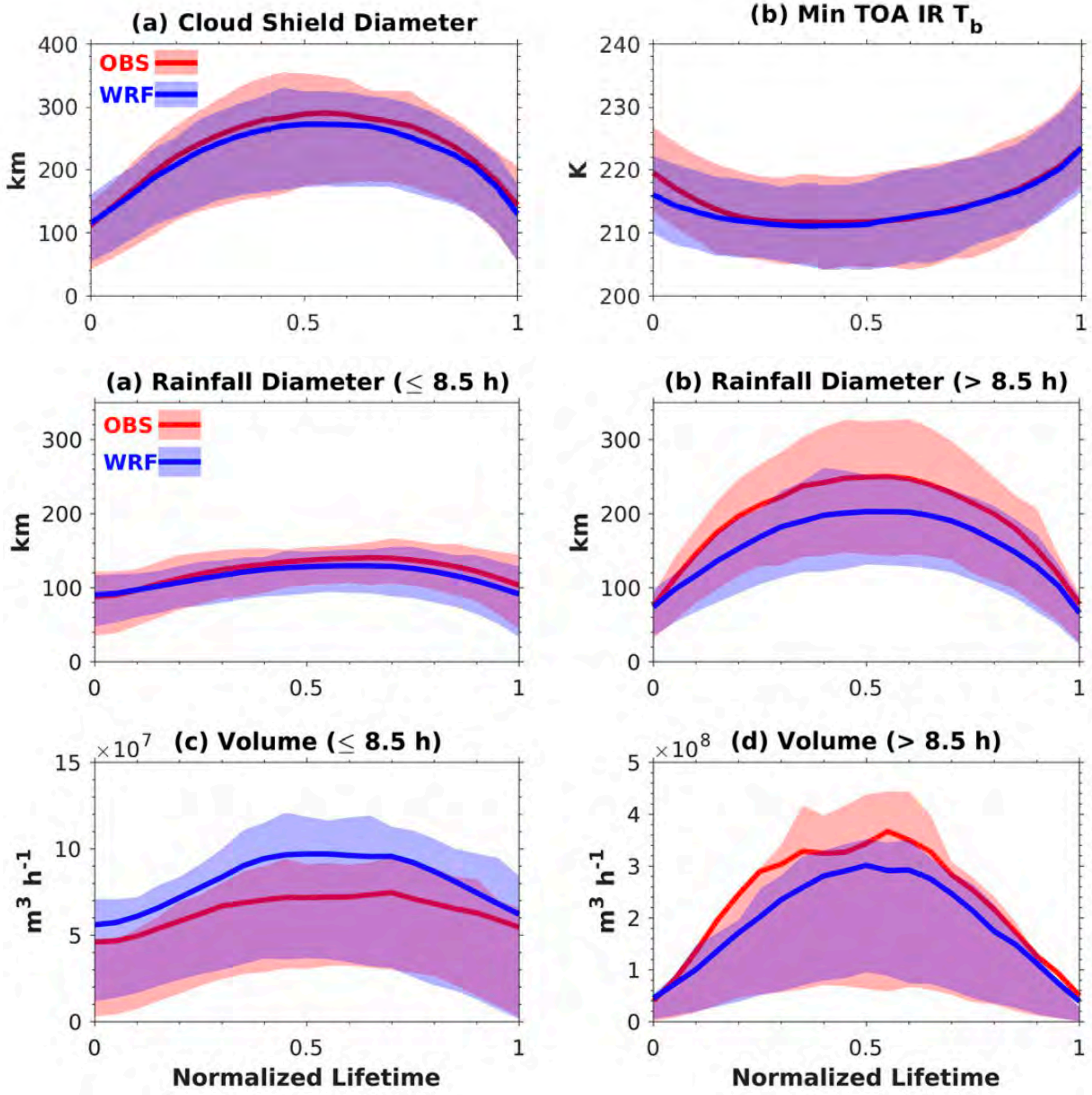

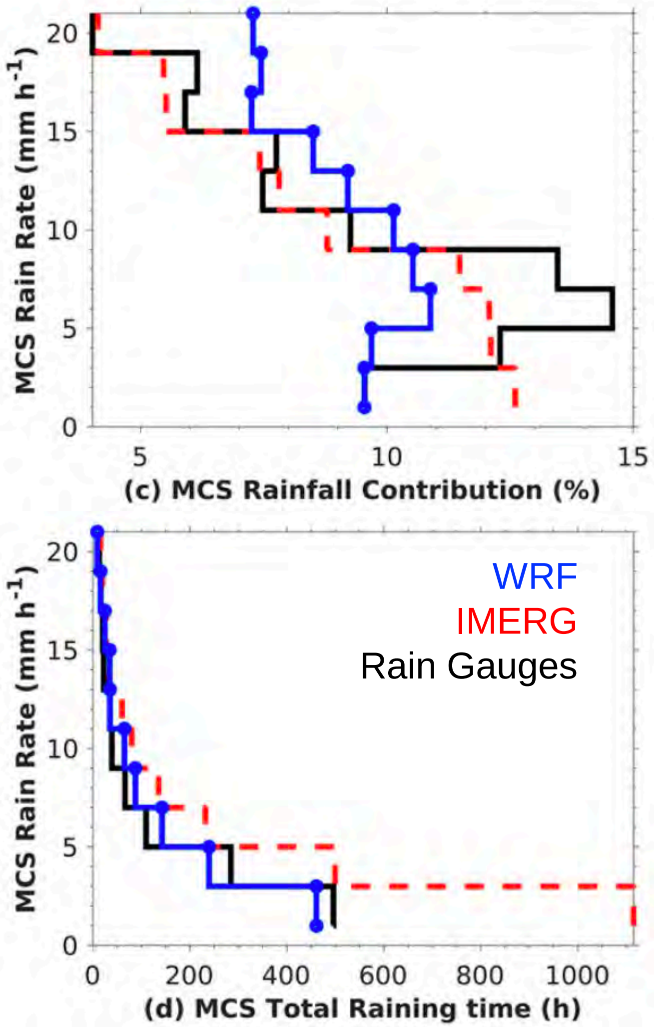

Simulated Convective Cell Evaluation

Zhang, Z., et al., 2022, to be submitted.

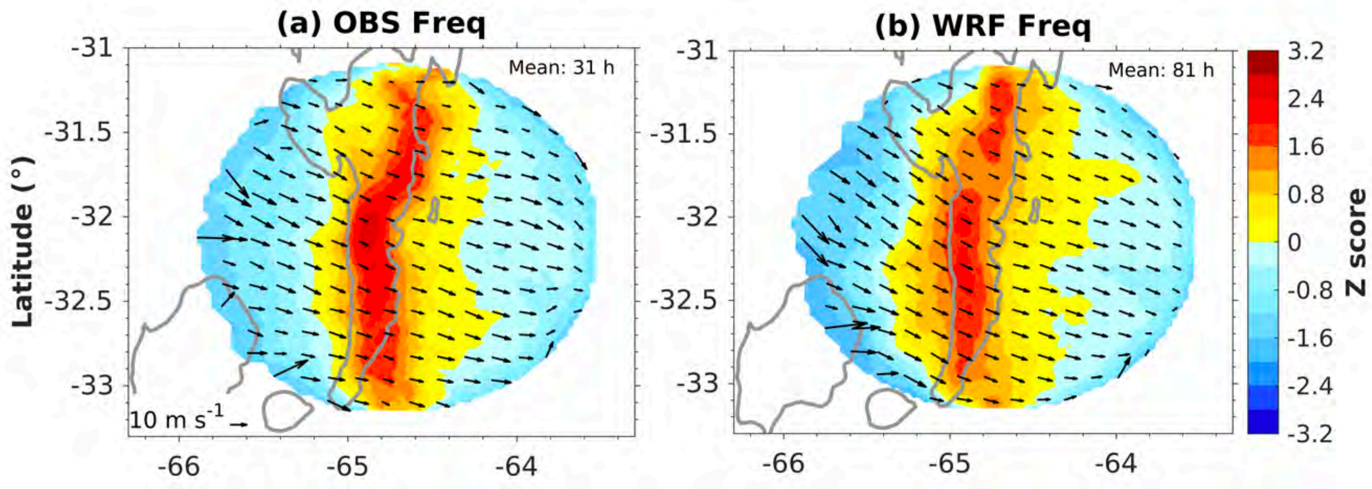

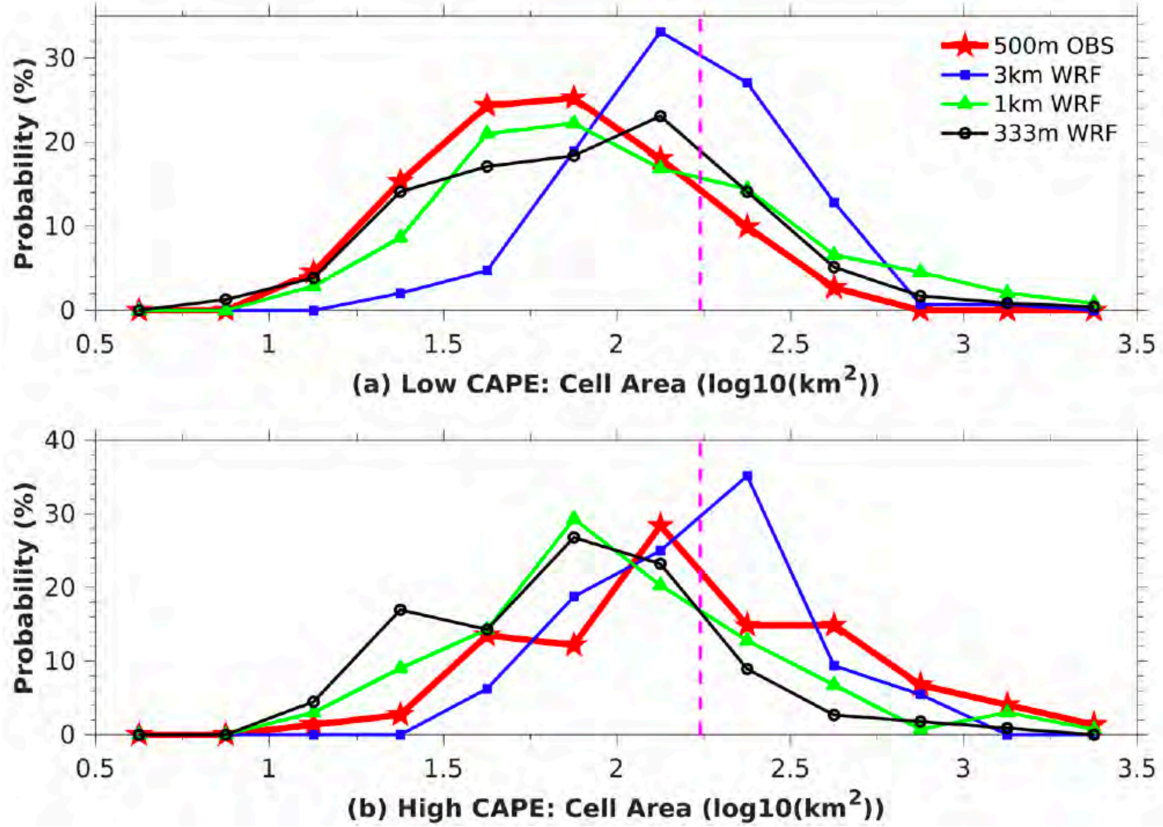

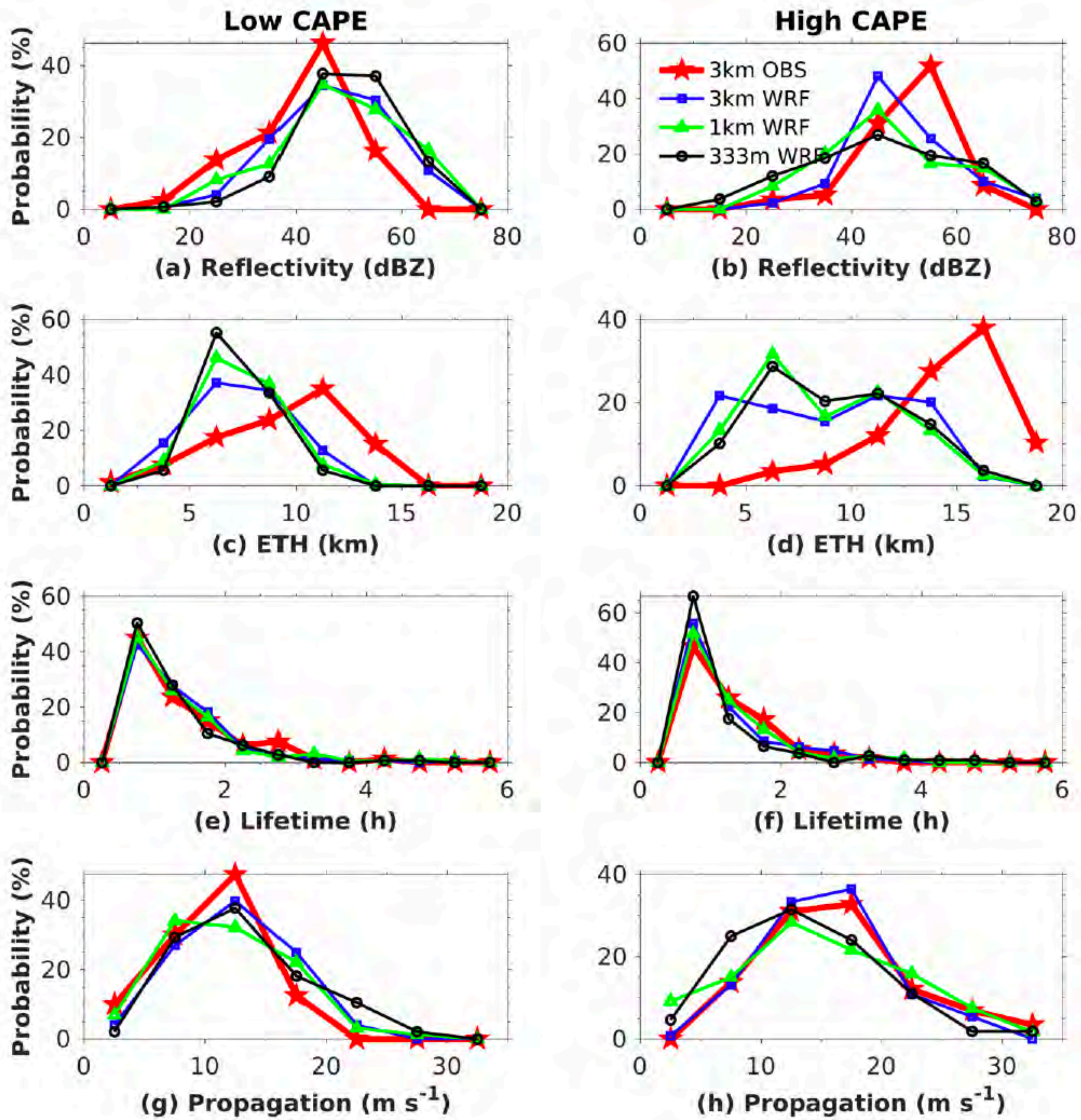

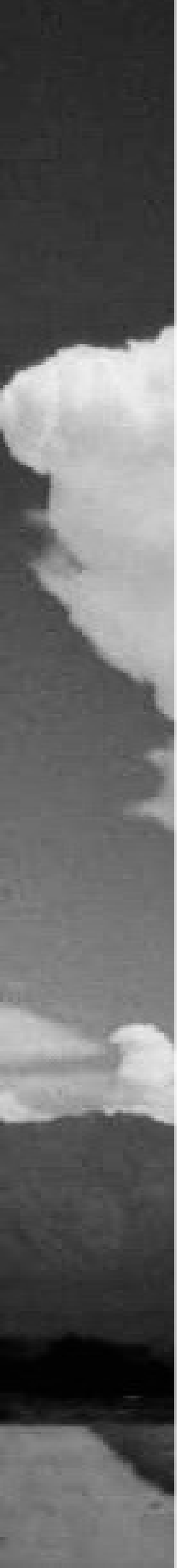

Aerosol Effects on Deep Convection

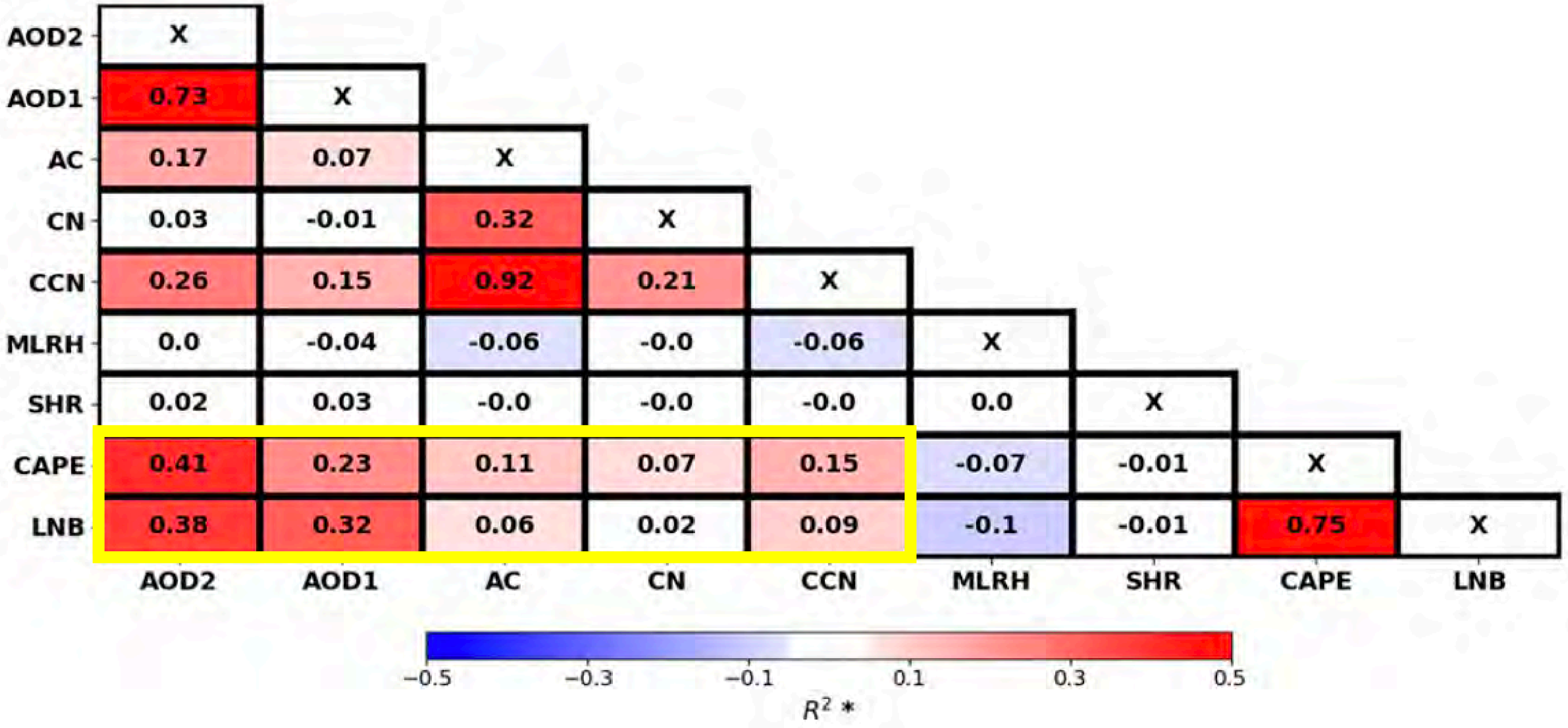

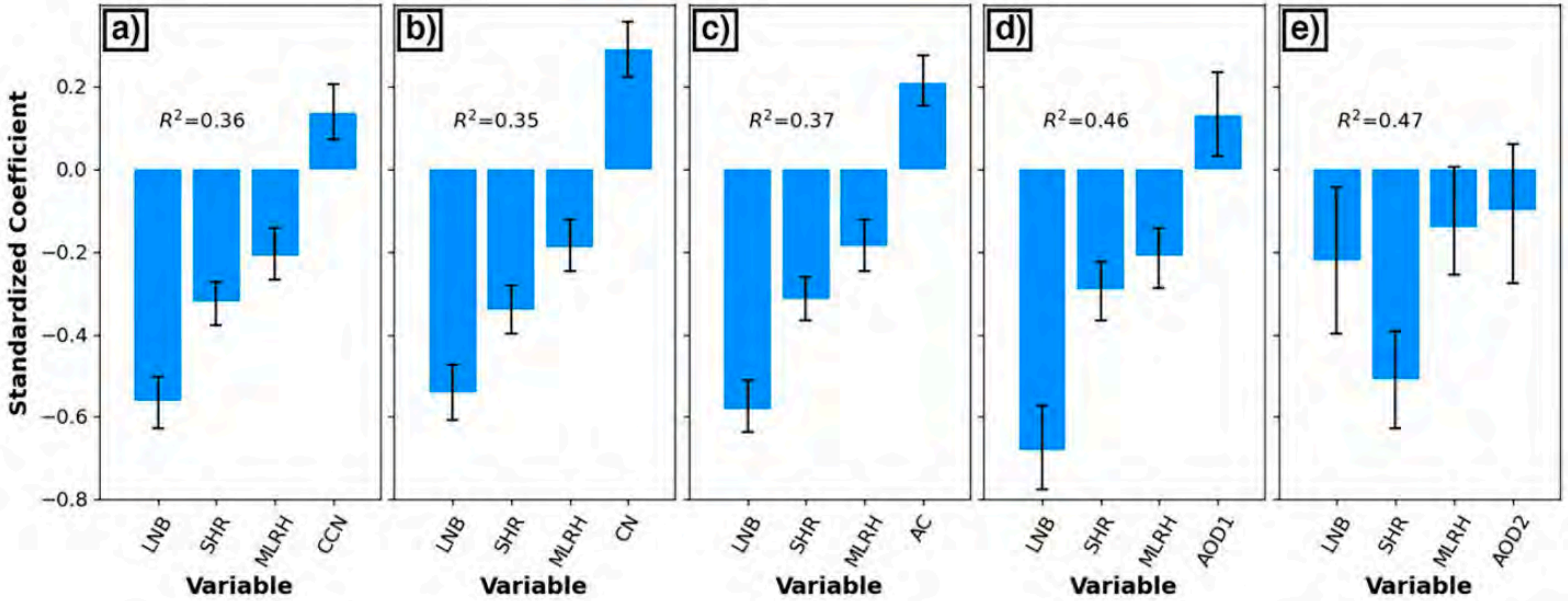

Veals, P., et al., 2022: Indications of a decrease in the depth of deep convective cores with increasing aerosol concentration during the CACTI campaign. *J. Atmos. Sci.*, 79, doi:10.1175/JAS-D-21-0119.1.

Processes Reflected in Detailed Hemispheric RHI Structures

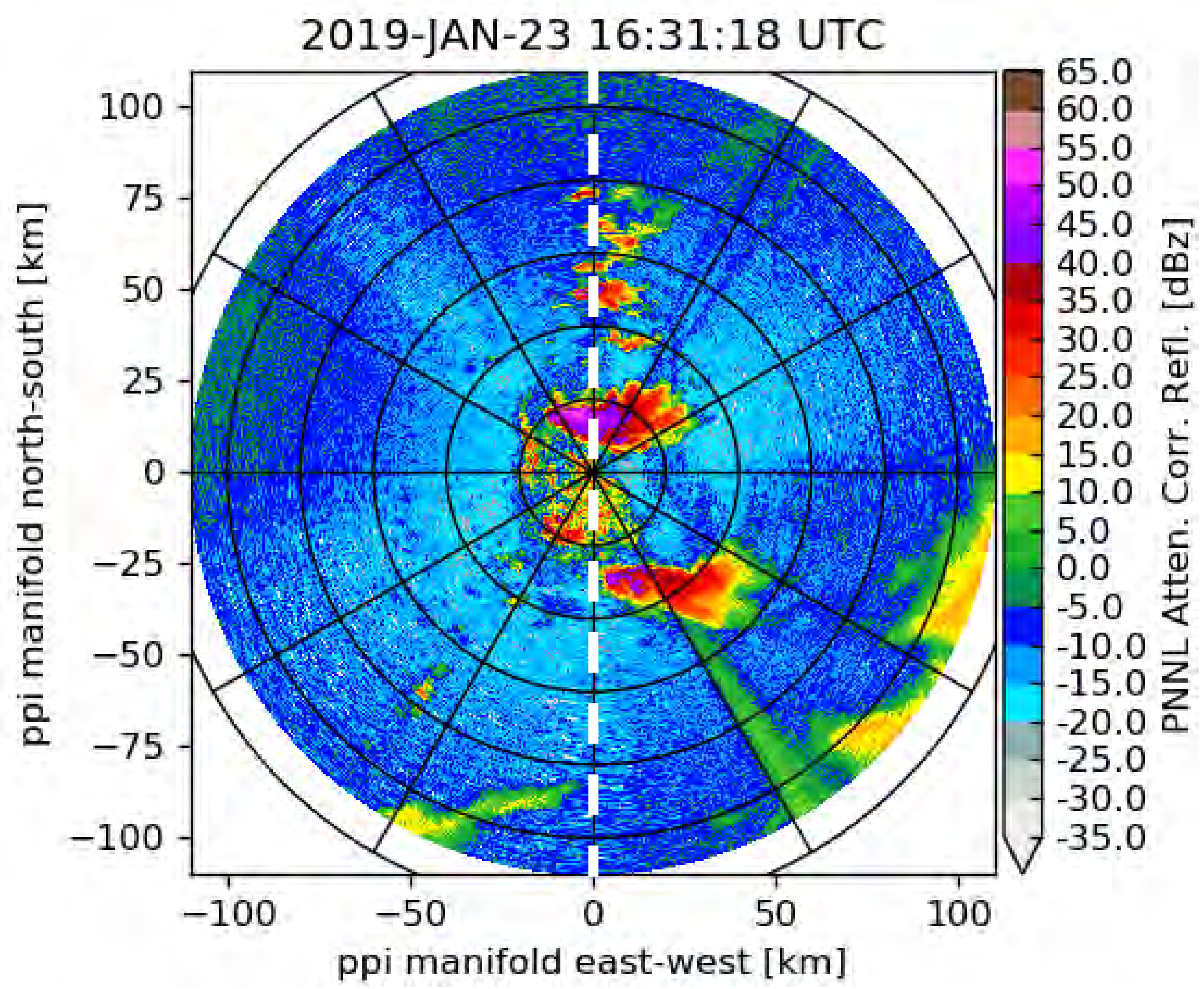

6 C-band HSRHIs (every 30° azimuthally) twice in a row every 15 minutes

6 X-band HSRHIs (every 30° azimuthally) 3 times in a row every 15 minutes

South-North HSRHI

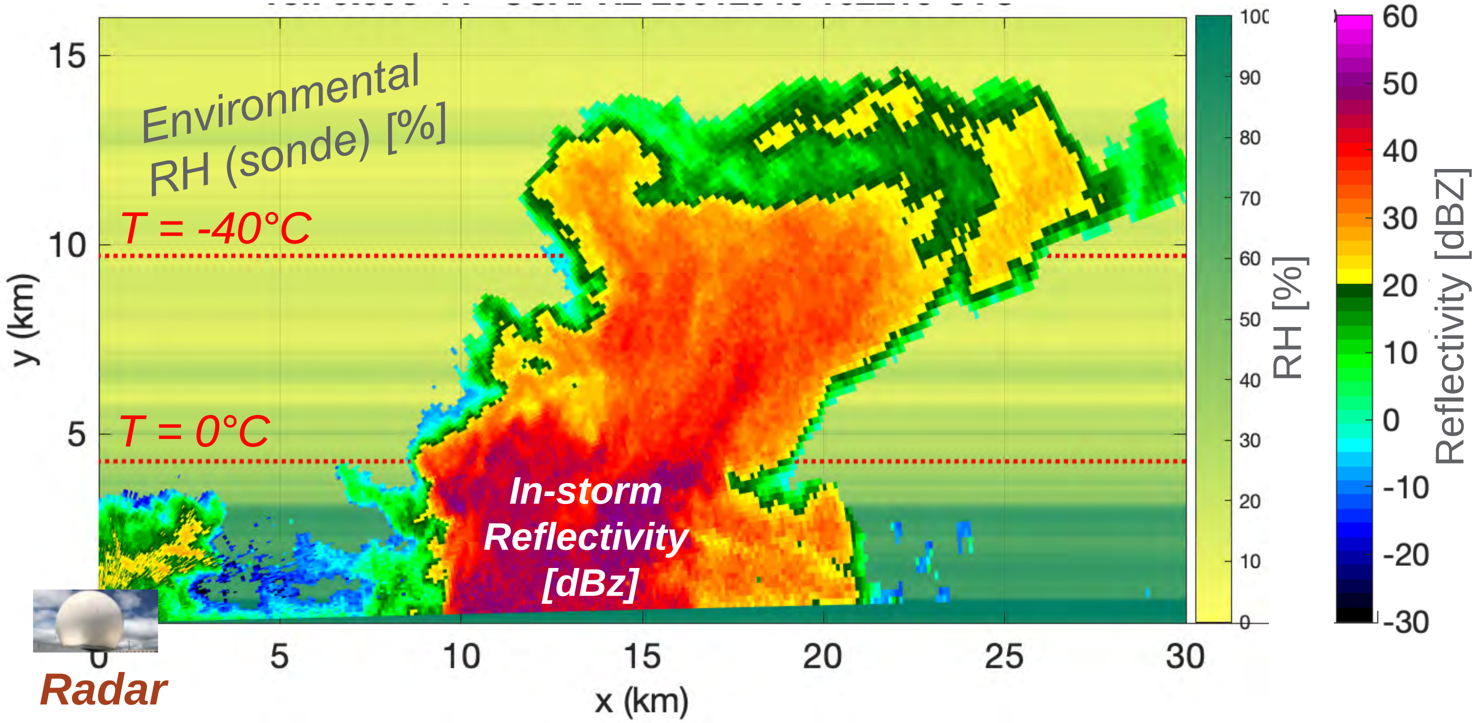

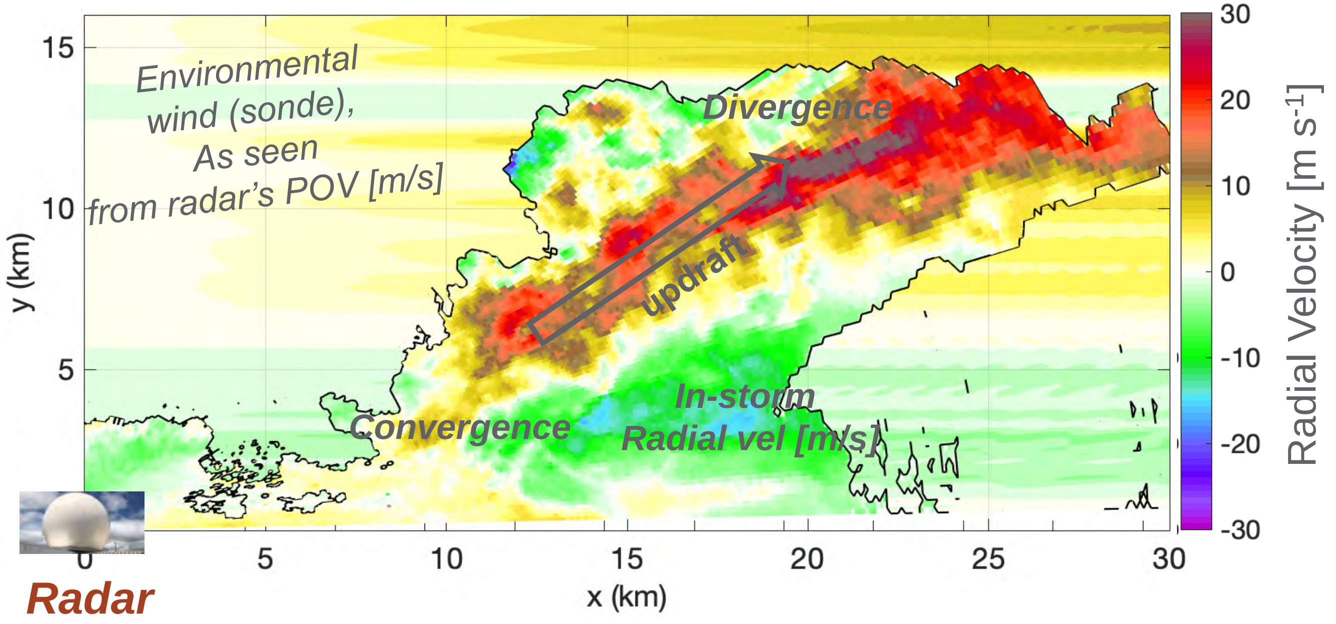

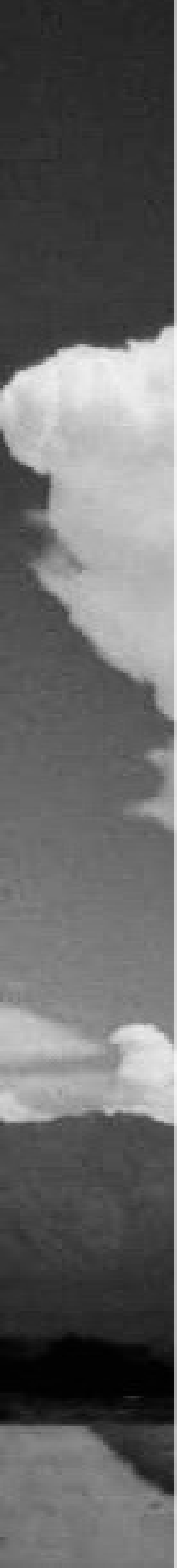

Pacific Northwest NATIONAL LABORATORY

Summary

- A tremendous number of CACTI cloud, aerosol, radiation, and atmospheric state datastreams and products (228) from the AMF1, CSAPR2, and G-1 are now available with most on the ARM archive: https://www.arm.gov/research/campaigns/amf2018cacti
- A lot of work has been done and continues to be done to build extensive cloud databases from which statistical studies and case studies can be performed focusing on a range of environmental controls on cloud and precipitation evolution as well as cloud and precipitation effects on the environment.
    - This has resulted in several studies targeting improved understanding and modeling of aerosol-cloud interactions, warm drizzle, deep convection initiation, and deep convective upscale growth.
- There is a tremendous number of further opportunities to explore many datasets that have yet to be analyzed and to build on the foundation laid by the development of many tools and products, particularly related to the life cycles of clouds, aerosols, and their interactions.
    - Please contact me with questions or to discuss ideas (adam.varble@pnnl.gov)

Pacific Northwest NATIONAL LABORATORY

Integrated Cloud, Land-Surface, & Aerosol System Study ICLASS

ARM

ASR Atmospheric System Research

NSF

Thank you

Research was supported by DOE ASR via PNNL’s ICLASS project and NSF. CACTI was supported by DOE ARM.

Contact: adam.varble@pnnl.gov

U.S. DEPARTMENT OF ENERGY BATTELLE

PNNL is operated by Battelle for the U.S. Department of Energy

Early stages of the 25 January 2019 storm that reached nearly 21 km ASL. Photo courtesy of Ramón Alberto Acuña (SMN).

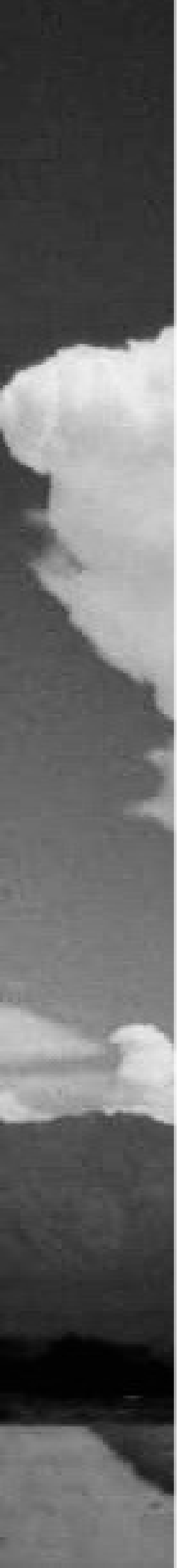

CACTI Observing Facilities (AMF1, G-1, CSAPR2)

Varble, A. C., et al., 2021: Utilizing a Storm-Generating Hotspot to Study Convective Cloud Transitions: The CACTI Experiment. *BAMS,* 102, E1597-E1620, doi:10.1175/BAMS-D-20-0030.1.

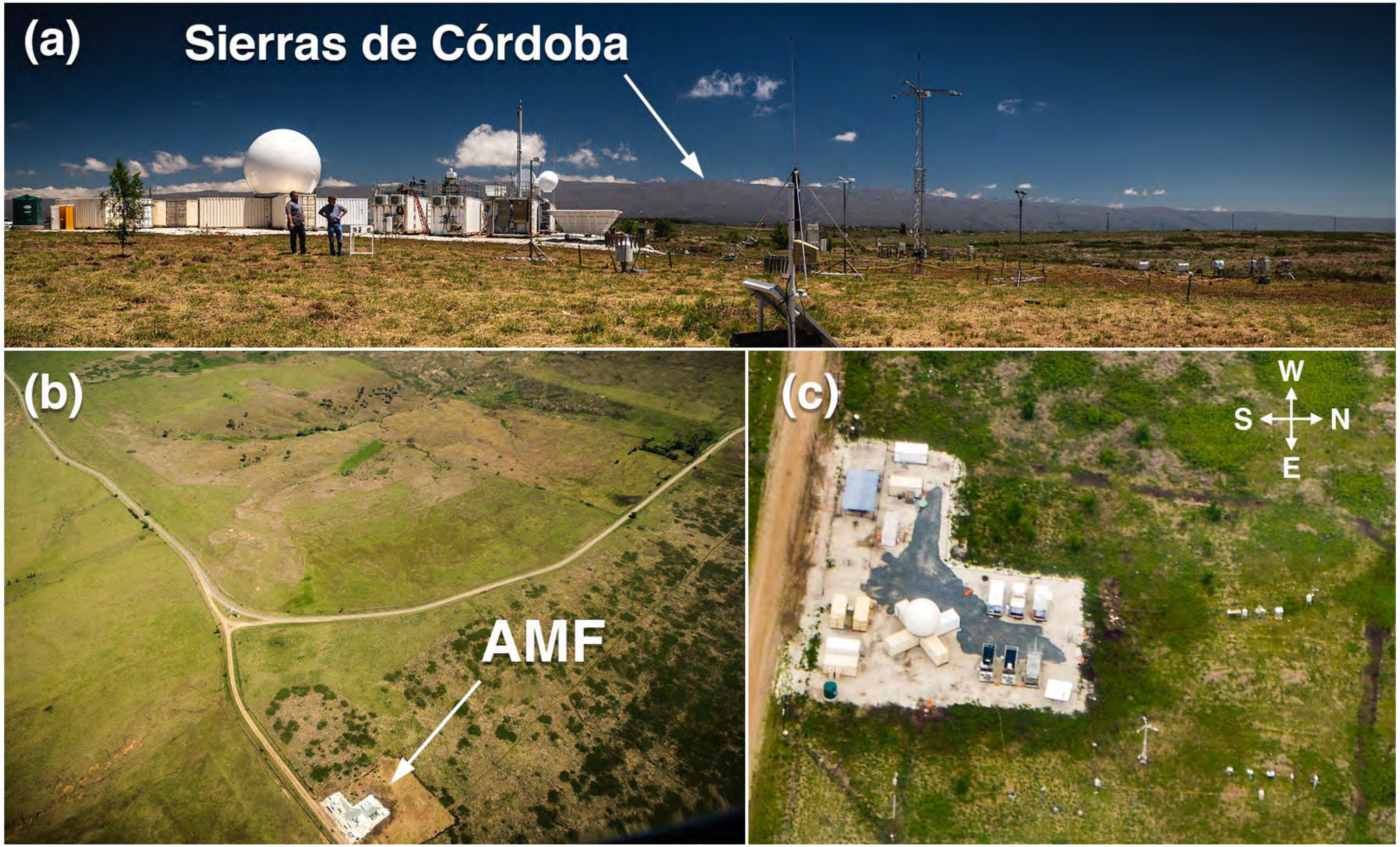

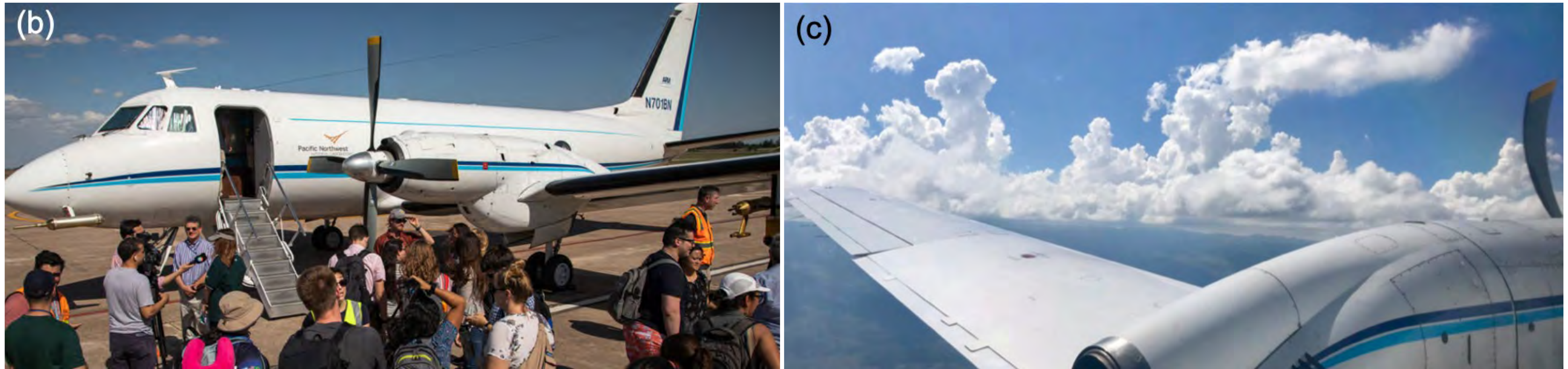

Surface-Based Measurements

Ground-Based Instruments and Measurements	
Cloud and Precipitation Measurements	**Instrumentation**
Cloud and Precipitation Kinematic and Microphysical Retrievals	C-band Scanning ARM Precipitation Radar, Ka/X-band Scanning ARM Cloud Radar, Ka-band ARM Zenith Radar, Radar Wind Profiler
Heights of Cloud Bases/Tops, Sizes, and Vertical Winds	ARM Cloud Digital Cameras
Cloud Base Height	Ceilometer, Micropulse Lidar, Doppler lidar
Cloud Scene/Fraction	Total Sky Imager
Raindrop Size Distribution, Fall Speeds, and Rainfall	Parsivel Laser and 2D Video Disdrometers, Tipping and Weighing Bucket Rain Gauges, Optical Rain Gauge, Present Weather Detector
Liquid Water Path	2-Channel, High-Frequency, and Profiling Microwave Radiometers
Atmospheric State Measurements	**Instrumentation**
Precipitable Water	2-Channel, High-Frequency, and Profiling Microwave Radiometers
Surface Pressure, Temperature, Humidity, Winds, and Visibility	Surface Meteorological Stations (4 sites)
Vertical Profiles of Temperature, Humidity, and Winds	Radiosondes (2 sites), Radar Wind Profiler, Profiling Microwave Radiometer, Atmospheric Emitted Radiation Interferometer
Boundary Layer Winds and Turbulence	Doppler Lidar, Sodar
Surface Condition Measurements	**Instrumentation**
Surface Heat Fluxes and Energy Balance, CO_2 Flux, Turbulence, and Soil Temperature and Moisture	Eddy Correlation Flux Measurement System, Surface Energy Balance System
Aerosol and Trace Gas Measurements	**Instrumentation**
Aerosol Backscatter Profile	Micropulse Lidar, Doppler Lidar, Ceilometer
Aerosol Optical Depth	Cimel Sun Photometer, Multifilter Rotating Shadowband Radiometer
Cloud Condensation Nuclei (CCN) Concentration	Dual Column CCN counter
Condensation Nuclei (CN) Concentration	Fine and Ultrafine Condensation Particle Counters
Ice Nucleating Particle (INP) Concentration	Filters processed in Colorado State University Ice Spectrometer
Aerosol Chemical Composition	Aerosol Chemistry Speciation Monitor, Single Particle Soot Photometer
Aerosol Scattering and Growth	Ambient and Variable Humidity Nephelometers
Aerosol Absorption	Particle Soot Absorption Photometer
Aerosol Size Distribution	Ultra-High Sensitivity Aerosol Spectrometer, Scanning Mobility Particle Sizer, Aerodynamic Particle Sizer
Trace Gas Concentrations	O_3, CO, N_2O, H_2O Monitoring Systems
Radiation Measurements	**Instrumentation**
Radiative Fluxes	Broadband Direct, Diffuse, and Total Downwelling Downwelling Radiation Radiometers, Broadband Upwelling Radiation Radiometers, Ground and Sky Infrared Thermometers, AERI, Narrow Field of View 2-Channel Zenith Radiometer, Hemispheric and Zenith Shortwave Array Spectroradiometers, Multifilter Radiometer, Multifilter Rotating Shadowband Radiometer, Cimel Sun Photometer, Surface Energy Balance System, 2-Channel, High-Frequency, and Profiling Microwave Radiometers

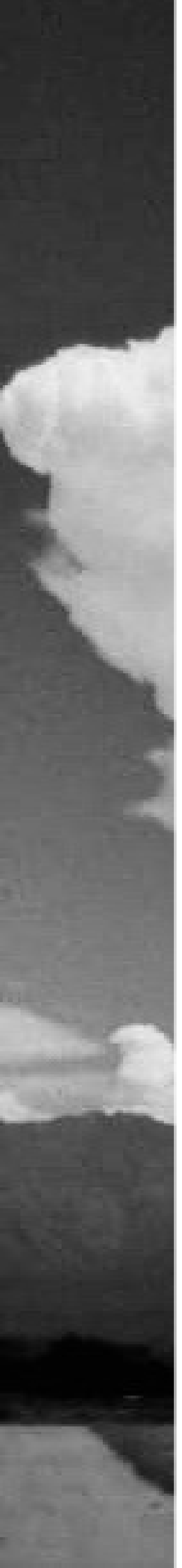

G-1 Flights

Flight	Time (UTC)	Situation
1	13:02–17:01 Nov 4	Deepening orographic cumulus
2	13:09–17:05 Nov 6	Deep convection initiation; likely warm rain
3	12:10–16:10 Nov 10	Deepening orographic cumulus prior to deep convection initiation
4	16:48–20:00 Nov 12	Elevated deep convection, low-level stable cumulus and stratus
5	14:00–18:00 Nov 14	Clear air aerosol sampling
6	13:05–16:00 Nov 15	Clear air aerosol sampling
7	14:05–18:00 Nov 16	Boundary layer and elevated orographic cumulus
8	12:18–16:30 Nov 17	Congestus along cold front; wind-blown dust; mountain wave
9	15:10–19:06 Nov 20	Orographic cumulus; strong inversion
10	18:22–20:27 Nov 21	Orographic congestus and deep convection initiation
11	14:31–18:11 Nov 22	Stratiform anvil sampling along radar north-south scans
12	16:17–20:25 Nov 24	Orographic cumulus line; strong inversion
13	15:51–19:07 Nov 25	Orographic cumulus line; potential decoupling from boundary layer
14	15:08–18:50 Nov 28	Orographic congestus and deep convection initiation
15	14:16–16:32 Nov 29	Orographic congestus and deep convection initiation
16	16:20–18:47 Dec 1	Elevated drizzle in orographic stratocumulus; possible ice
17	12:06–16:11 Dec 2	Elevated drizzle in widespread clouds; possible ice; gravity waves in cloud layer
18	16:03–20:09 Dec 3	Boundary layer coupled orographic cumulus; strong inversion
19	17:51–19:45 Dec 4	Deepening congestus and some deep convection initiation
20	12:04–15:28 Dec 5	Mid-level clouds; congestus and some deep convection initiation
21	15:01–19:01 Dec 7	Orographic cumulus; strengthening inversion
22	16:06–19:30 Dec 8	Clear air aerosol sampling

G-1 Measurements

Aircraft Instruments and Measurements	
Positioning Measurements	**Instrumentation**
Position/Aircraft parameters	Aircraft Integrated Meteorological Measurement System-20, Global Positioning System (GPS) DSM 232, C-MIGITS III (Miniature Integrated GPS/INS Tactical System), VectorNav-200 GPS/INS, Video Camera P1344
Atmospheric State Measurements	**Instrumentation**
Pressure, Temperature, Humidity, Winds, Turbulence	Gust Probe, Rosemount 1221F2, Aircraft Integrated Meteorological Measurement System-20, Tunable Diode Laser Hygrometer, GE-1011B Chilled Mirror Hygrometer, Licor LI-840A, Rosemount 1201F1 and E102AL
Aerosol and Trace Gas Measurements	**Instrumentation**
Aerosol Sampling	Aerosol Isokinetic Inlet, Counterflow Virtual Impactor (CVI) Inlet
Aerosol Optical Properties	Single Particle Soot Photometer, 3-wavelength Integrating Nephelometer, 3-wavelength Particle Soot Absorption Photometer, 3-wavelength Single Channel Tricolor Absorption Photometer
Aerosol Chemical Composition	Single Particle Mass Spectrometer (miniSPLAT)
Aerosol Size Distribution	Ultra-High Sensitivity Aerosol Spectrometer, Scanning Mobility Particle Sizer, Passive Cavity Aerosol Spectrometer, Optical Particle Counter Model CI-3100, Dual Polarized Cloud and Aerosol Spectrometer (CAS)
CN Concentration	Fine (1 on Isokinetic Inlet and 1 on CVI Inlet) and Ultrafine CPCs
CCN Concentration	Dual-column CCN counter
INP Concentration	Filter Collections for Colorado State University Ice Spectrometer
Trace Gas Concentrations	N_2O, CO, O_3, and SO_2 Monitoring Systems
Cloud and Precipitation Measurements	**Instrumentation**
Hydrometeor Size Distribution	Fast Cloud Droplet Probe, 2-Dimensional Stereo Probe, High Volume Precipitation Sampler 3, Cloud and Aerosol Precipitation Spectrometer (CAPS; includes Cloud Imaging Probe, CAS, and Hotwire Sensor)
Hydrometeor Imagery	Cloud Particle Imager
Liquid Water Content	Particle Volume Monitor 100-A, Multi-Element Water Content Meter, Hotwire Sensor from CAPS

RELAMPAGO Hydrologic Sites Downstream of CACTI Domain

Nesbitt S. W., et al., 2021, *BAMS,* doi:10.1175/BAMS-D-20-0029.1.

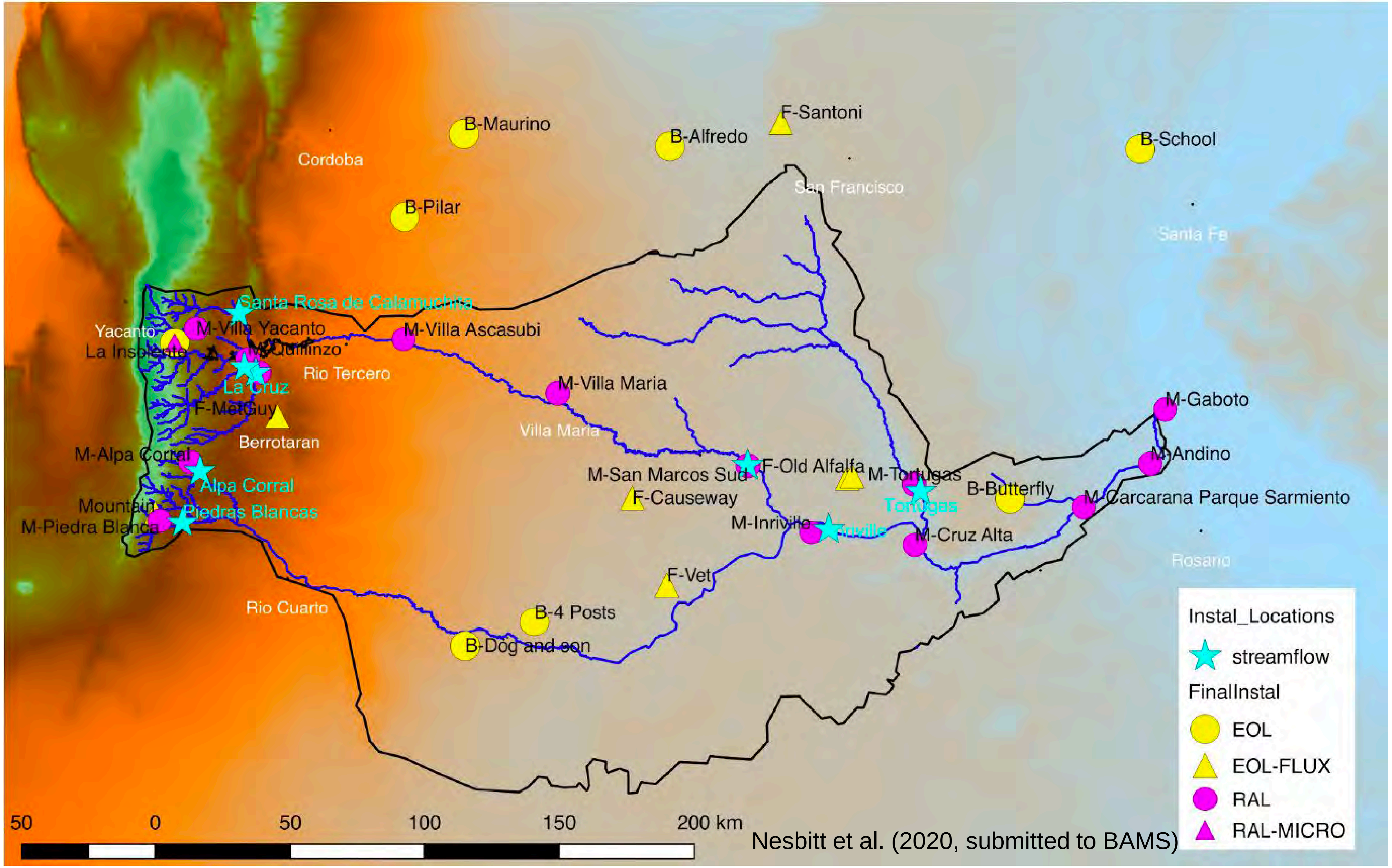

Nesbitt et al. (2020, submitted to BAMS)

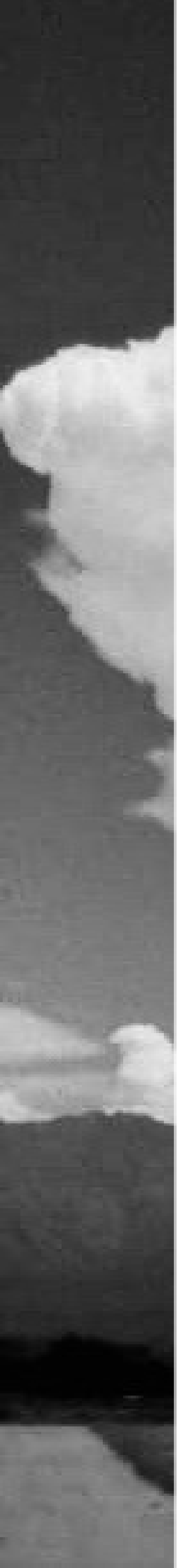

Pacific Northwest
NATIONAL LABORATORY

Environmental Conditions During CACTI

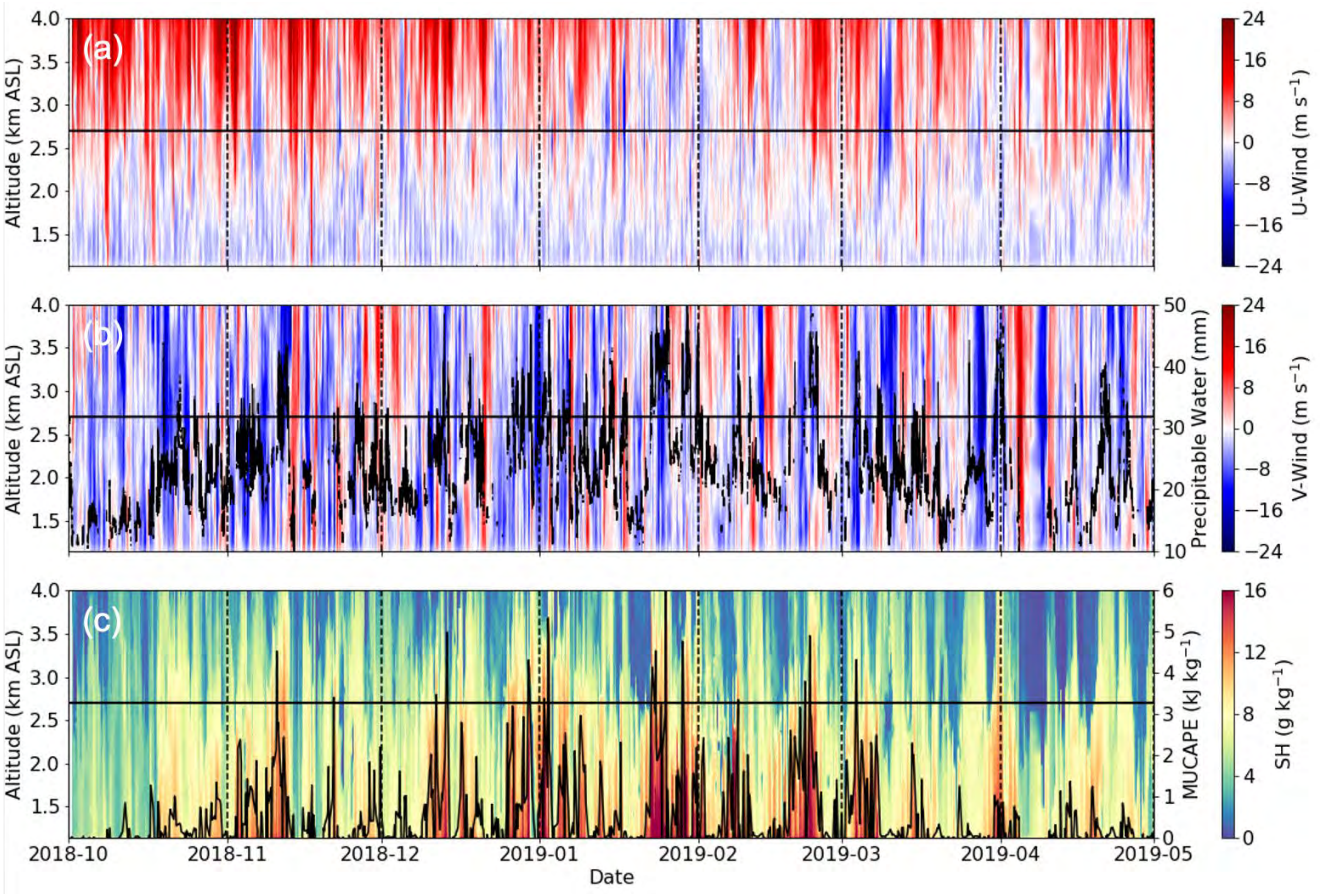

Varble, A. C., et al., 2021, *BAMS,* doi:10.1175/BAMS-D-20-0030.1.

Convective Environmental Condition Distributions and Diurnal Cycles

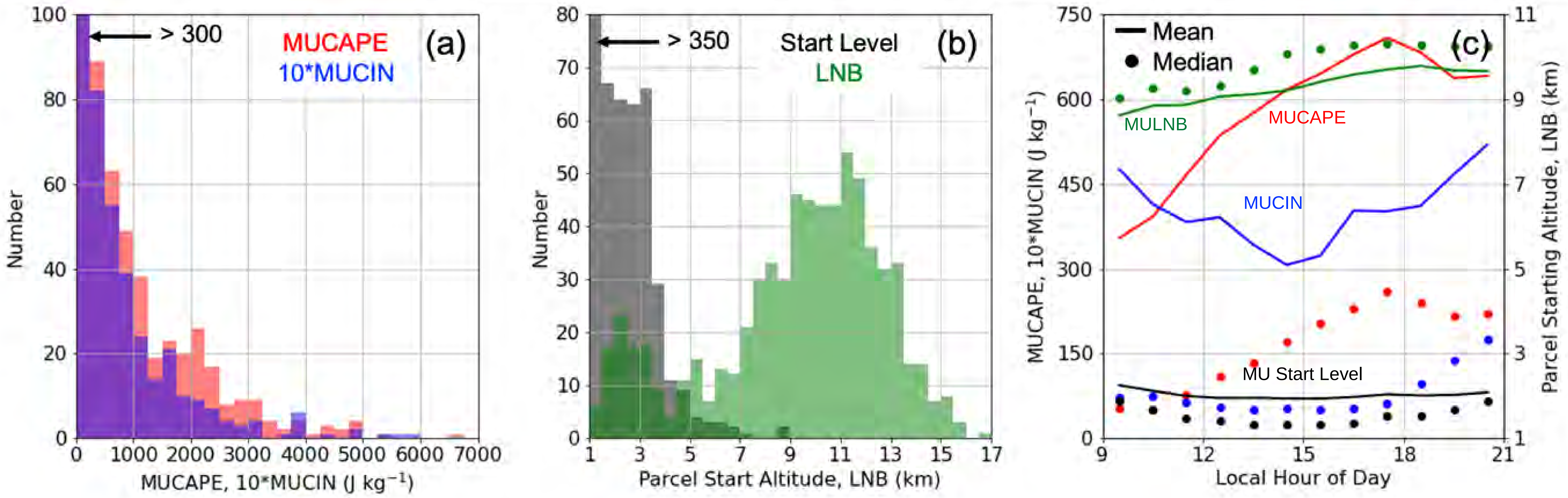

Varble, A. C., et al., 2021, *BAMS,* doi:10.1175/BAMS-D-20-0030.1.

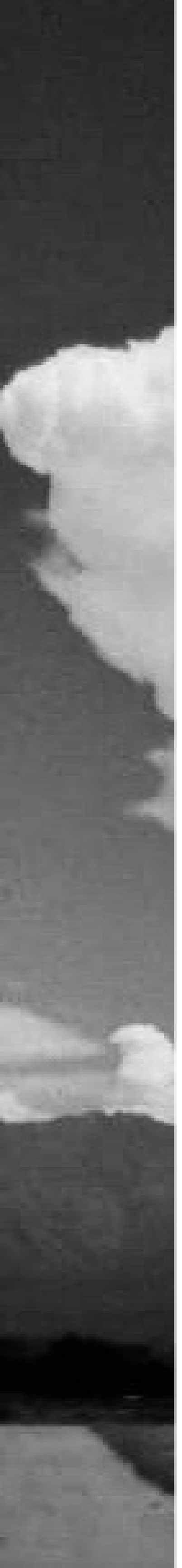

Stratocumulus Drizzle Case

Wind shear layer lifts with cloud top during drizzle onset, and the cloud remains coupled with the boundary layer. CCN concentrations do not decrease during this time, indicating drizzle onset is controlled by the lifting mechanism.

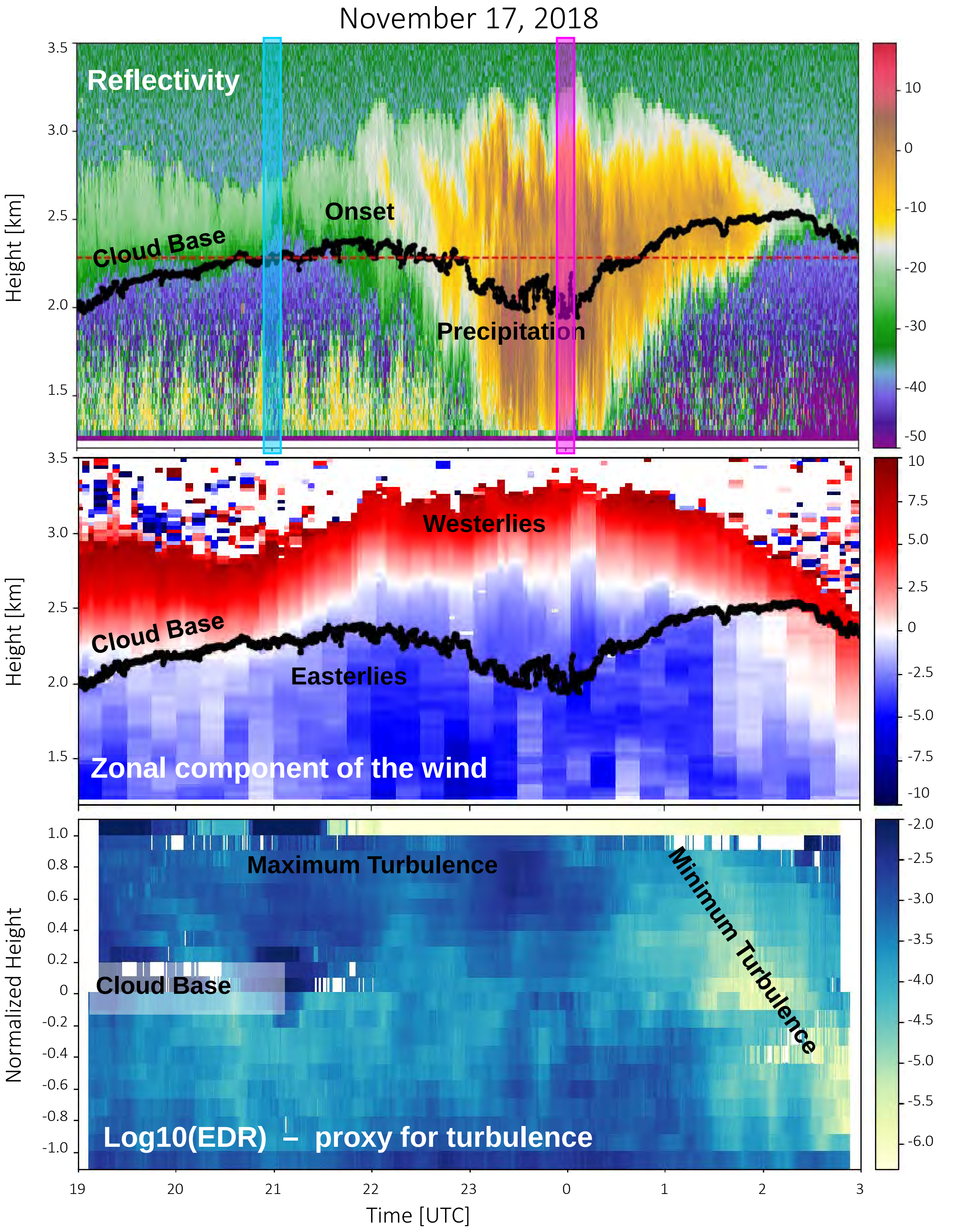

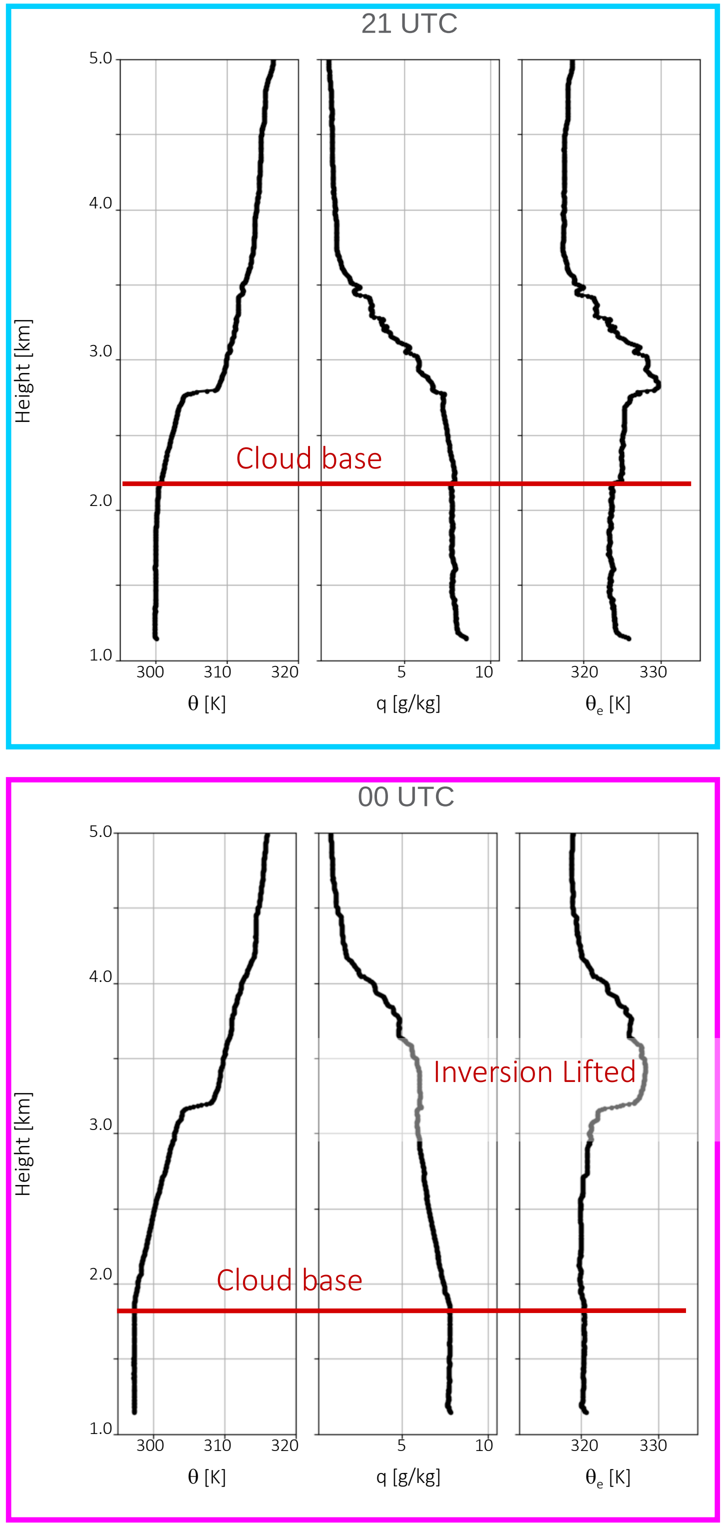

Stratocumulus Drizzle Case

Wind shear layer remains constant and cloud depth does not increase during drizzle onset. The cloud decouples from the boundary layer during drizzle onset, indicating a potentially key role for lower CCN concentrations aloft.

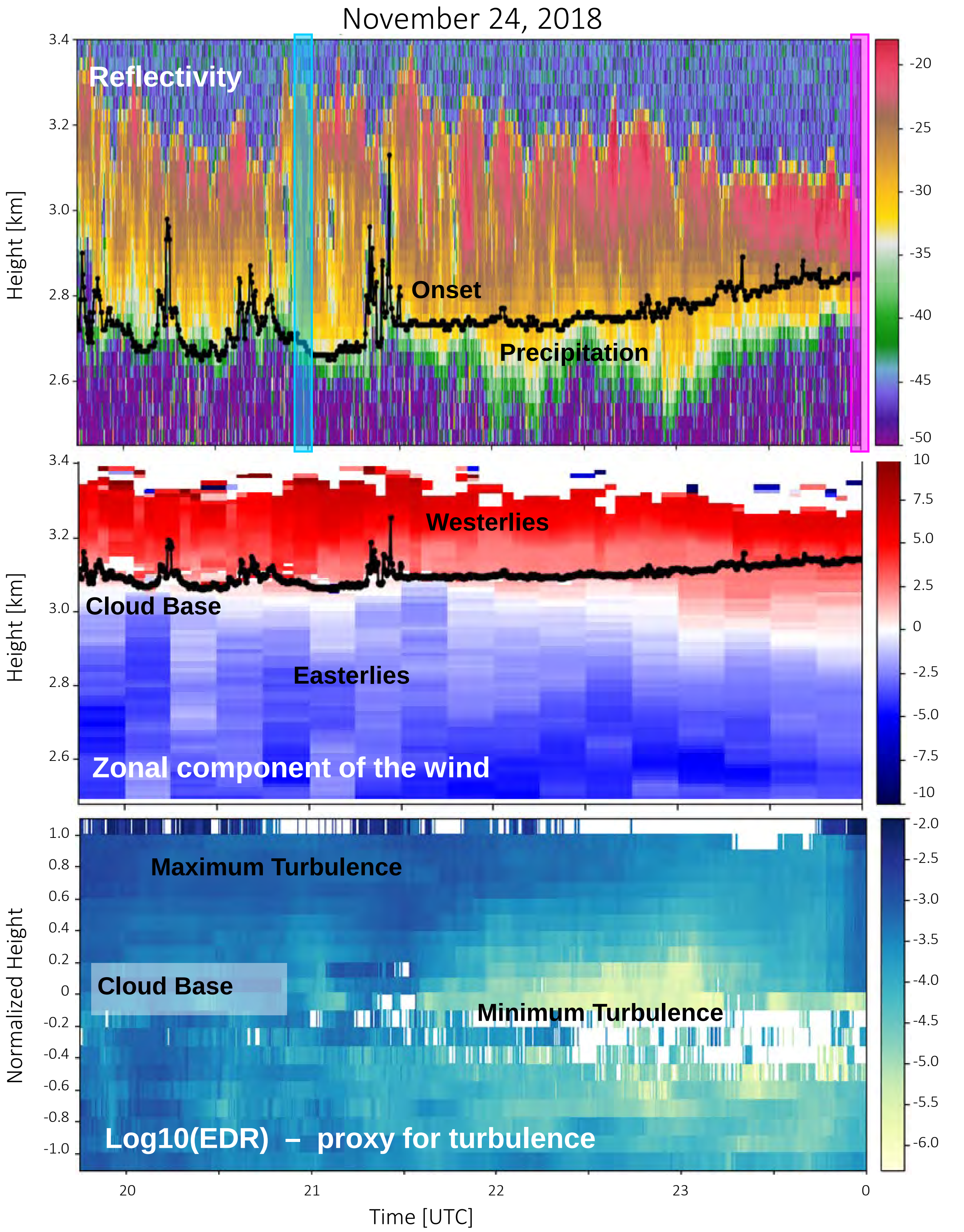

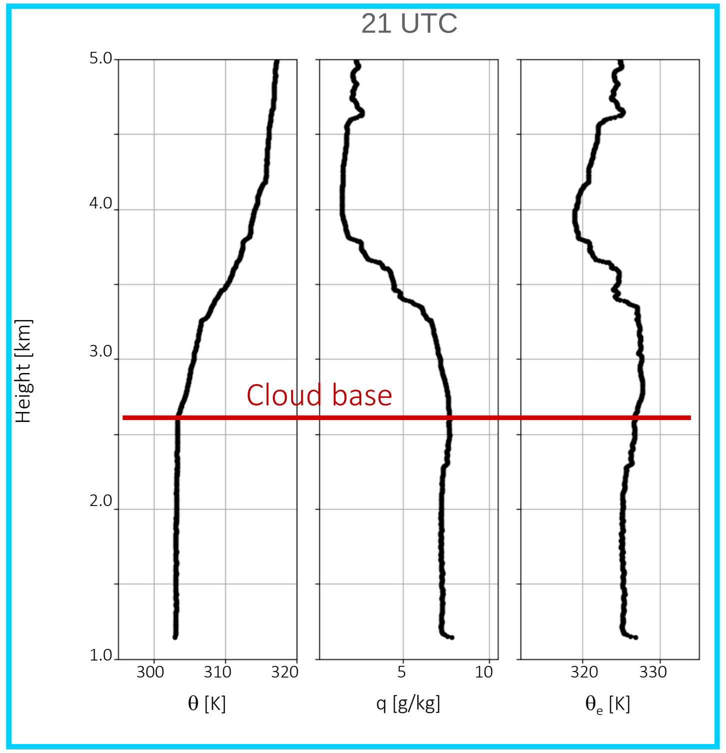

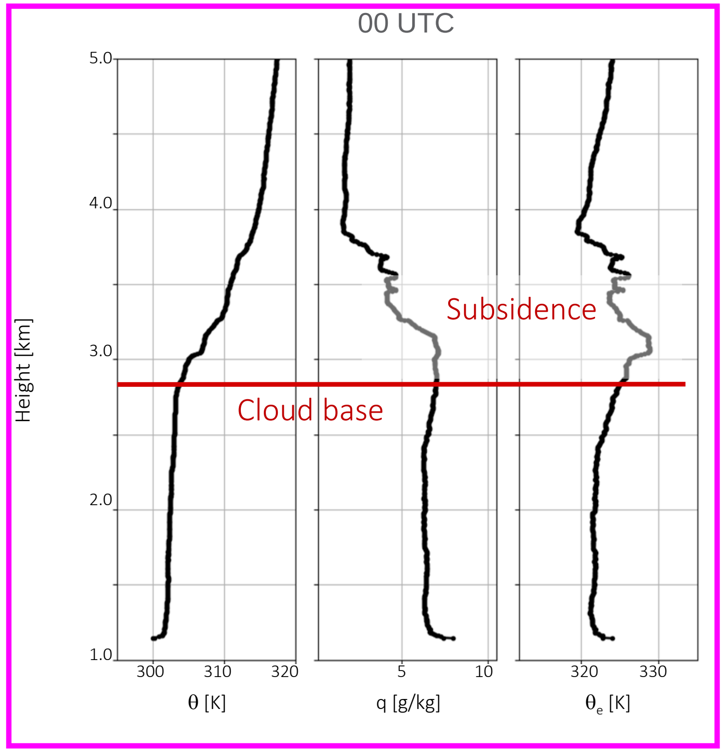

Success vs. Failure Thermodynamic Variability

Dense sounding networks during RELAMPAGO-mobile missions show considerable low level thermodynamic, particularly moisture, variability that greatly impacts convective inhibition and the level of free convection.

Upper PBL to lower troposphere moisture changes rapidly in time prior to deep convection initiation.

Just before deep convection initiation, CAPE and CIN are similar for both success and fail cases.

Marquis J. N., et al., 2021, *Mon. Wea. Rev.*, doi:10.1175/MWR-D-20-0391.1.

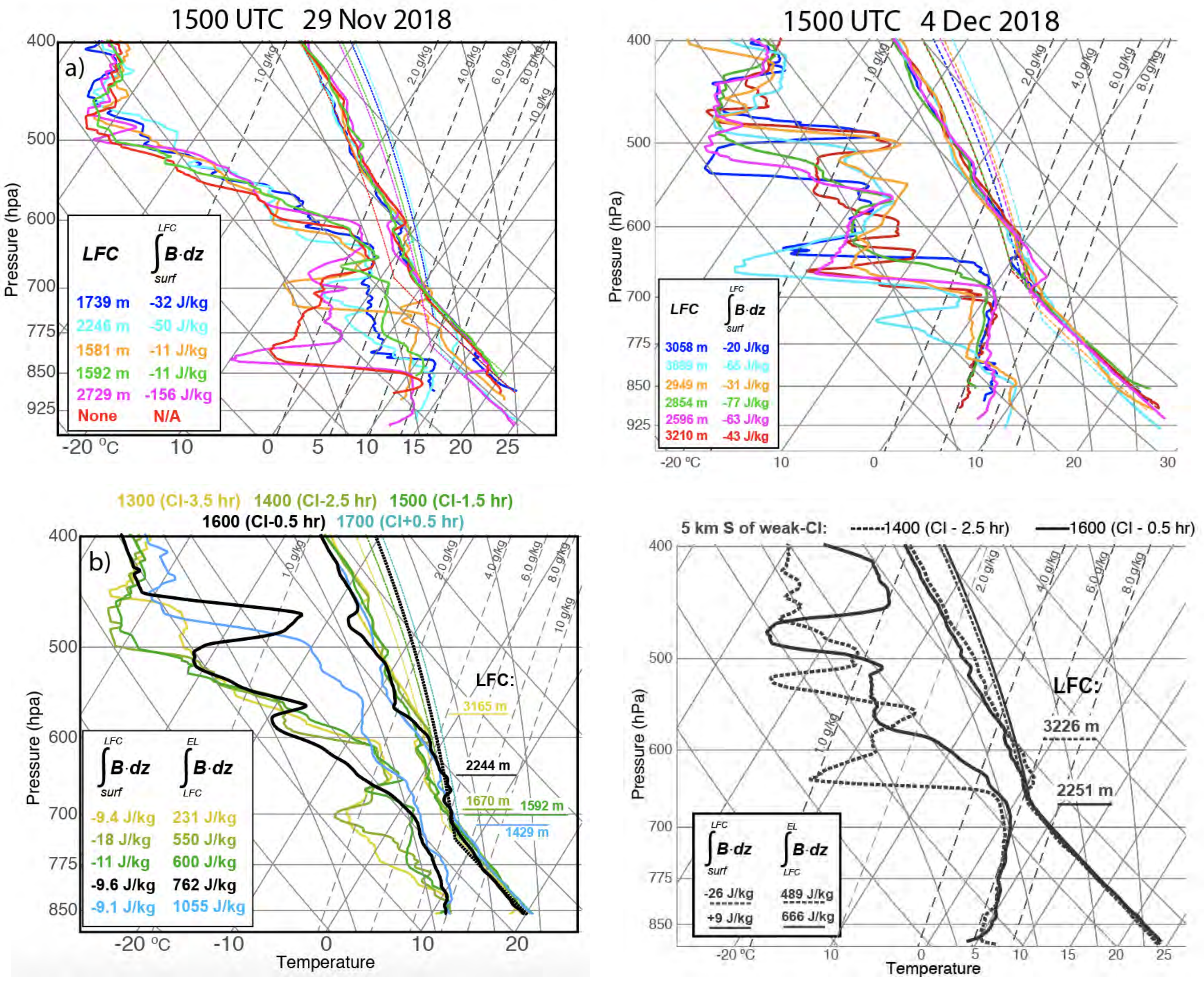

Success vs. Failure Circulations

Dual-Doppler analyses and soundings highlight significantly different low level kinematic conditions on 29 Nov and 4 Dec.

29 Nov has a much shallower easterly upslope flow and regions of enhanced meridional-mean convergence indicating more robust mesoscale convergence that is also suggested by more widespread orographic congestus coverage.

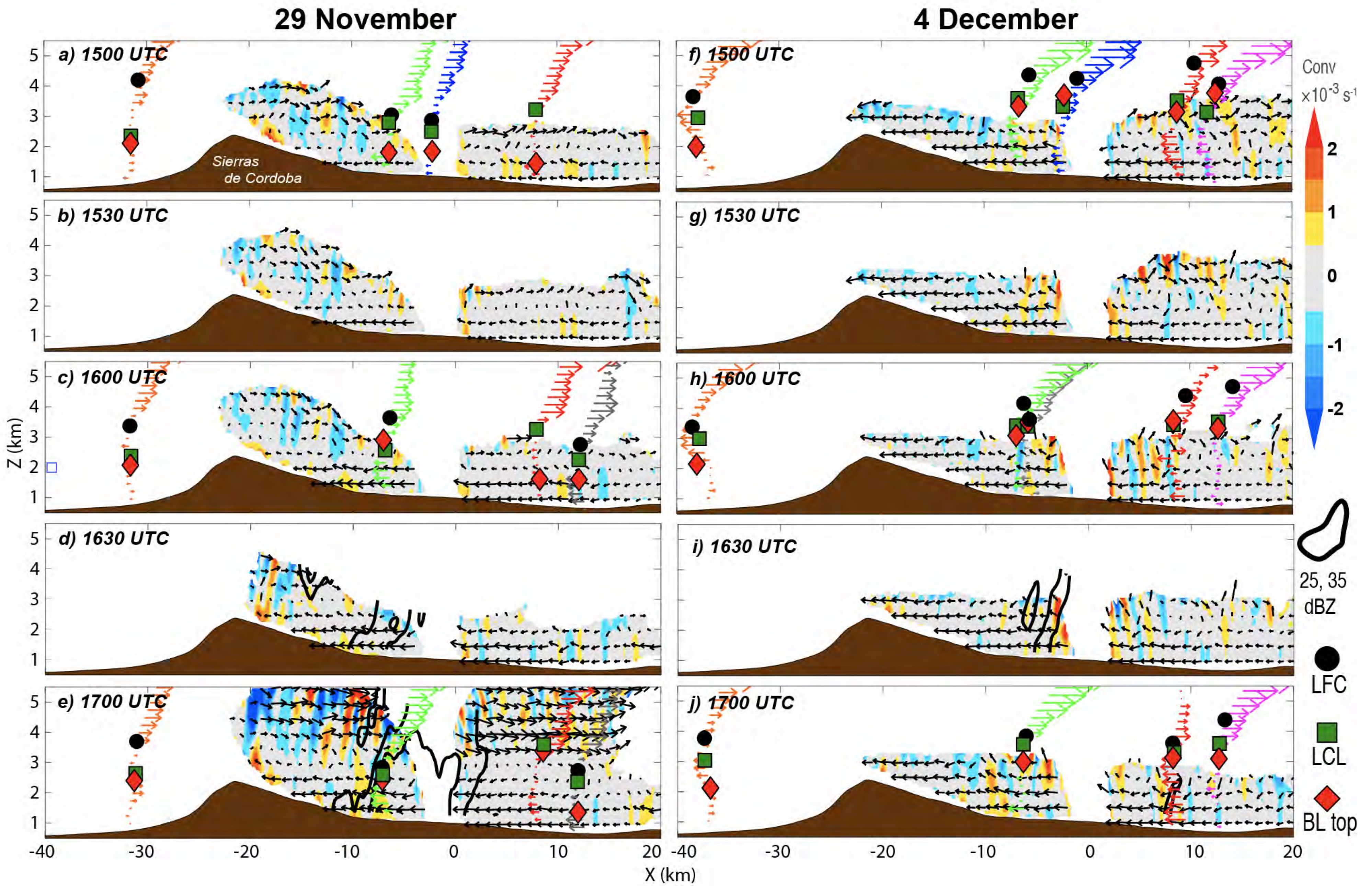

Marquis J. N., et al., 2021, *Mon. Wea. Rev.*, doi:10.1175/MWR-D-20-0391.1.

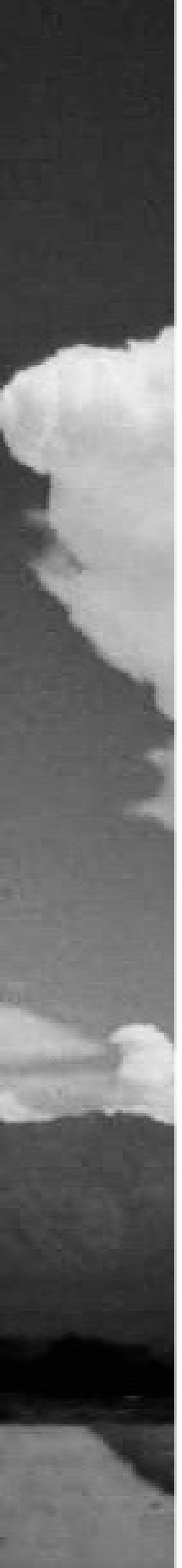

Success vs. Failure Updrafts

Maximum updraft widths on 29 Nov approach 5 km with some being coherent for more than 15-30 minutes and correlated with the most robust low level reflectivity areas downshear.

Maximum updraft widths on 4 Dec remain < 3 km and are similar to the scale of boundary layer thermals.

These results indicate that mesoscale convergence may promote wider updrafts that can overcome buoyancy dilution by entrainment aloft.

Marquis J. N., et al., 2021, *Mon. Wea. Rev.*, doi:10.1175/MWR-D-20-0391.1.

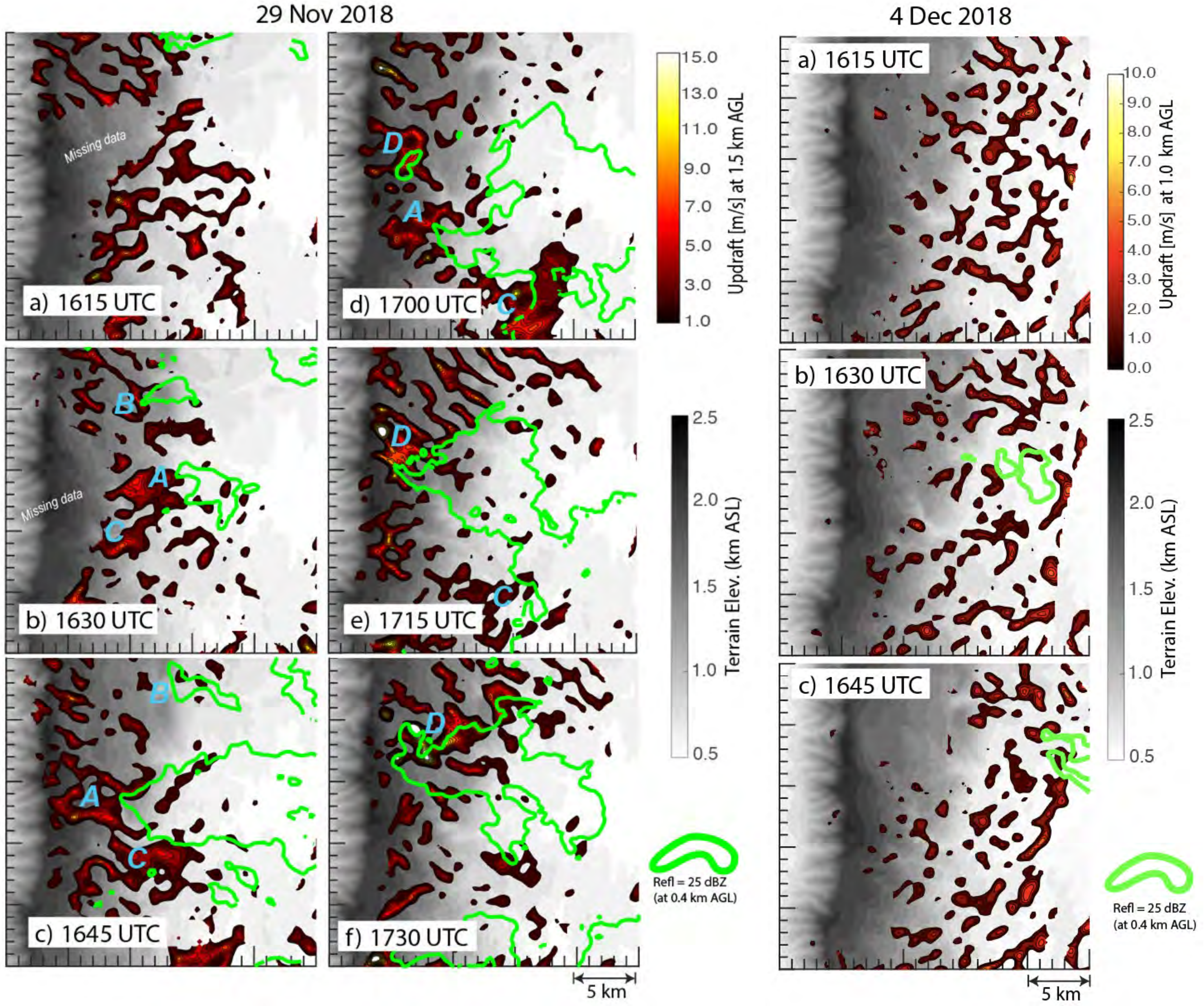

Marquis et al. (2021)

Tracked Cell Upscale Growth

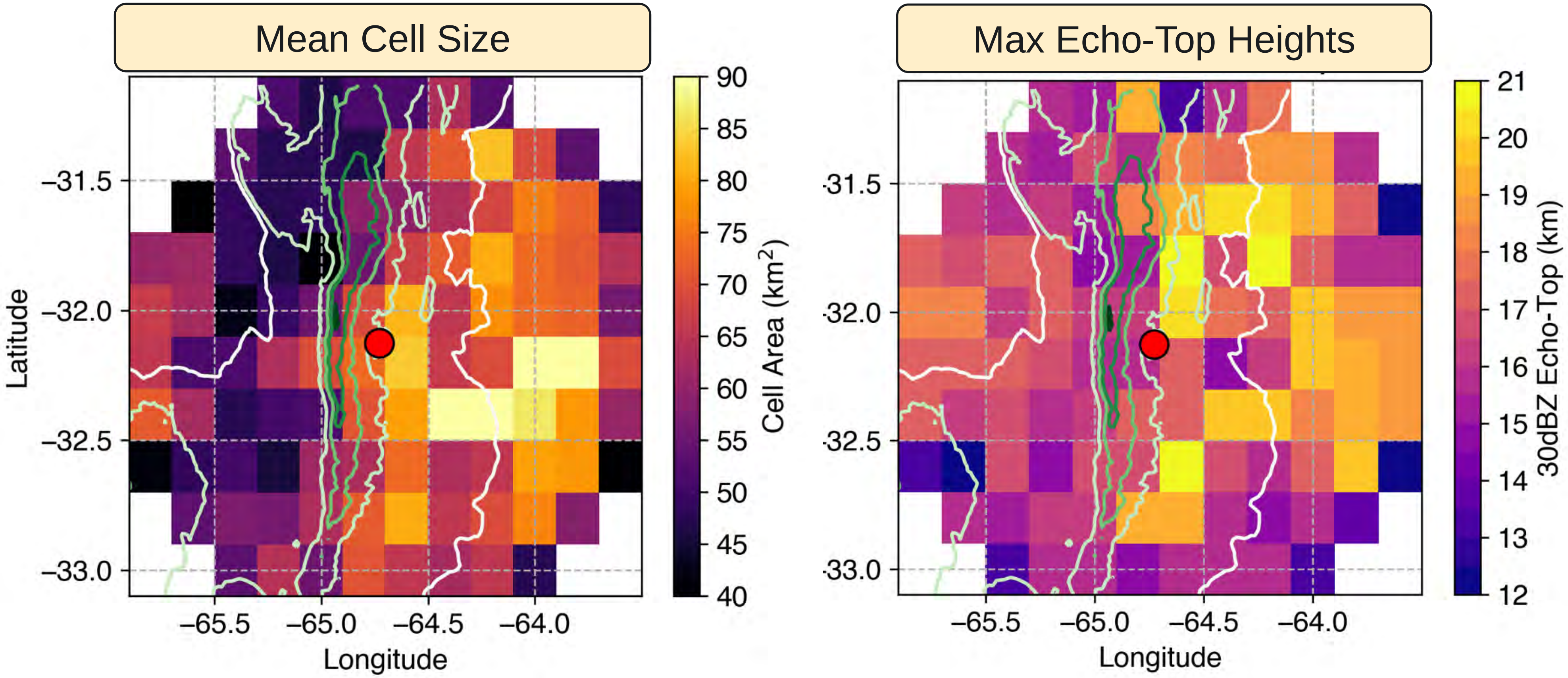

Feng, Z, et al., 2022, *MWR*, doi:10.1175/MWR-D-21-0237.1.

Increasing cell size east of the terrain is correlated with increasing radar echo top heights, and these increases occur immediately east of the highest terrain.

The example below shows how some cells grow upscale in area and/or depth over hours while others do not, which we are using to study determinants of these differences.

WRF narrow cell reflectivity correlations with environment are very similar to observed

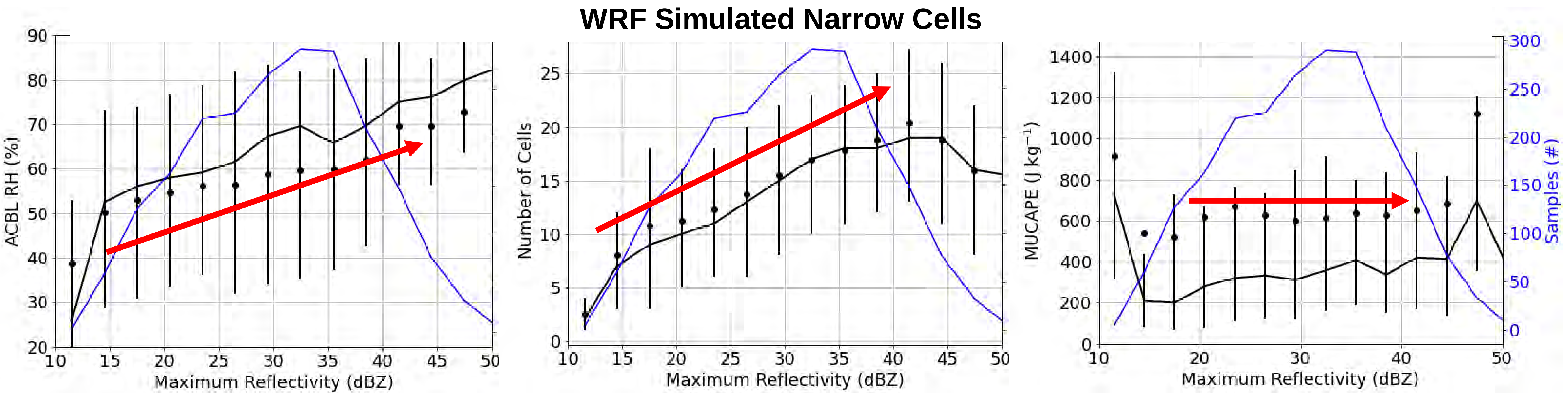

WRF reproduces observed correlations and can be mined for further information

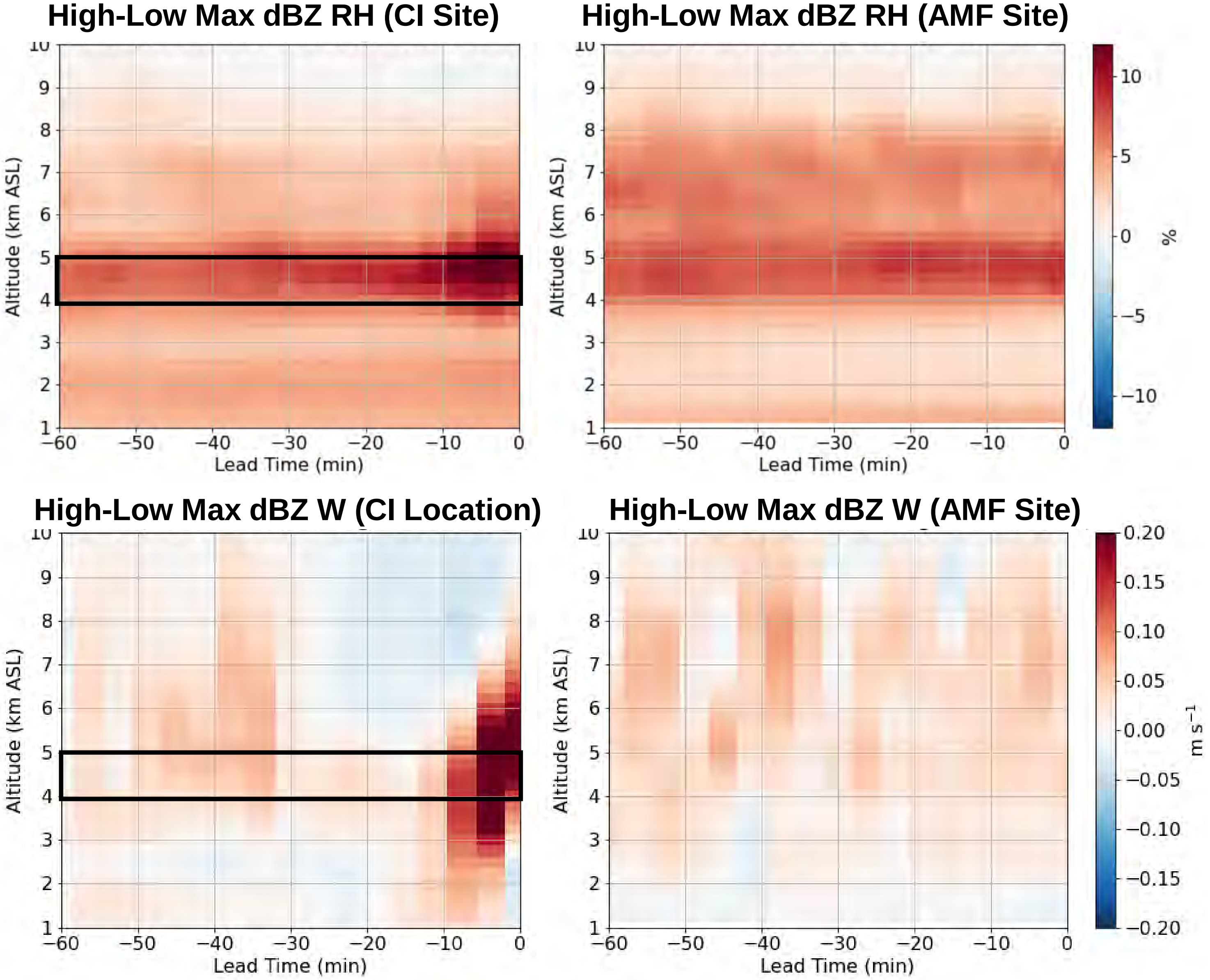

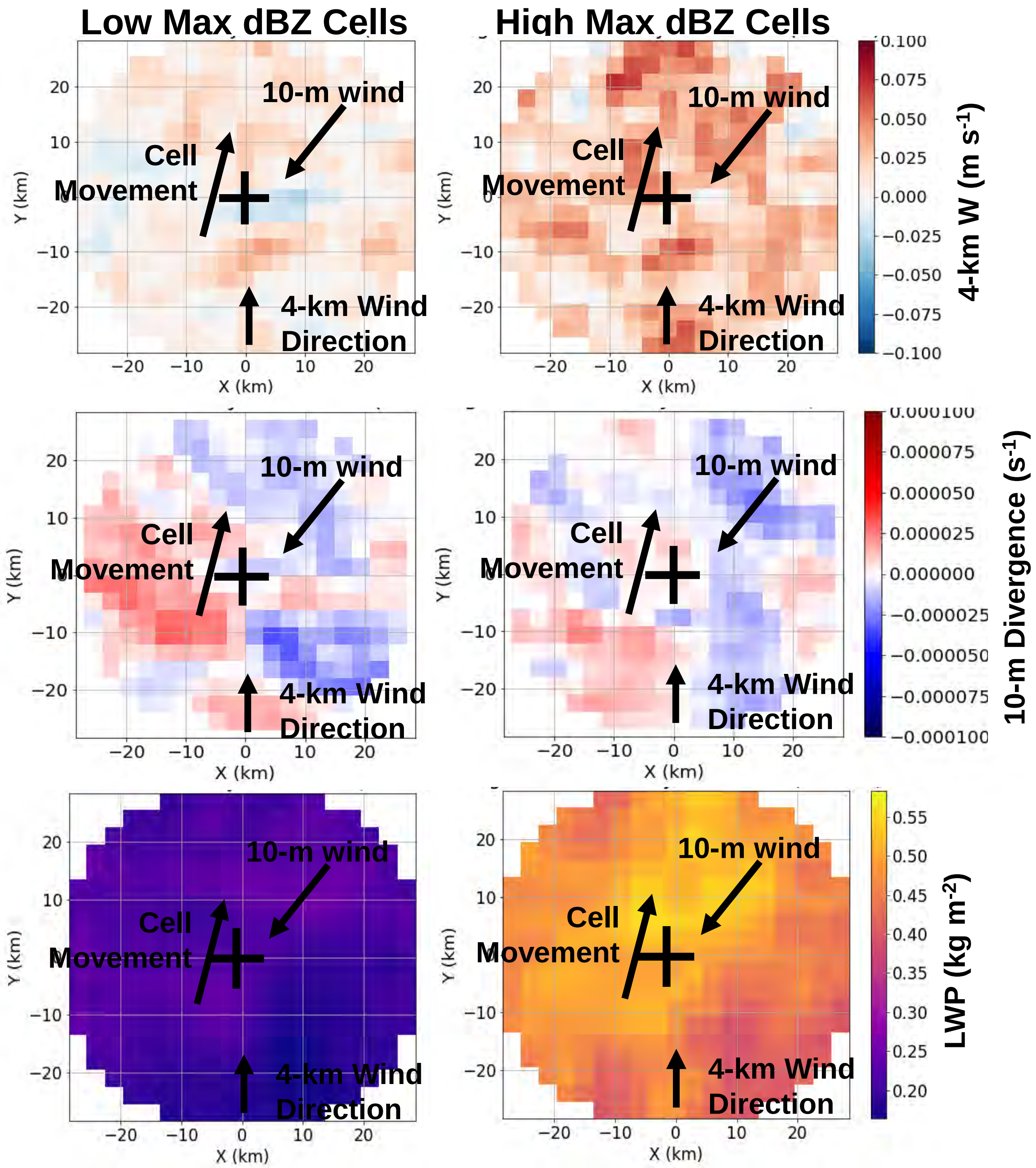

WRF time-height changes at CI locations for low vs. high max dBZ cells

RH (and theta-e) increase between 3 and 5 km leading up to CI associated with both cooling and moistening

High max reflectivity cells have the same patterns in time as low max reflectivity cells but accentuated

High max reflectivity cells have free tropospheric ascent 30-60 min prior to CI whereas low reflectivity cells have slight subsidence

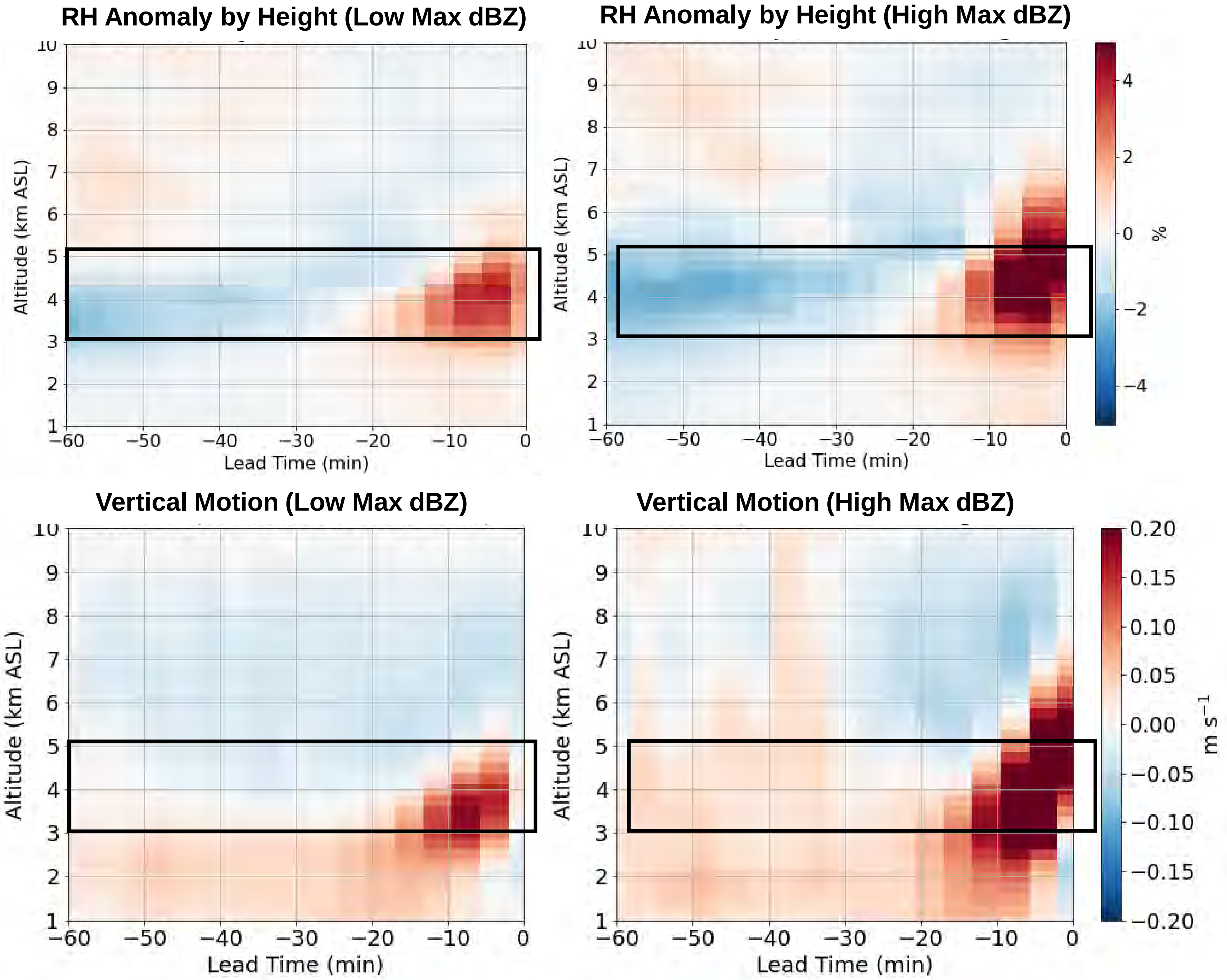

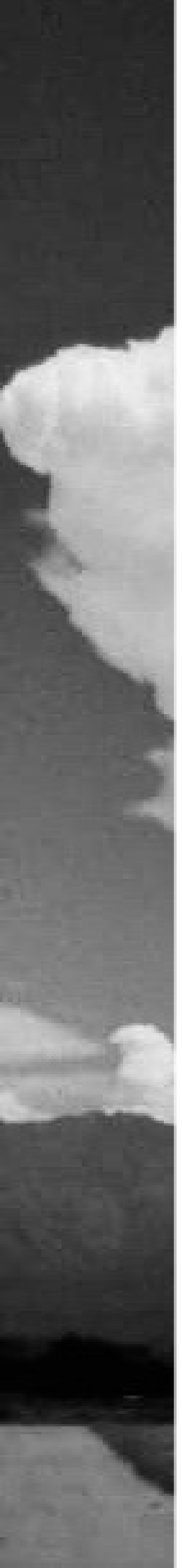

WRF cell coverage prior to CI correlate with moistening

Average 4-km RH rotated to the 4-km wind direction increases over and downstream of the CI location as cells propagate through the area

Low max reflectivity cells have the same patterns but with lesser RH and cell coverage (not shown)

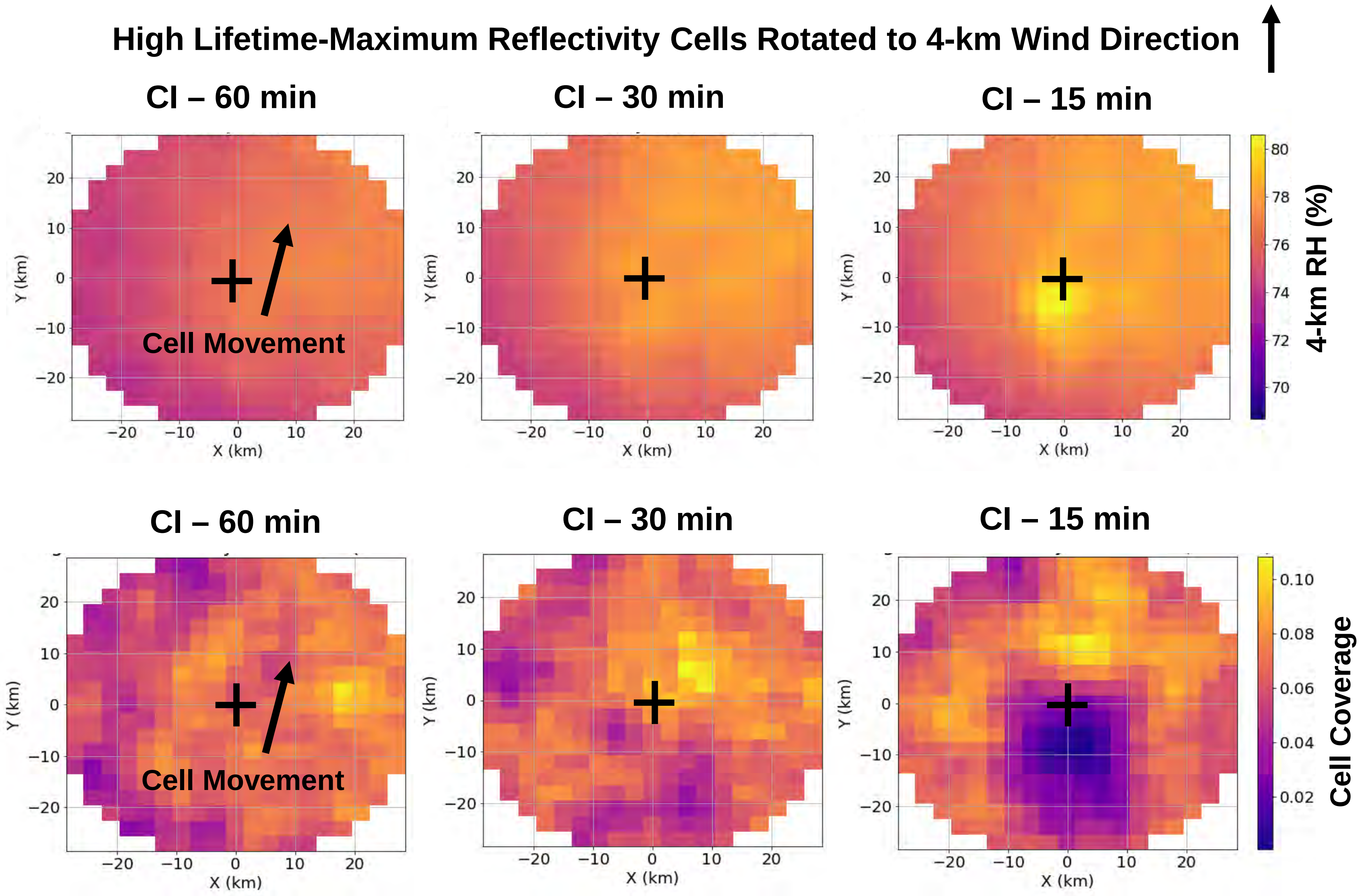

WRF MUCAPE distribution prior to CI

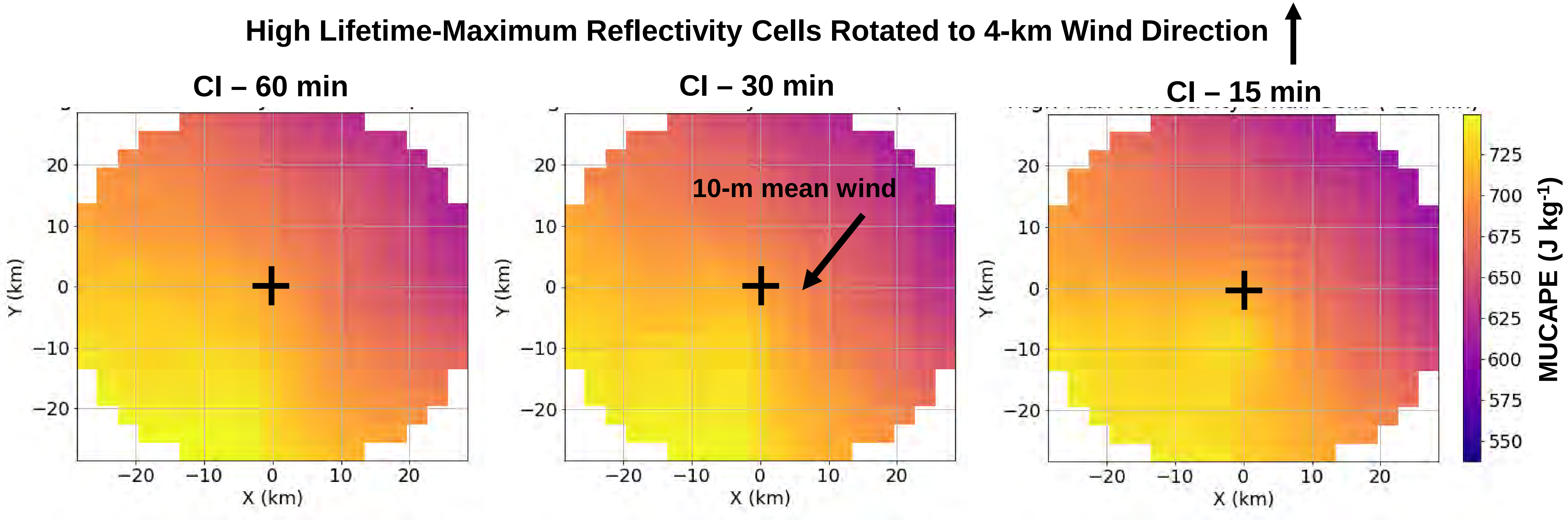

Diurnal cycles of narrow cell max reflectivity and number of cells in the domain

More numerous cells are most common overnight but greater max reflectivity associated with more cells in the domain does not change diurnally. Thus, this signal is not related to diurnal processes.

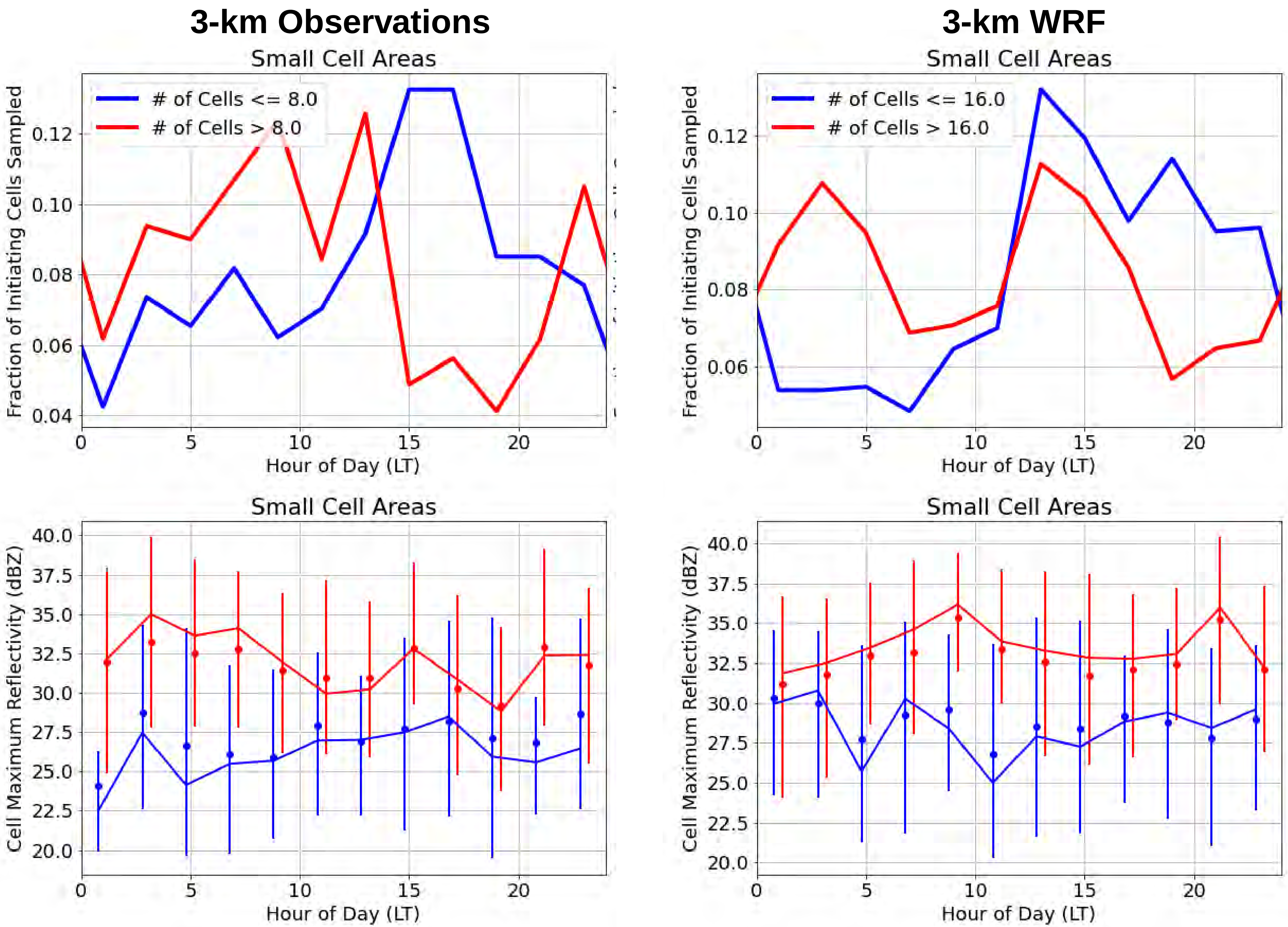

Campaign-long 3-km WRF Performance

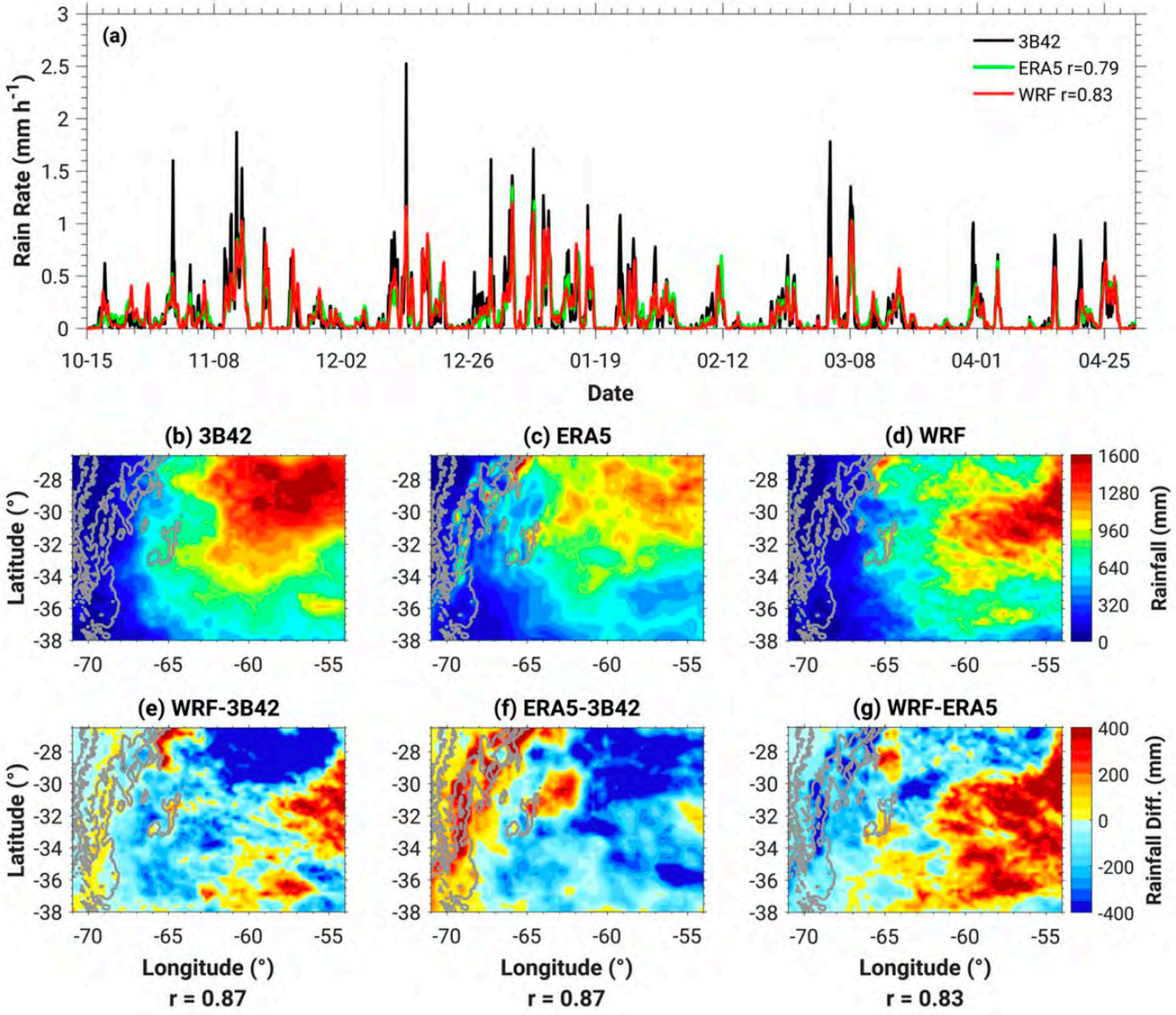

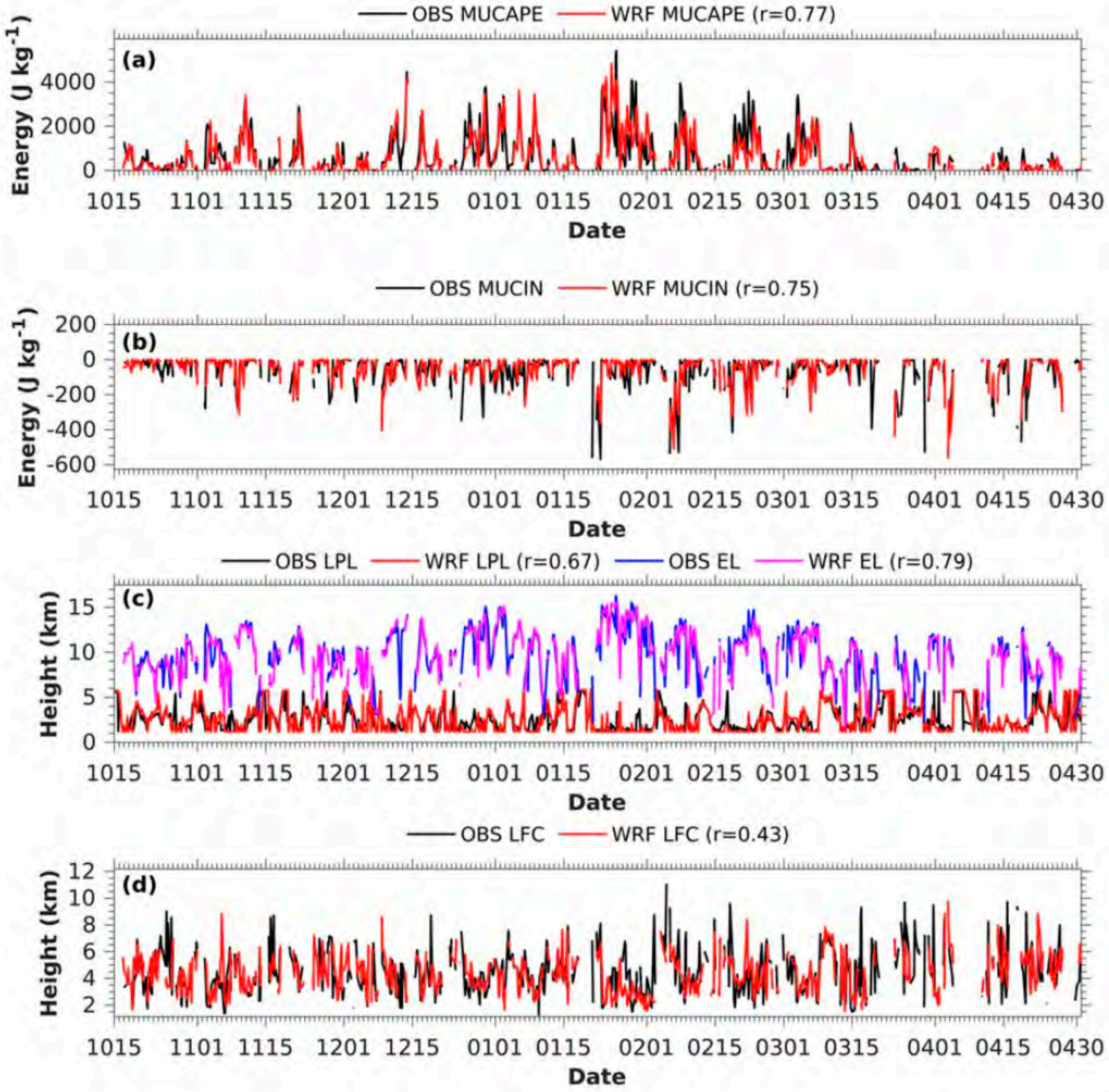

Zhang, Z., et al., 2021, *Mon. Wea. Rev.*, doi:10.1175/MWR-D-20-0411.1.

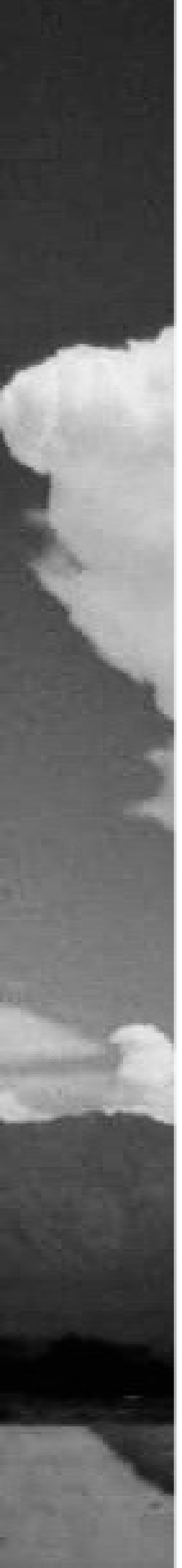

Radiosonde Statistics

Over 2700 soundings were launched, with many more during the IOP associated with RELAMPAGO missions.

Max CAPEs approached 8000 J kg^{-1}, max PW exceeded 60 mm, and 0-6 km bulk shear frequently surpassed 25 m s^{-1}.

Schumacher, R., et al., 2021: Convective-storm environments in subtropical South America from high-frequency soundings during RELAMPAGO-CACTI. *Mon. Wea. Rev*., 149, 1439-1458, doi:10.1175/MWR-D-20-0293.1.

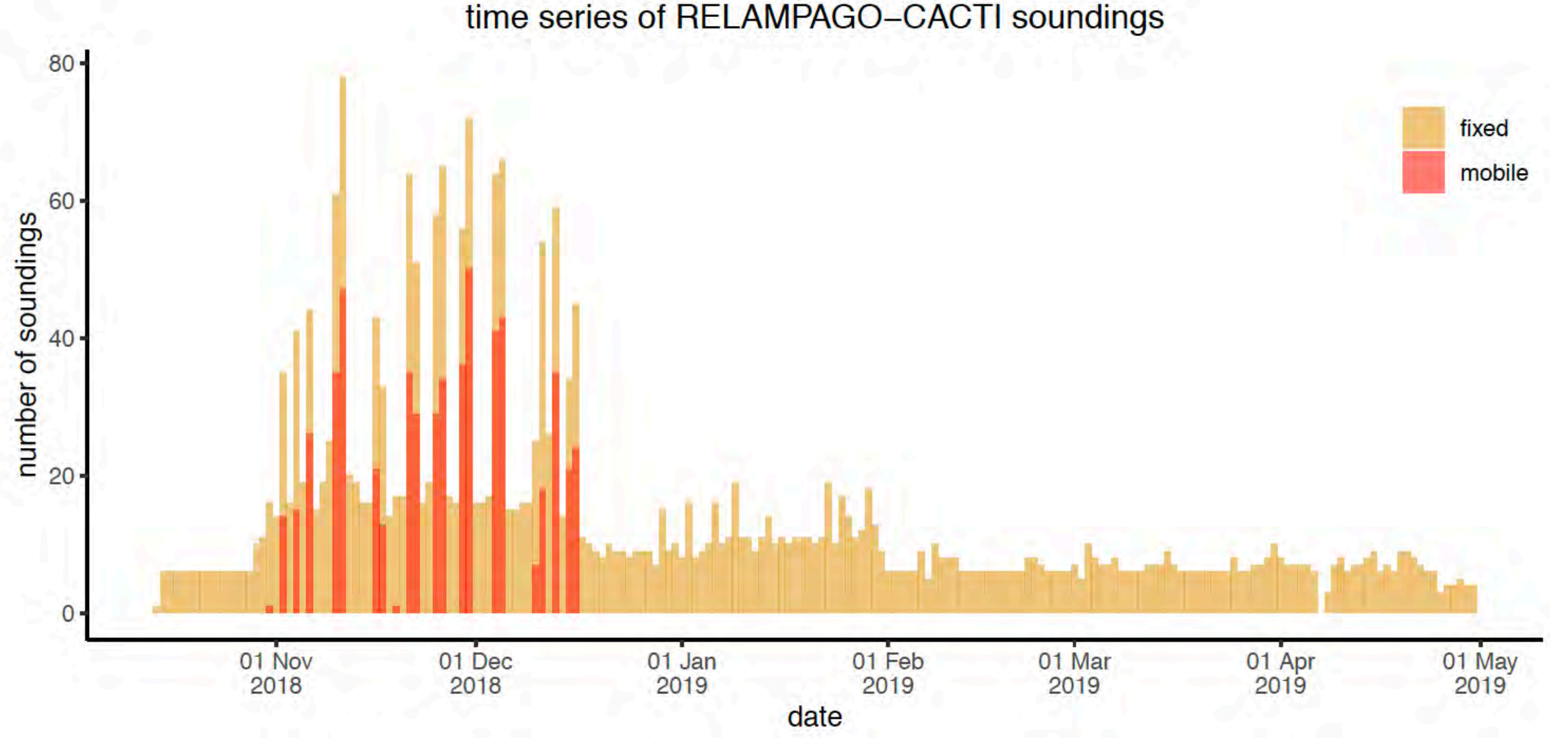

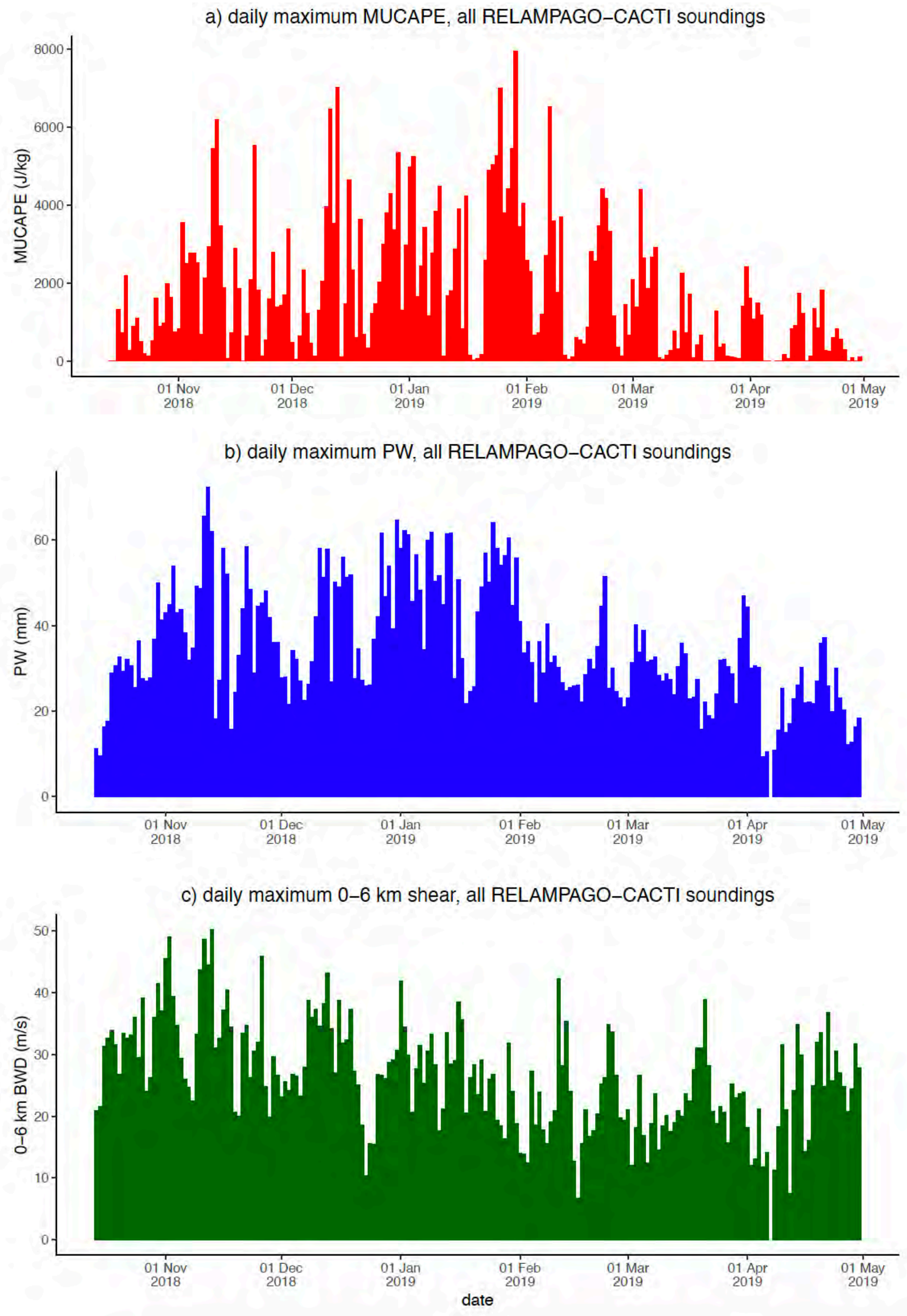

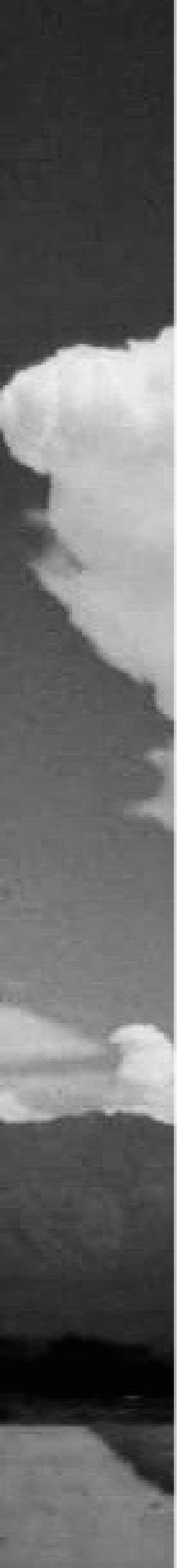

Pacific Northwest
NATIONAL LABORATORY

Low Level Jets and Cold Pools

As expected, a number of soundings exhibited northerly low level jets, which decreased in strength as they approached the SDC range.

These LLJs varied significantly in altitude from 500 m to > 2000 m. These more elevated LLJs may occur more frequently in this region as compared to the Great Plains.

A number of soundings were also launched in cold pools, which varied greatly in depth and intensity, similar to what has been found for observations over the Great Plains.

Schumacher, R., et al., 2021, *Mon. Wea. Rev.*, doi:10.1175/MWR-D-20-0293.1.

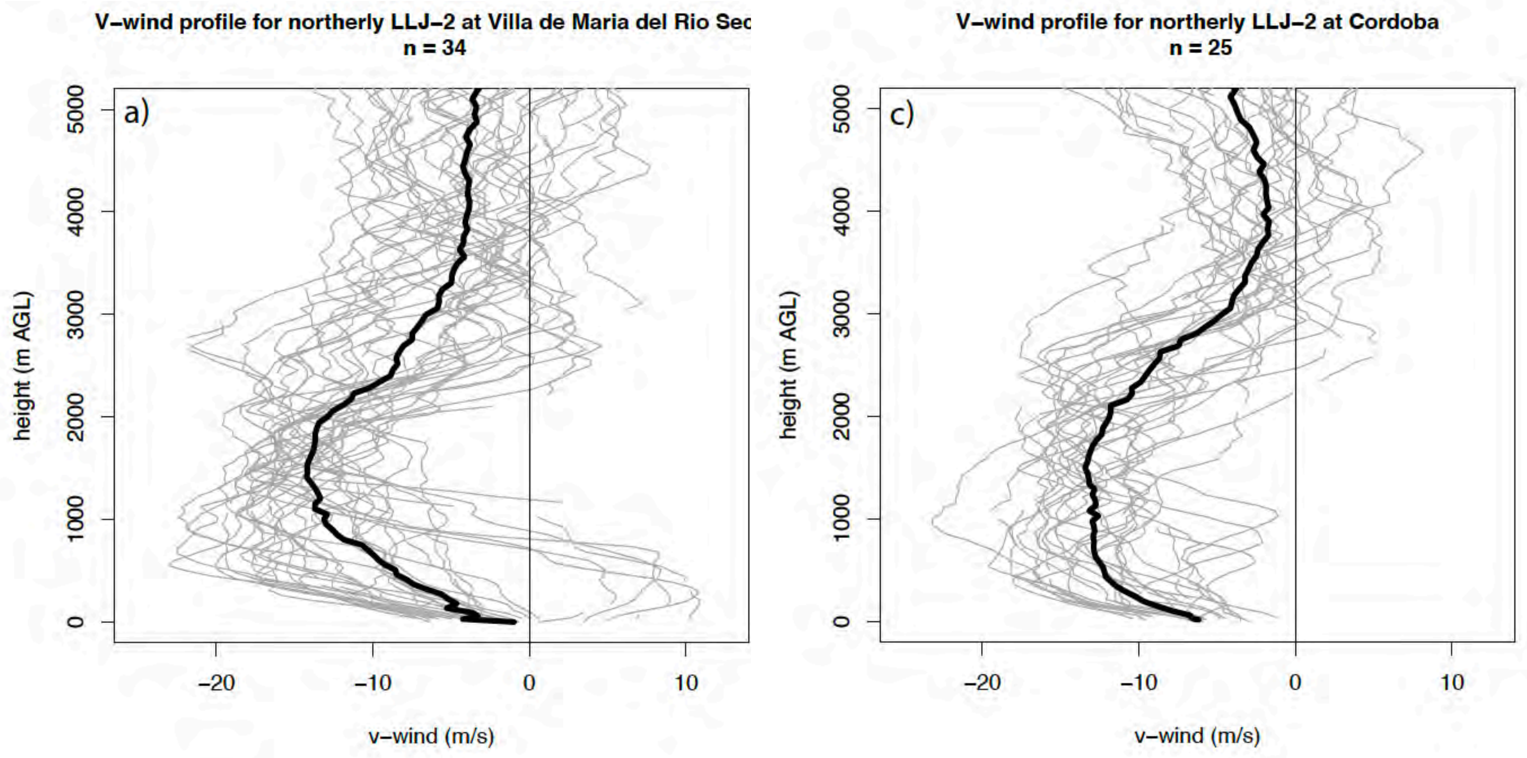

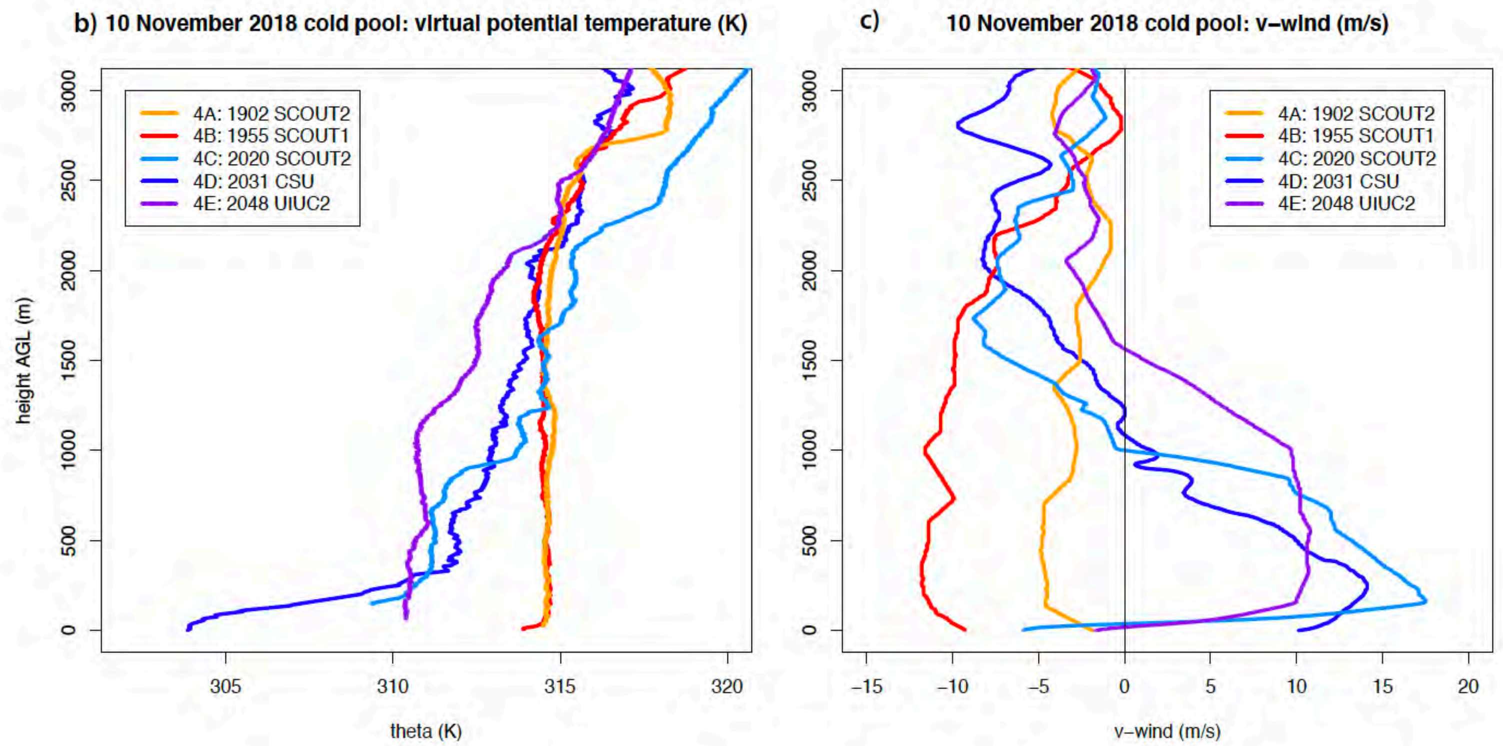

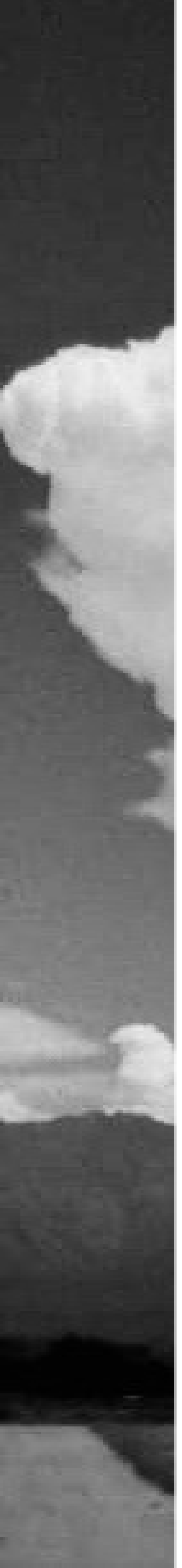

Pacific Northwest NATIONAL LABORATORY

Severe Weather

RELAMPAGO had many objectives related to observing and understanding high impact weather.

Environments favorable to supercells and significant hail were very common, and many supercells and hailstorms were observed (e.g., right), particularly in the immediate lee of the high terrain.

Significant tornado conditions were much rarer due to insufficient low level vertical wind shear and storm-relative helicity.

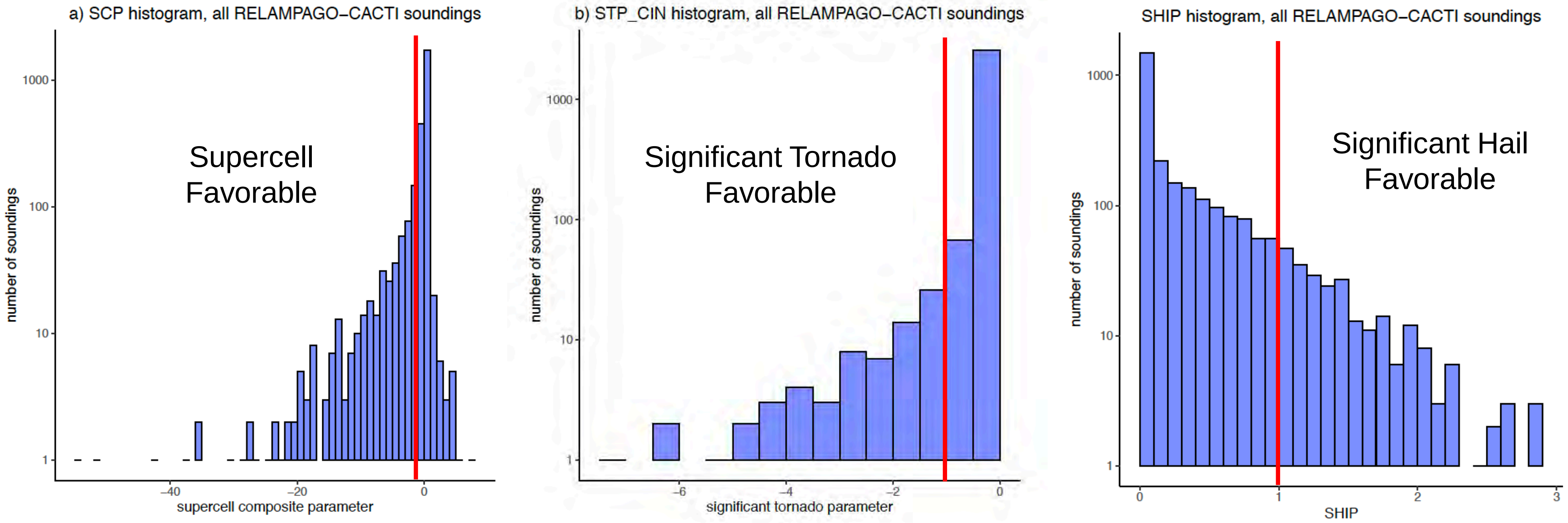

Schumacher, R., et al., 2021, *Mon. Wea. Rev.*, doi:10.1175/MWR-D-20-0293.1.

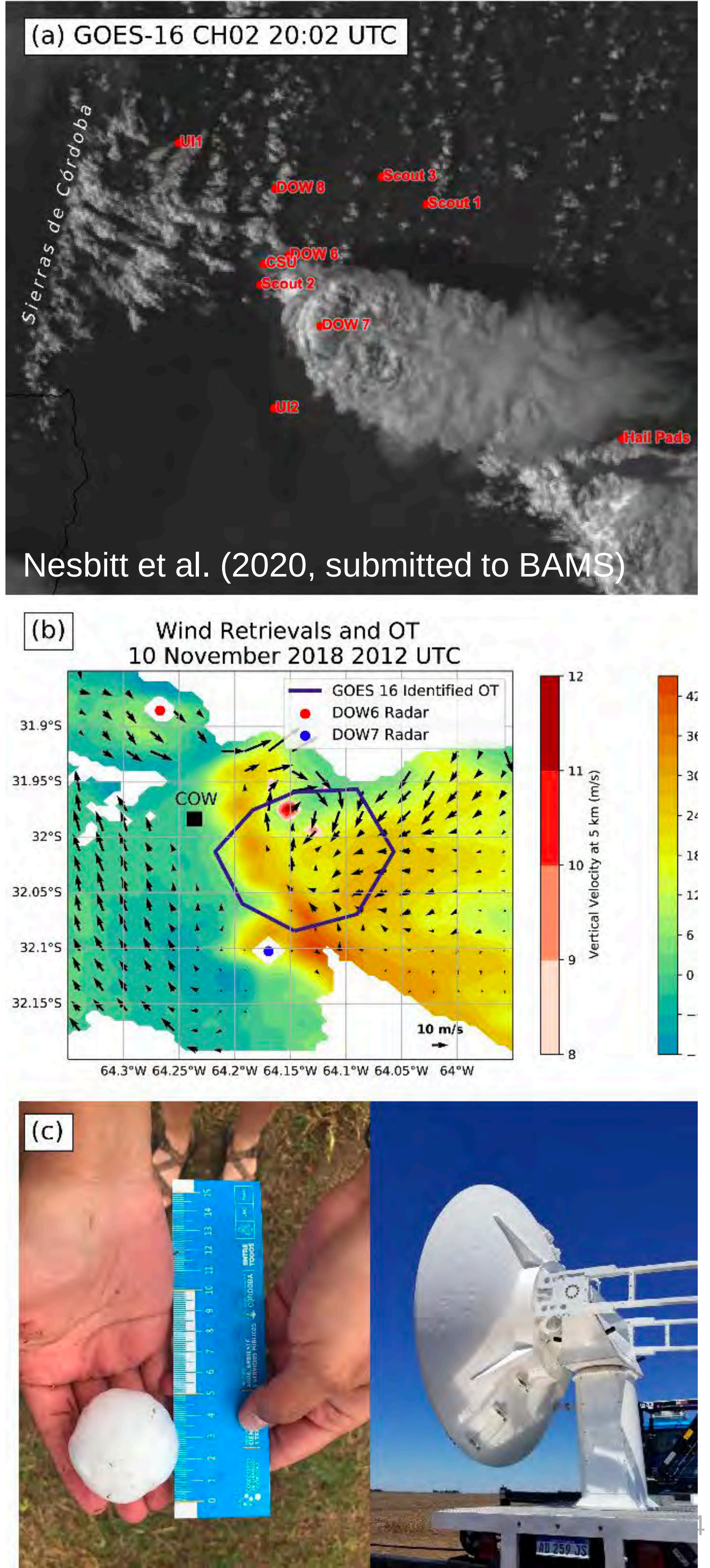

Nesbitt et al. (2020, submitted to BAMS)

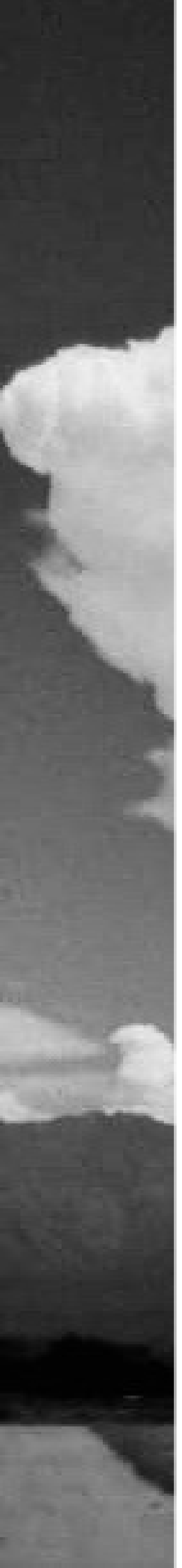

Extreme Deep Convection

Investigations are also ongoing into the extreme convection observed including this case on January 25, 2019.

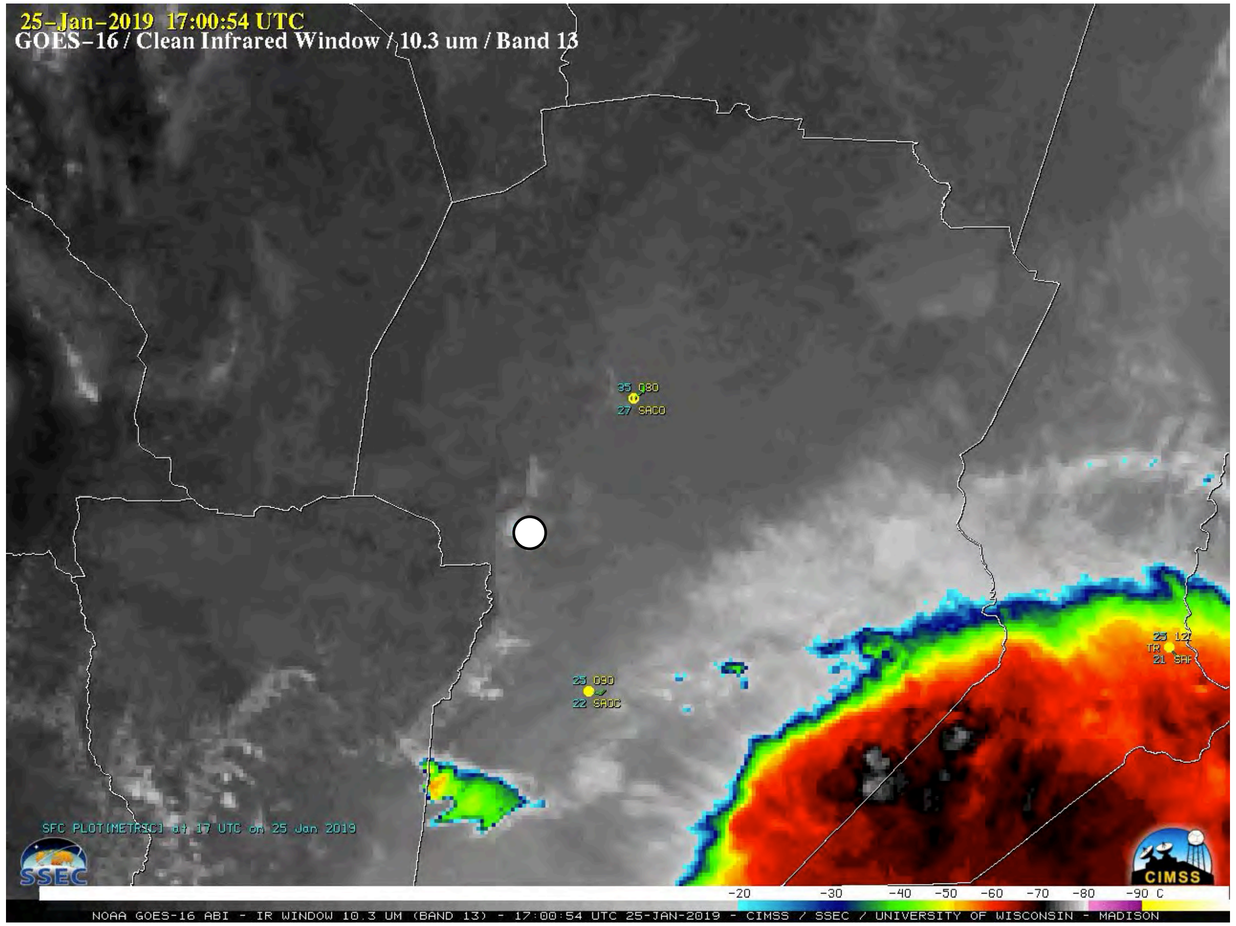

Cordoba Jan. 25 Soundings

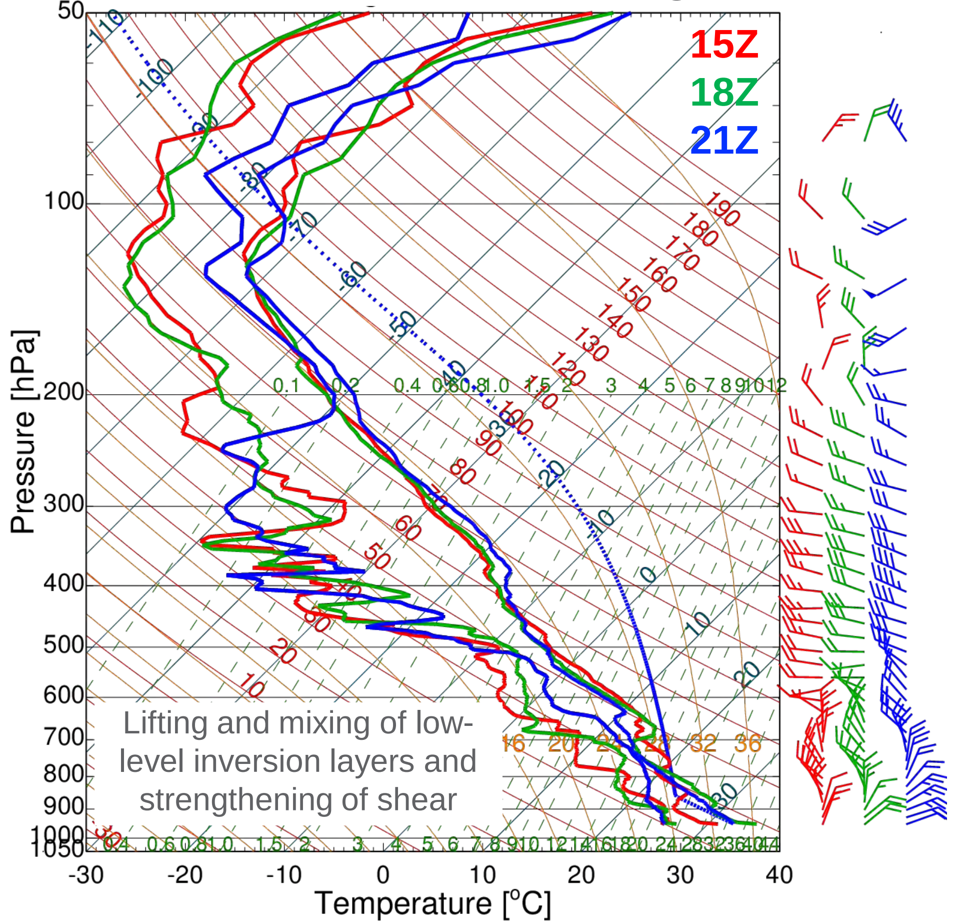

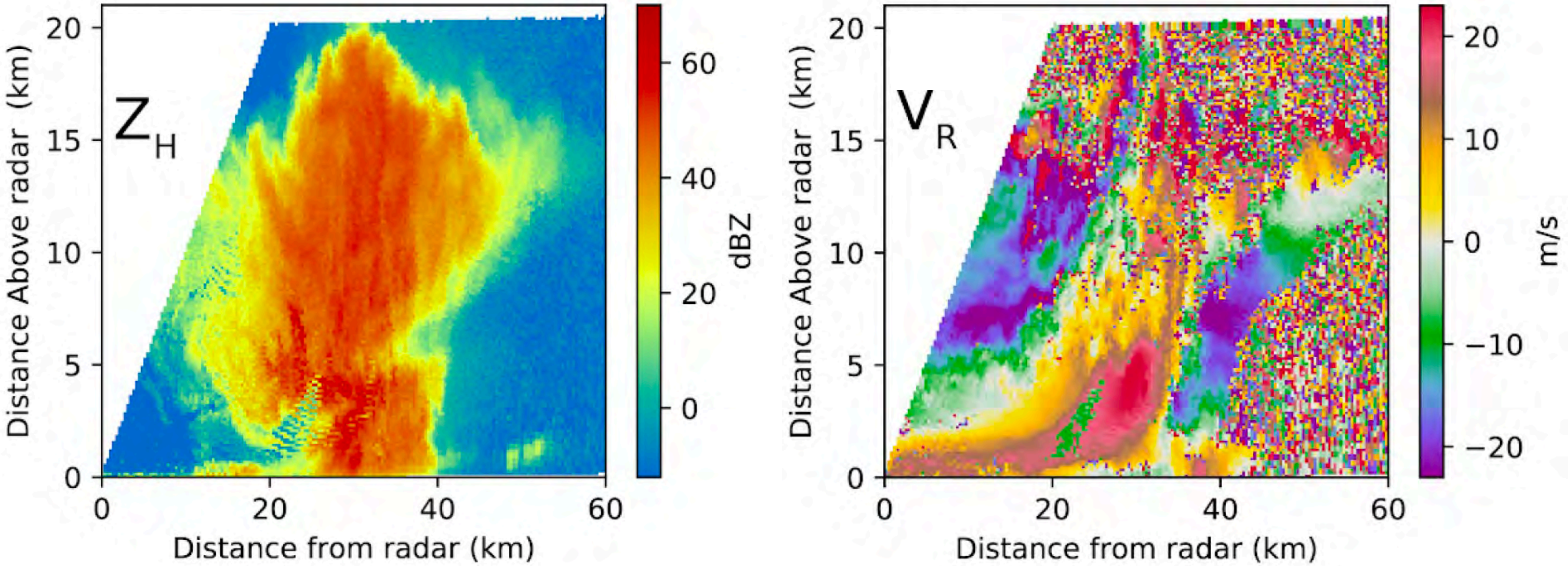

Nesbitt S. W., et al., 2021, *BAMS,* doi:10.1175/BAMS-D-20-0029.1.

Opportunities to Leverage Detailed HSRHI Scans

Tracked cells are being linked with rapid scan GOES-16 data and routine hemispheric RHI scans (e.g., 30º azimuth to right) along each radial spoke in the PPI view below

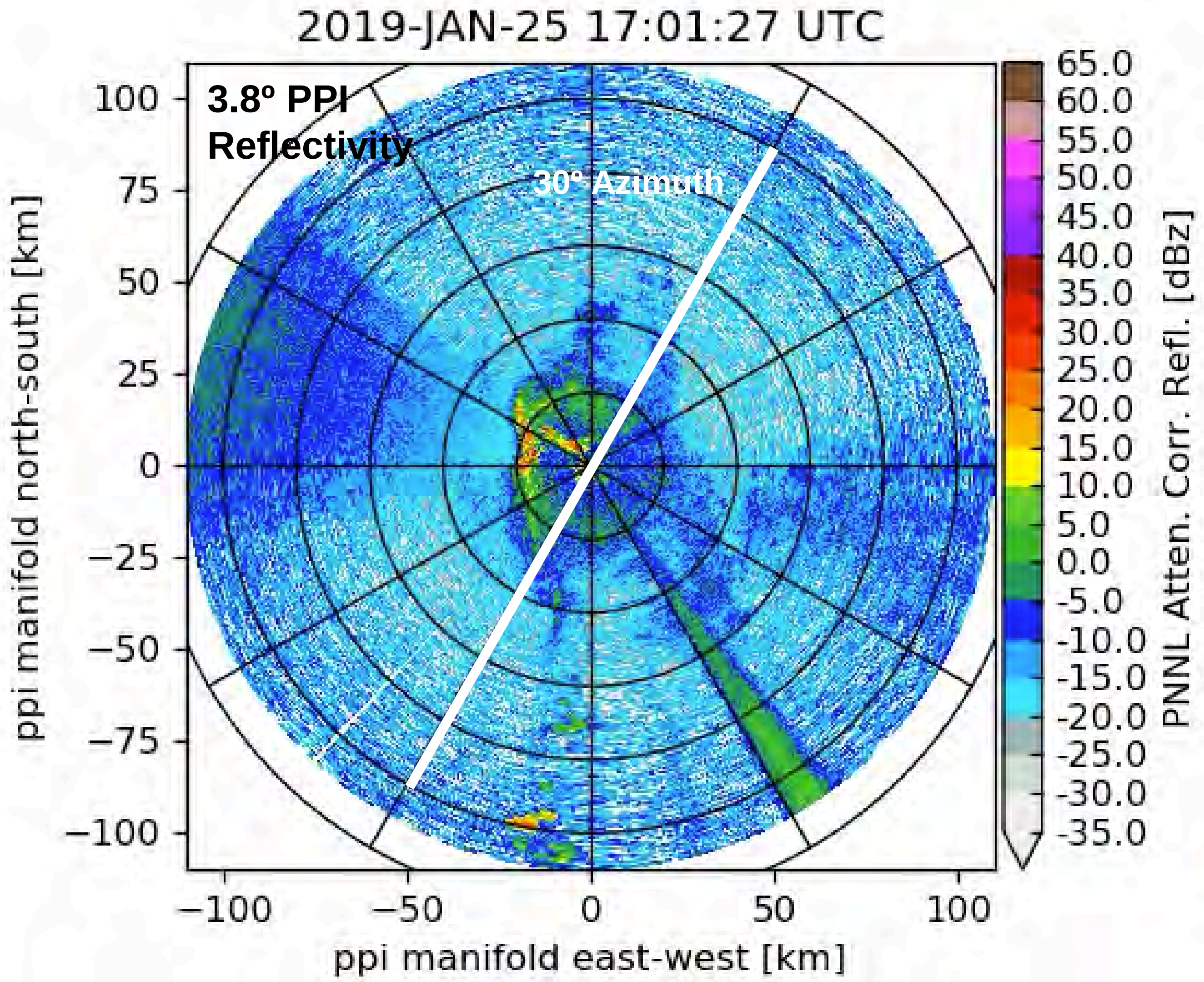

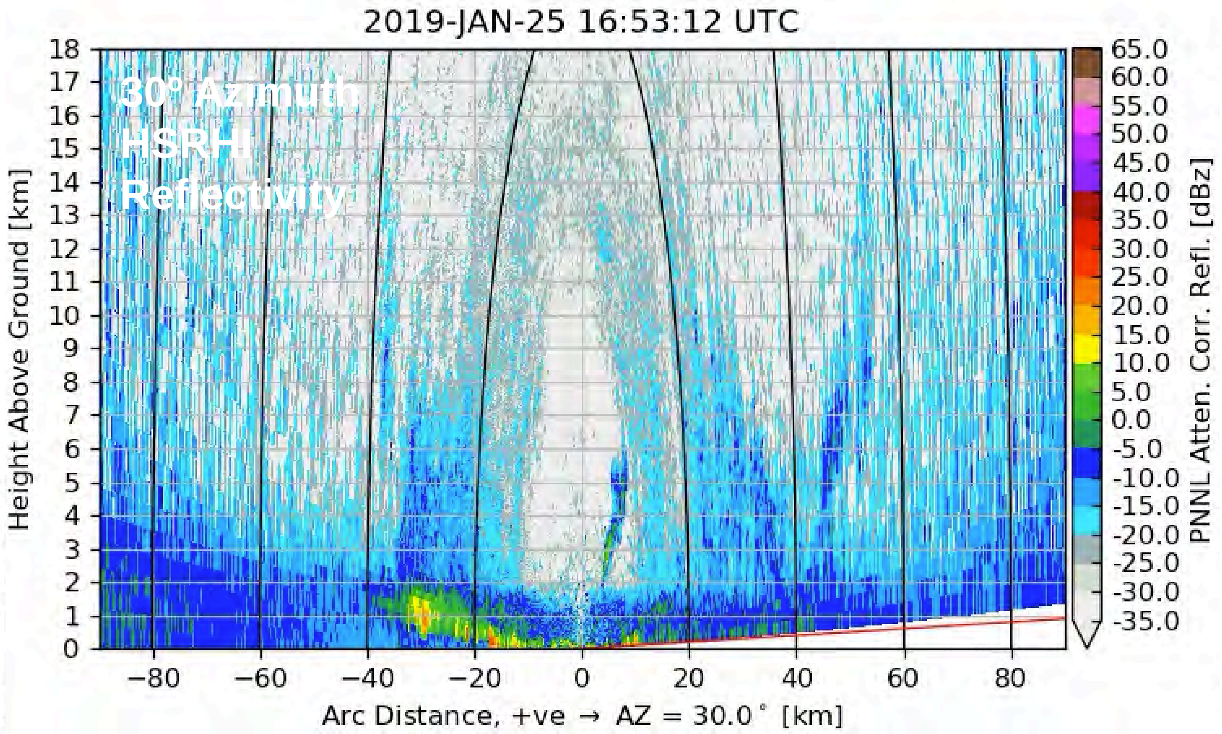

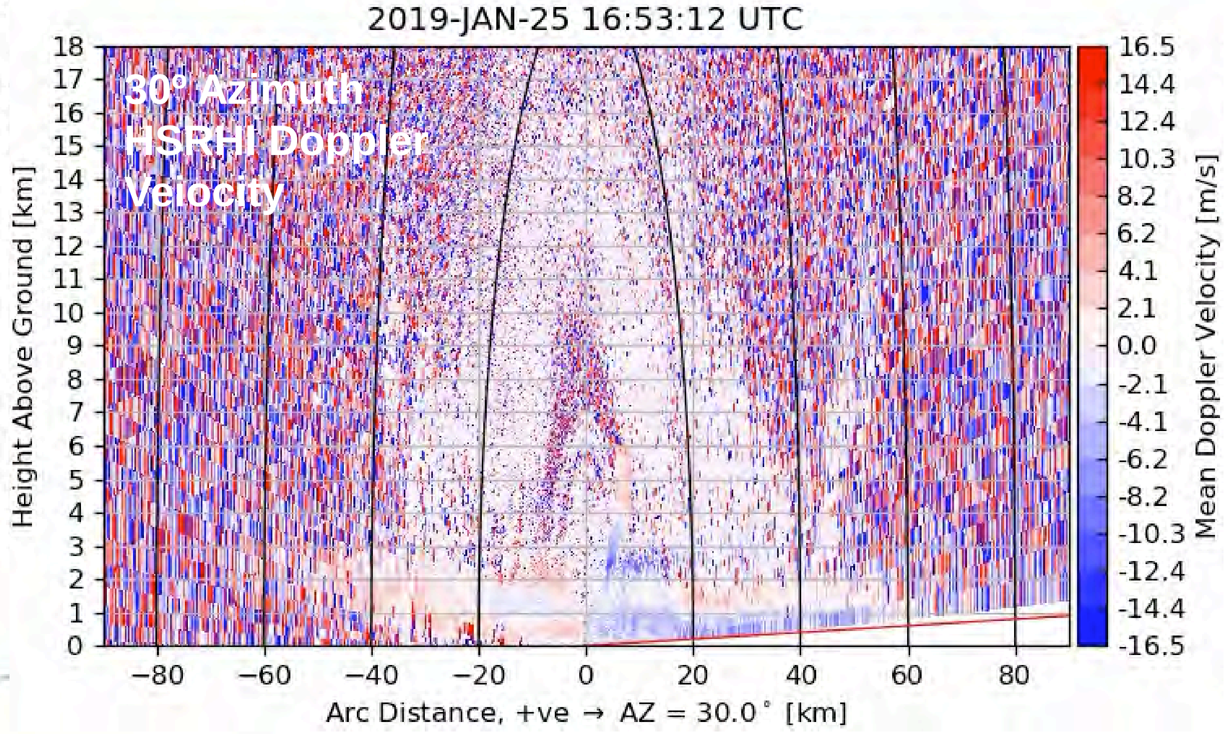

Detailed Microphysical and Kinematic Evolution

South to North

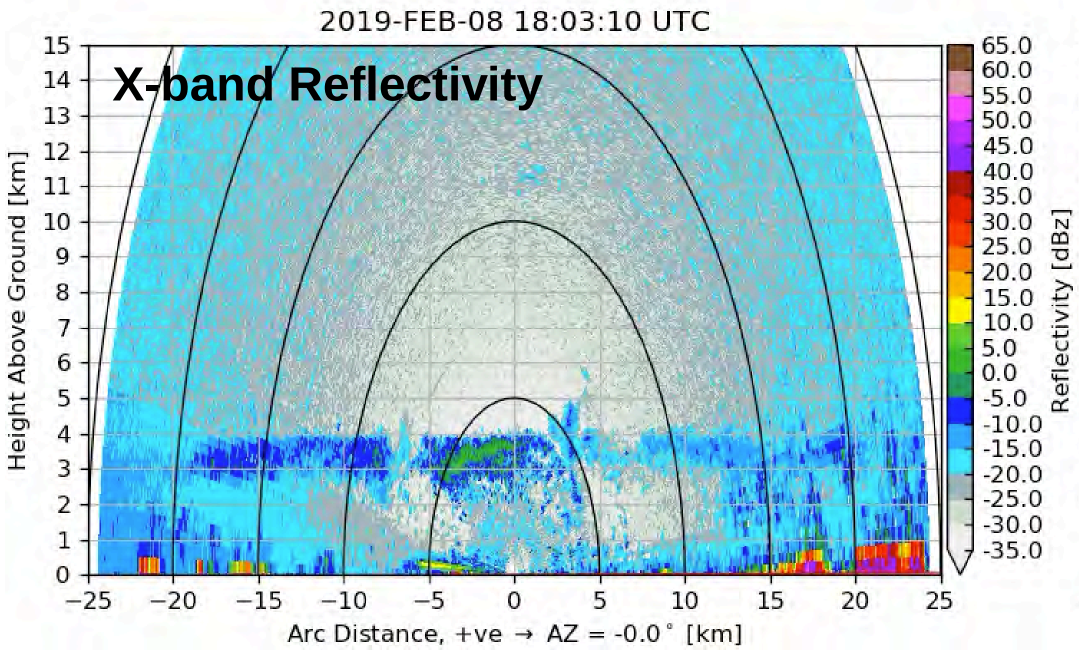

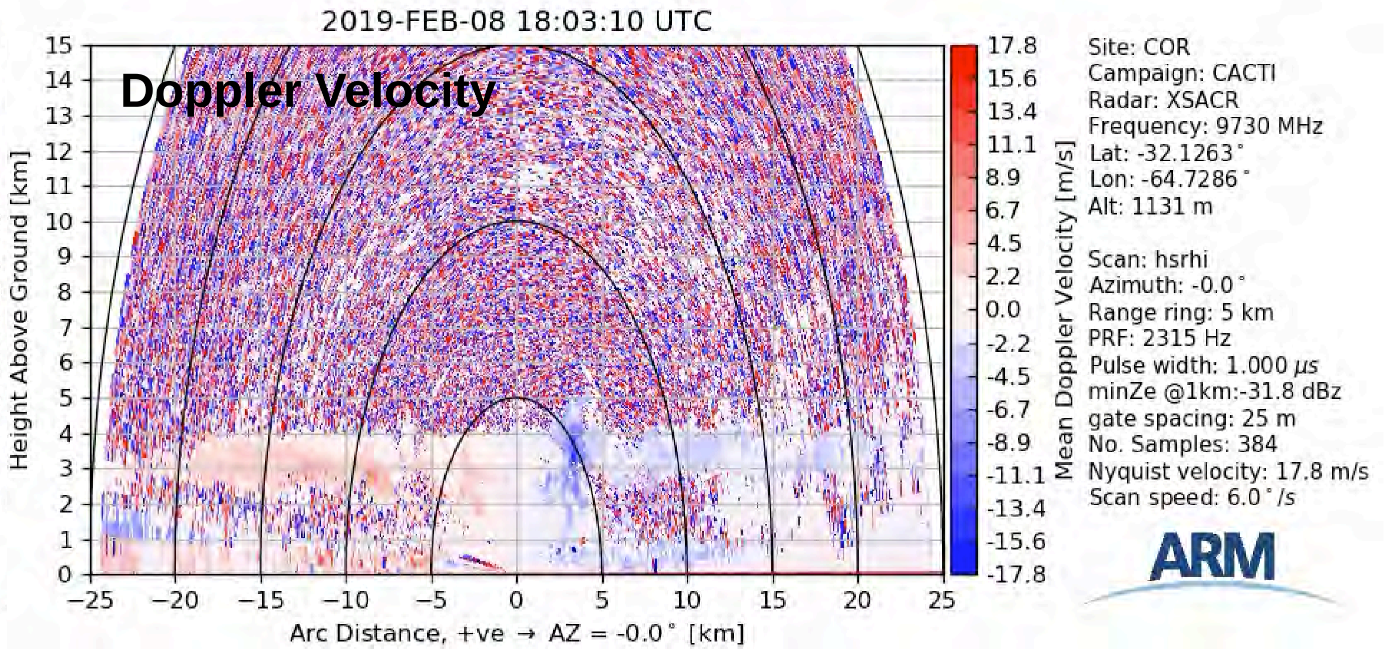

Images from Joseph Hardin and Nitin Bharadwaj

West to East

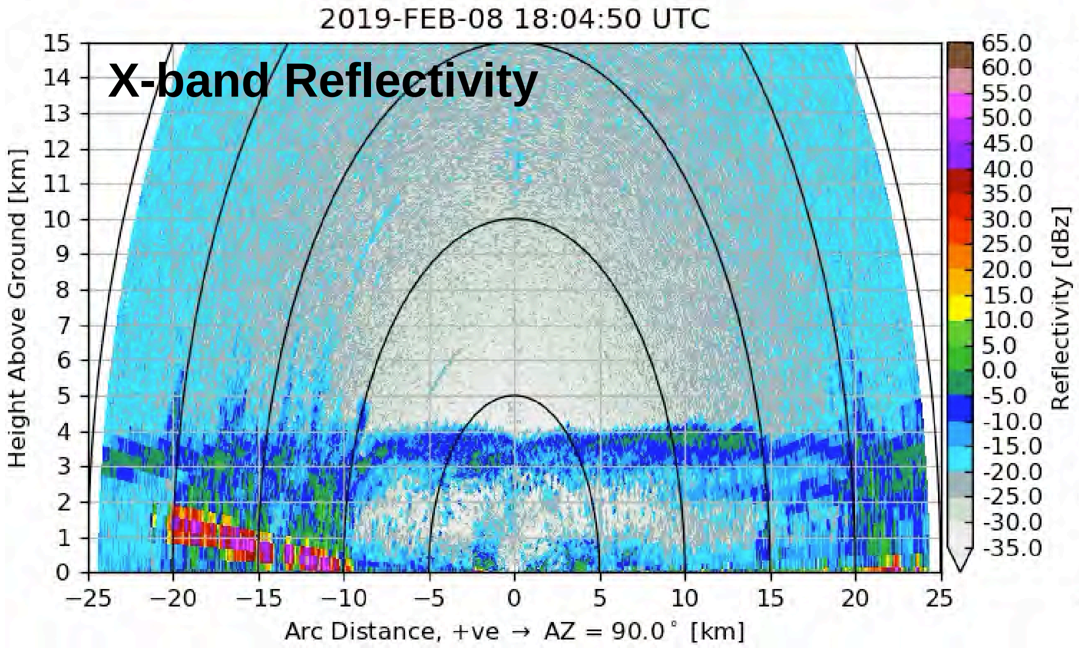

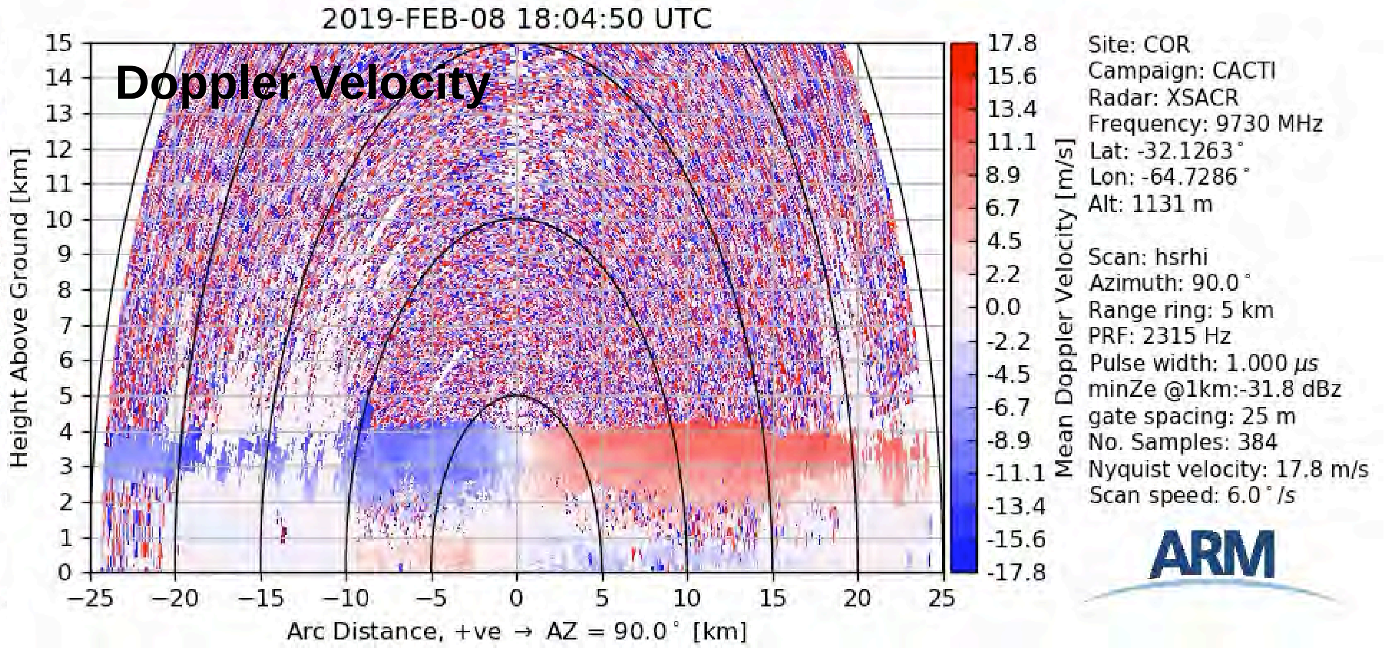

HSRHI Objects Connected to Cell Tracks

Horizontal Scan

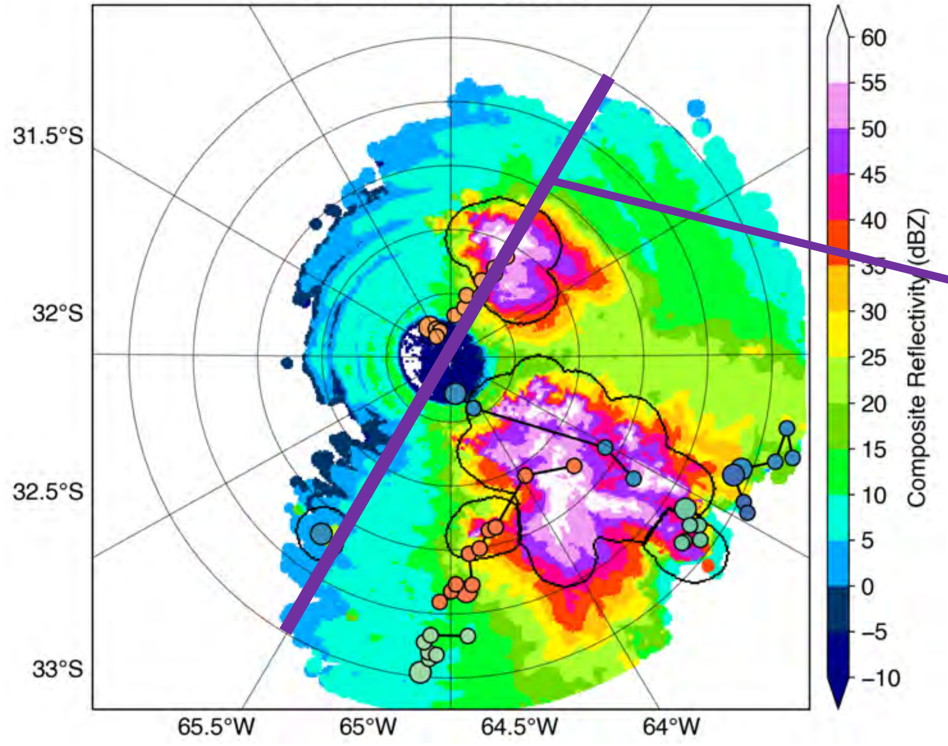

Detailed Vertical Scan

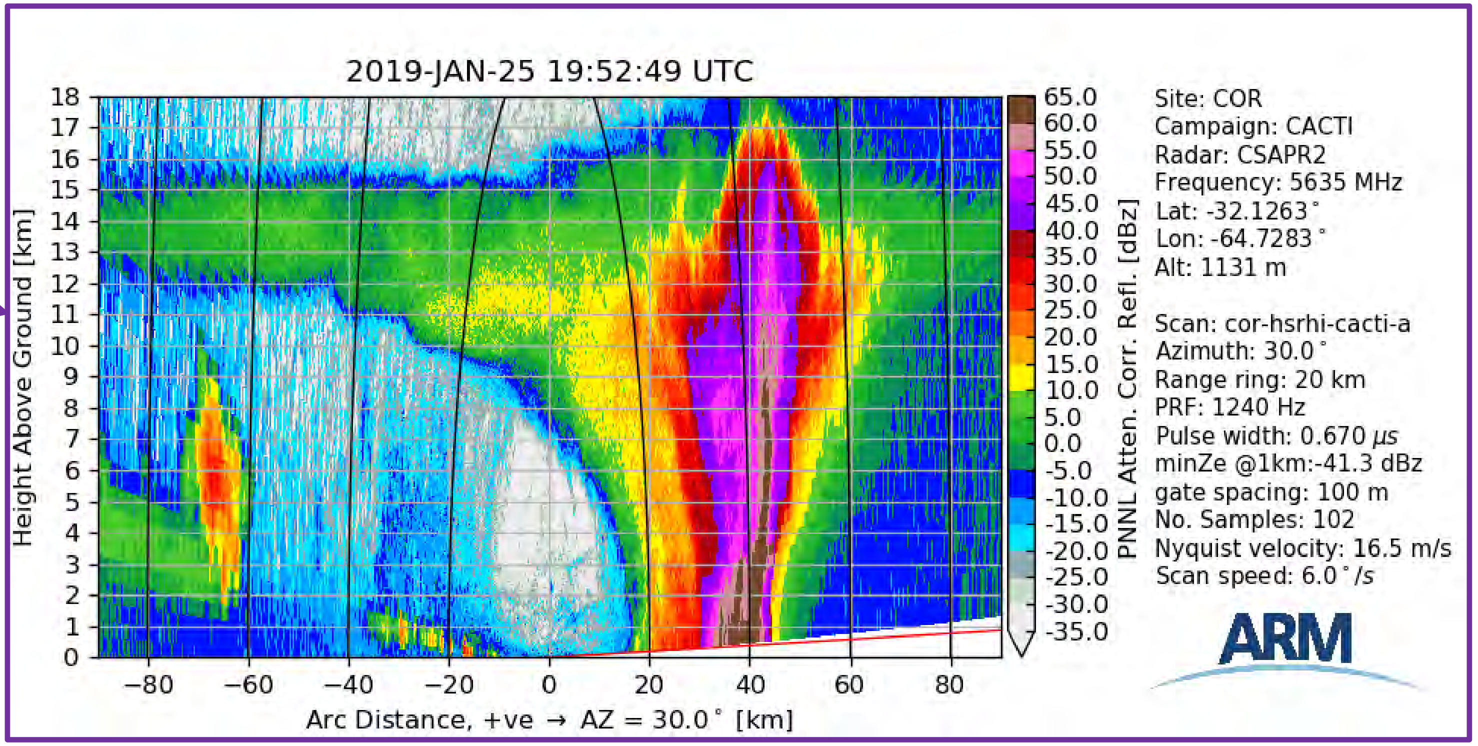

Our extensive database of HSRHI scans is being used to identify detailed HSRHI objects that are being tied to the PPI-tracked objects.